Table of contents:

1. Experimental details and characterization data

General considerations. All reactions were carried out under an inert-gas atmosphere (dry argon or nitrogen) using standard Schlenk or glove box techniques. The starting material C_3Cl_6 (*Sigma Aldrich*) was purified by flash chromatography (*c*-hexane) prior to use. All other commercially available substances were used as received. [*n*Bu$_4$N]$_2$[(Cl$_3$Si)$_2$C–C(SiCl$_3$)$_2$] ([*n*Bu$_4$N]$_2$[**B**]) was synthesized according to a literature procedure.[S1] Reaction solvents were dried over sodium (*n*-hexane, *n*-pentane), sodium/benzophenone (Et_2O, THF), CaH_2 (CH_2Cl_2), or *n*-BuLi (NMe_2Et) and freshly distilled prior to use. MeOH and a solution of Me_3SnCl in THF were stored over molecular sieves (3 Å; several weeks in the case of MeOH). CD_2Cl_2 and $CDCl_3$ were stored over molecular sieves (4 Å). NMR spectra were recorded on a *Bruker* DPX-250, *Bruker* Avance II 300, or *Bruker* Avance III HD 500 (equipped with a Prodigy BBO 500 S1 probe) spectrometers. ^{1}H/^{13}C{^{1}H} NMR spectra were referenced against (residual) solvent signals (CD_2Cl_2: 5.32 ppm/53.84 ppm, $CDCl_3$: 7.26 ppm/77.16 ppm;[S2] s = singlet, d = doublet, t = triplet, m = multiplet). ^{29}Si NMR spectra were calibrated against external $SiMe_4$ (δ(^{29}Si) = 0 ppm); whenever present, $SiCl_4$ (δ(^{29}Si) = −18.9 ppm)[S3] was used as internal standard. The CW EPR spectrum was recorded at room temperature on an EMXnano (*Bruker*) tabletop EPR spectrometer using its Xenon controlling/recording software. UV/vis absorption spectra were recorded at room temperature using a *Varian* Cary 60 Scan UV/vis spectrophotometer. IR spectra were recorded using a *JASCO* FT/IR-4200 spectrometer equipped with a *PIKE* Technologies GladiATR unit. Multiple scans per measurement were accumulated to increase the signal-to-noise ratio (s = strong signal, m = medium signal, w = weak signal). The cyclic voltammogram of [*n*Bu$_4$N][**1**] was recorded at room temperature in a one-chamber, three electrode cell using an *EG&G* Princeton Applied Research 263A potentiostat with a platinum disk working electrode (diameter 2.00 mm). The reference electrode was a silver wire on which AgCl had been deposited by immersing the wire into HCl/HNO_3 (3:1). [*n*Bu$_4$N][B(C$_6$F$_5$)$_4$] was employed as the supporting electrolyte. All potential values are referenced against the FcH/FcH$^+$ redox couple (FcH = ferrocene; $E_{1/2}$ = 0 V). The LDI-MS spectra was recorded on a MALDI LTQ Orbitrap XL (*Thermo Fisher Scientific*) in the negative-ion mode. The resolution was set to 60000. The sample spots were prepared inside a glove box: A suspension of the sample in Et_2O was transferred to the sample holder by a transfer pipette to form a thin layer of material after evaporation. A desiccator was used to bring the sample holder from the glove box to the mass spectrometer. The laser energy was set to 50 µJ and 20 to 30 spectra were accumulated to increase the signal/noise ratio. The isotopic pattern of the molecular anion species was compared to the theoretical pattern calculated from the elemental composition of the anion using the instrument software (Xcalibur). Flash chromatography was performed on a *Biotage* ISOLERA ONE with *Interchim* puriFlash cartridges. GC-MS (gas chromatography – mass spectrometry) data were recorded using a *Shimadzu* GCMS-QP 2010SE. The stationary phase (*Restek*) had a length of 60 m with an inner diameter of 0.32 mm. The analyte was diluted with CH_2Cl_2 prior to the measurement. To avoid overloading the MS, a solvent cut was used.

The oven was heated using methods **A** – **D**. After exiting the column, substances were ionized with 70 eV and cationic fragments were measured within a range of m/z = 30-900 (mass per charges).

A: Samples were injected at 200 °C and transferred onto column using a split liner and a flow rate of 1.86 mL/min, carried by helium gas. The oven was heated from 50 °C for 1 min, the temperature was subsequently elevated at a rate of 20 °C/min up to 250 °C and held for 49 min, then elevated again at a rate of 25 °C/min up to 270 °C and held for 5 min.

B: Samples were injected at 200 °C and transferred onto column using a split liner and a flow rate of 1.86 mL/min, carried by helium gas. The oven was heated from 50 °C for 1 min, the temperature was subsequently elevated at a rate of 10 °C/min up to 250 °C and held for 30 min, then elevated again at a rate of 25 °C/min up to 270 °C and held for 5 min.

C: Samples were injected at 200 °C and transferred onto column using a split liner and a flow rate of 1.86 mL/min, carried by helium gas. The oven was heated from 50 °C for 1 min, the temperature was subsequently elevated at a rate of 20 °C/min up to 200 °C and held for 40 min, then elevated again at a rate of 25 °C/min up to 270 °C and held for 5 min.

D: Samples were injected at 180 °C and transferred onto column using a split liner and a flow rate of 1.86 mL/min, carried by helium gas. The oven was heated from 50 °C for 1 min, the temperature was subsequently elevated at a rate of 20 °C/min up to 180 °C and held for 25 min, then elevated at a rate of 20 °C/min up to 250 °C and held for 5 min, then elevated again at a rate of 25 °C/min up to 270 °C and held for 5 min.

The amount of Si-bonded Cl atoms in [**1**]$^-$ and **2** was determined by quenching an aliquot of the pure substance dissolved in CH_2Cl_2 with MeOH in a closed vessel. After stirring for 30 min, the mixture was titrated with aqueous NaOH (0.1 M) to determine the amount of liberated HCl; the titrations were repeated at least three times.

Note:

1. In the reaction protocols compiled below, the reaction equations show the theoretically required stoichiometries of the individual reactants, which can slightly deviate from the stoichiometries used in practice, mainly for reasons of convenience.

2. The synthesis of [1]$^-$ proceeds quantitative. Therefore, in all syntheses, *in situ* generated [1]$^-$ is used without further analysis or purification.

Synthesis of [*n*Bu$_4$N][1].

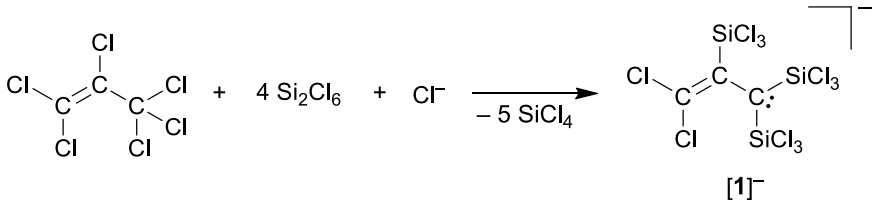

Neat Si_2Cl_6 (1.39 mL, 2.17 g, 8.07 mmol) was added dropwise with stirring at room temperature to a Schlenk flask containing a solution of [*n*Bu$_4$N]Cl (0.560 g, 2.01 mmol) and C_3Cl_6 (0.28 mL, 0.49 g, 1.97 mmol) in CH_2Cl_2 (25 mL). *Caution*: A slow drop rate is important because the reaction is strongly exothermic. After stirring for 12 h at room temperature, all volatiles were removed under reduced pressure and [*n*Bu$_4$N][**1**] was obtained as a brown sticky solid. Yield: 1.33 g (1.77 mmol, 90%). *Note*: The stirring time can be reduced but should not be less than 1 h.

^{1}H NMR (500.2 MHz, CD_2Cl_2, 298 K): δ = 3.16 (m, 8H; C*H*$_2$N), 1.63 (m, 8H; C*H*$_2$CH$_2$N), 1.43 (m, 8H; CH$_3$C*H*$_2$), 1.02 ppm (t, $^3J_{HH}$ = 7.4 Hz, 12H; C*H*$_3$).

^{13}C{^{1}H} NMR (125.8 MHz, CD_2Cl_2, 298 K): δ = 137.3 (Cl_2C=$CSiCl_3$), 135.8 (Cl_2C=$CSiCl_3$), 59.4 (*C*H$_2$N), 50.3 (*C*(SiCl$_3$)$_2$), 24.3 (*C*H$_2$CH$_2$N), 20.1 (CH$_3$*C*H$_2$), 13.7 ppm (*C*H$_3$).

^{29}Si{^{1}H} NMR (99.4 MHz, CD_2Cl_2, 298 K): δ = –8.4 (Cl$_3$*Si*C=), –16.7 ppm ((*Si*Cl$_3$)$_2$C).

LDI-MS(–): *m*/*z* = 508.59 ([$C_3Cl_2(SiCl_3)_3$]$^-$; calc: 508.58).

Note: (i) [*n*Bu$_4$N]Cl can be replaced by [Et$_4$N]Cl, [Ph$_4$P]Cl, or [Ph$_3$P=N=PPh$_3$]Cl. (ii) 1,2-Dichlorobenzene is also a suitable solvent. (iii) The anion [**1**]$^-$ is also obtained when 6 eq or 10 eq of Si_2Cl_6 are employed. (iv) An increase in the reaction temperature to 39.6 °C does not lead to a higher degree of silylation.

Synthesis of [Ph_4P][1] to obtain single-crystalline material for X-ray analysis.

In the glove box, neat Si_2Cl_6 (0.109 g, 0.405 mmol) was added via syringe dropwise with stirring at room temperature to a screw-capped vial, charged with a solution of [Ph_4P]Cl (0.038 g, 0.101 mmol) and C_3Cl_6 (0.025 g, 0.101 mmol) in CH_2Cl_2 (0.5 mL). After stirring for 12 h at room temperature and slow evaporation of all volatiles, brown single crystals of [Ph_4P][**1**] were obtained together with some microcrystalline material. Yield: 0.084 g (0.099 mmol, 98%). After manual crystal picking for X-ray analysis, the remaining sample was dissolved in CD_2Cl_2, transferred to an NMR tube, and the tube was flame-sealed under vacuum. The ^{1}H, $^{13}C\{^{1}H\}$, and $^{29}Si\{^{1}H\}$ NMR spectra of the solution showed only the signals of [Ph_4P][**1**].

^{1}H NMR (500.2 MHz, CD_2Cl_2, 298 K): δ = 7.95 – 7.91 (m, 4H; Ph_4P), 7.79 – 7.75 (m, 8H; Ph_4P), 7.65 – 7.60 (m, 8H; Ph_4P).

$^{13}C\{^{1}H\}$ NMR (125.8 MHz, CD_2Cl_2, 298 K): δ = 137.4 ($Cl_2C{=}CSiCl_3$), 136.2 (d, $^{4}J_{CP}$ = 3.0 Hz; C-*p*), 135.6 ($Cl_2C{=}CSiCl_3$), 134.8 (d, $^{2}J_{CP}$ = 10.3 Hz; C-*m*), 131.1 (d, $^{3}J_{CP}$ = 12.9 Hz; C-*p*), 117.9 (d, $^{1}J_{CP}$ = 89.6 Hz; C-*i*), 50.3 ($C(SiCl_3)_2$).

$^{29}Si\{^{1}H\}$ NMR (99.4 MHz, CD_2Cl_2, 298 K): δ = –8.5 ($Cl_3SiC{=}$), –16.7 ppm ($(SiCl_3)_2C$).

Reaction of C_3Cl_6 with 1 eq of Si_2Cl_6 and catalytic amounts of [*n*Bu_4N]Cl.

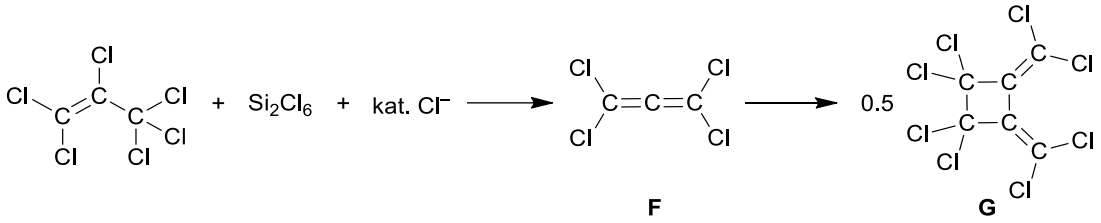

In the glove box, neat Si_2Cl_6 (0.026 g, 0.097 mmol) was added via syringe dropwise at room temperature to an NMR tube charged with a solution of [*n*Bu_4N]Cl (0.002 g, 0.007 mmol) and C_3Cl_6 (0.026 g, 0.105 mmol) in CD_2Cl_2 (0.5 mL). The tube was flame-sealed under vacuum. An NMR-spectroscopic investigation 1.5 h after mixing the compounds revealed the formation of perchloroallene **F**, its dimer **G** and $SiCl_4$ as the only reaction products. $^{13}C\{^1H\}$ NMR data were in accord with values from the literature.[S4,S5]

F:

$^{13}C\{^1H\}$ NMR (75.5 MHz, $CDCl_3$, 298 K): δ =196.8 (C=*C*=C), 104.4 ppm (*C*=C=*C*).

See below for the NMR data of **G**.

Synthesis of G through reaction of C_3Cl_6 with 1 equiv. of Si_2Cl_6 and catalytic amounts of [*n*Bu_4N]Cl.

A solution of [*n*Bu_4N]Cl (0.024 g, 0.086 mmol) in CH_2Cl_2 (6 mL) was added dropwise with stirring at –78 °C over a period of 30 min to a Schlenk flask containing a solution of C_3Cl_6 (0.302 g, 1.21 mmol) and Si_2Cl_6 (0.323 g, 1.20 mmol) in CH_2Cl_2 (10 mL). A subsequent GC-MS measurement revealed the formation of tetrachloroallene (**F**) and its dimer **G** besides some residual C_3Cl_6. The reaction mixture was allowed to warm to room temperature and stirring was continued for 1 d to ensure the quantitative dimerization of the tetrachloroallene. All volatiles were removed under reduced pressure and the colorless residue was extracted with *n*-pentane (5 × 5 mL). The combined *n*-pentane solutions were evaporated under reduced pressure to furnish a colorless solid. Colorless single crystals of **G** were obtained through slow evaporation of an *n*-pentane solution. Yield: 0.104 g (0.292 mmol, 48%). $^{13}C\{^1H\}$ NMR data were in accord with values from the literature[S5] and the structure was also confirmed by own X-ray crystallographic measurements (the solid-state structure of **G** is known[S6]).

$^{13}C\{^1H\}$ NMR (75.5 MHz, $CDCl_3$, 298 K): δ = 132.9 (Cl_2C–*C*=CCl_2), 127.5 (Cl_2C–C=*C*Cl_2), 89.4 ppm (Cl_2*C*–C=CCl_2).

Synthesis of 1• though oxidation of [*n*Bu$_4$N][1] with SbCl$_5$.

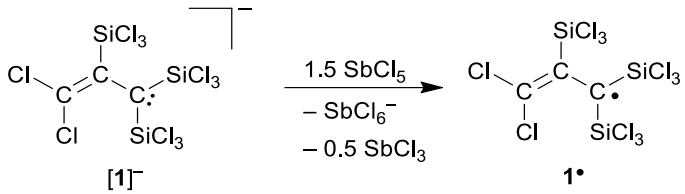

In the glove box, neat Si_2Cl_6 (0.28 mL, 0.44 g, 1.6 mmol) was added dropwise via syringe at room temperature to a Schlenk flask charged with a solution of [*n*Bu$_4$N]Cl (0.111 g, 0.399 mmol) and C_3Cl_6 (0.098 g, 0.394 mmol) in CH_2Cl_2 (3.0 mL). After stirring for 1 h at room temperature, all volatiles were removed under reduced pressure. The residue was re-dissolved in CH_2Cl_2 (2.0 mL) and a substoichiometric amount of $SbCl_5$ (0.118 g, 0.395 mmol) in CH_2Cl_2 (0.5 mL) was added via syringe with stirring at room temperature (unconsumed [**1**]$^-$ is easy to remove from **1**•). The color of the reaction mixture changed immediately from dark brown to dark blue. After further stirring for 5 min, *n*-hexane (20 mL) was added, whereupon a beige solid precipitated. The precipitate was removed by filtration and all volatiles were removed from the clear blue filtrate under reduced pressure to obtain a blue oily residue. The radical **1**• was isolated from this oil as an intensely blue-colored, waxy solid by distillation/sublimation (10^{-3} mbar, oil bath: 90 °C). Yield: 0.104 g (0.204 mmol, 78% with respect to $SbCl_5$, assuming that 1.5 eq of $SbCl_5$ are consumed to generate 1 eq of **1**•). **1**• was examined by EPR spectroscopy. Details regarding the preparation of an EPR sample of **1**• are given below.

Note: Attempts at the oxidation of [**1**]$^-$ with various other oxidizing agents either yielded only traces of **1**•, or showed no reaction, or resulted in complete decomposition of [**1**]$^-$.

Table S1. Screening of suitable oxidizing agents for the oxidation of [**1**]$^-$.

Oxidizing agents	**Outcome**
$FeCl_3$, $CuCl_2$	Negligible amount of **1**• is formed; the majority of [**1**]$^-$ remains untouched
$K_3[Fe(CN)_6]$, $[FeCp_2][TsO]$, $(Cl_3Si)_2C=C(SiCl_3)_2$[S1]	No reaction occurs
$Pb(OAc)_4$, Cl_2, DDQ, $Ag[NO_3]$, $[NO][BF_4]$	Complete decomposition of [**1**]$^-$

Reaction of 1• with 1,4-cyclohexadiene.

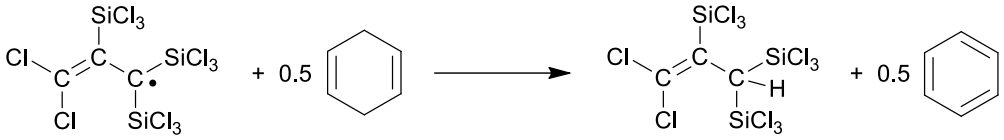

1• **2**

In the glove box, an NMR tube was charged with **1•** (0.020 g, 0.039 mmol) and CD_2Cl_2 (0.5 mL). The tube was flame-sealed under vacuum. An NMR-spectroscopic investigation of the intensely blue-colored solution showed only the (slightly broadened) signals of CD_2Cl_2 and traces of **2** as a contaminant. The tube was opened inside the glove box and its content was transferred to a new NMR tube, charged with 1,4-cyclohexadiene (0.024 g, 0.300 mmol). The tube was flame-sealed under vacuum. After 6 h, the blue color had vanished, and an NMR-spectroscopic investigation of the slightly beige solution revealed the clean formation of **2** and C_6H_6 in the expected 2:1 ratio.

Note: The common radical scavenger *n*Bu_3SnH proved to be unsuitable due to unwanted reactions between *n*Bu_3SnH and the Cl_3Si moieties of **1•**.

Attempted reaction of 2 with azobis(isobutyronitrile) (AIBN).

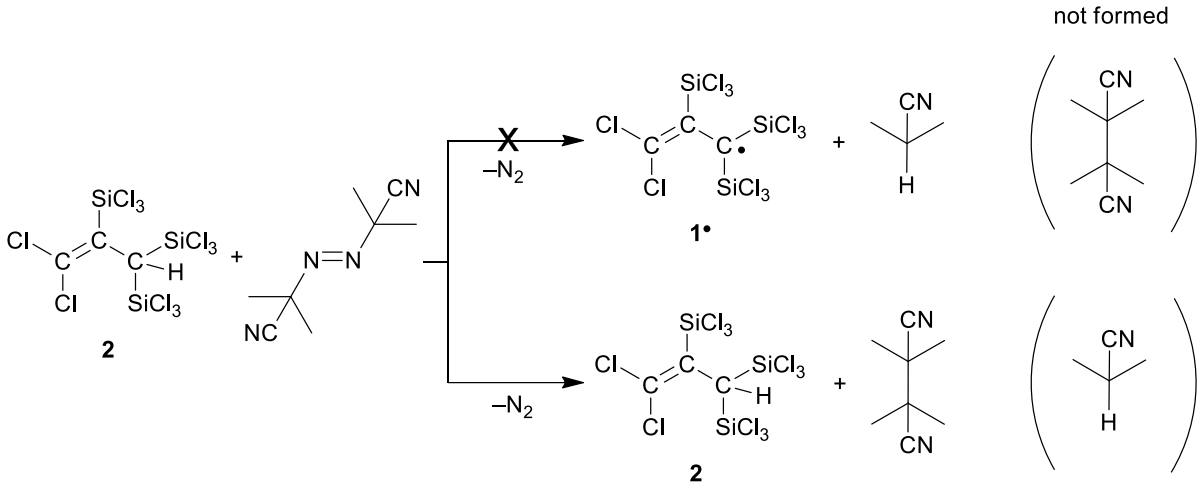

In the glove box, an NMR tube was charged with **2** (0.042 g, 0.082 mmol), AIBN (0.021 g, 0.128 mmol), and C_6D_{12} (0.5 mL). The tube was flame-sealed under vacuum. An NMR-spectroscopic investigation of the colorless solution showed mainly the signals of **2**, while most of the AIBN remained undissolved. The NMR tube was heated to 90 °C for 20 h, whereupon the undissolved AIBN largely vanished. Upon cooling to room temperature, colorless single crystals grew. An NMR-spectroscopic investigation of the colorless solution revealed the formation of 2,2,3,3-tetramethylbutanedinitrile[S19] besides unreacted **2**. The crystals were identified as 2,2,3,3-tetramethylbutanedinitrile by means of X-ray crystallography.[S20]

Synthesis of 2.

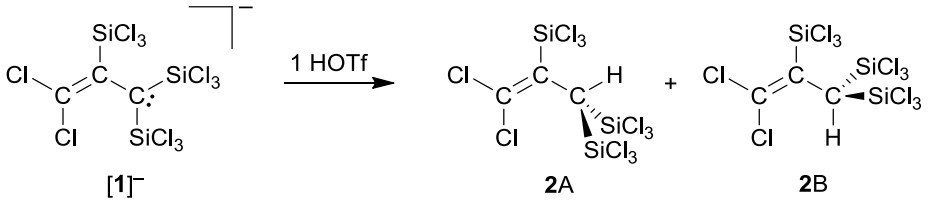

Neat Si_2Cl_6 (5.60 mL, 8.75 g, 32.5 mmol) was added dropwise with stirring at 0 °C to a Schlenk flask containing a solution of [*n*Bu_4N]Cl (2.29 g, 8.24 mmol) and C_3Cl_6 (2.01 g, 8.08 mmol) in CH_2Cl_2 (50 mL). After stirring for 12 h, neat HOTf (1.00 mL, 1.71 g, 11.4 mmol) was added via syringe at room temperature, whereupon the initially red-brown reaction mixture adopted a pale yellow color. After stirring for 6 h at room temperature, all volatiles were removed under reduced pressure. The orange, viscous residue was extracted with *n*-hexane (10 × 3 mL), and the combined extracts were evaporated under reduced pressure to obtain the crude product as a clear yellow liquid. After fractional distillation (89 °C, 10^{-3} mbar) **2** was isolated as a colorless oil, which partly solidified upon standing. Yield: 2.32 g (4.54 mmol, 56%). Conformer ratio **2**A:**2**B ≈ 2:1 (determined by ^{1}H NMR spectroscopy). The conformers **2**A/**2**B were assigned by means of their $^3J_{SiH}$ coupling constants: **2**A (s-*cis*) shows a smaller value than **2**B (s-*trans*).[S7,S8]

Note: In the first reaction step, Si_2Cl_6 can also be added at room temperature, but with a slow drop rate to avoid a fierce reaction. The stirring times can be reduced but should not be less than 1 h.

A:
^{1}H NMR (500.2 MHz, CD_2Cl_2, 298 K): δ = 3.75 ppm (s, $^2J_{HSi}$ = 16.5 Hz, $^3J_{HSi}$ = 11.2 Hz, 1H; C*H*($SiCl_3$)$_2$).

^{13}C{^{1}H} NMR (125.8 MHz, CD_2Cl_2, 298 K): δ = 140.0 (C=*C*$SiCl_3$), 126.7 (Cl_2*C*=C), 41.6 ppm (*C*H($SiCl_3$)$_2$).

^{29}Si NMR (99.4 MHz, CD_2Cl_2, 298 K): δ = –2.2 (d, $^2J_{SiH}$ = 16.5 Hz; CH(*Si*Cl_3)$_2$), –7.9 (d, $^3J_{SiH}$ = 11.2 Hz; C=C*Si*Cl_3).

B:
^{1}H NMR (500.2 MHz, CD_2Cl_2, 298 K): δ = 4.09 (s, $^2J_{HSi} \approx {}^3J_{HSi}$ = 16.7 Hz, 1H; C*H*($SiCl_3$)$_2$).

^{13}C{^{1}H} NMR (125.8 MHz, CD_2Cl_2, 298 K): δ = 140.1 (C=*C*$SiCl_3$), 126.6 (Cl_2*C*=C), 44.6 (*C*H($SiCl_3$)$_2$).

^{29}Si NMR (99.4 MHz, CD_2Cl_2, 298 K): δ = –1.1 (d, $^2J_{SiH}$ = 16.7 Hz; CH(*Si*Cl_3)$_2$, –10.0 ppm (d, $^3J_{SiH}$ = 16.6 Hz; C=C*Si*Cl_3).

EA (%): Found: C, 6.6; H, 0.3. Calc. for $C_3HCl_{11}Si_3$: C, 7.05; H, 0.2%.

GC-MS (EI, method A): **A**: rt = 15.1 min, *m*/*z* = 511.60 ([M$^•$]$^+$); **B**: rt = 15.3 min, *m*/*z* = 511.60 ([M$^•$]$^+$).

Deprotonation of 2 with [*n*Bu$_4$N]$_2$[B].

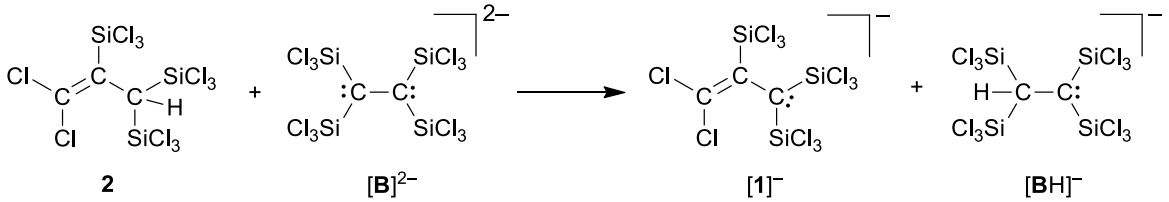

2 [**B**]$^{2–}$ [**1**]$^–$ [**B**H]$^–$

In the glove box, an NMR tube was charged with **2** (0.051 g, 0.100 mmol), [*n*Bu$_4$N]$_2$[**B**] (0.052 g, 0.050 mmol), and CD_2Cl_2 (0.5 mL). The tube was flame-sealed under vacuum. Immediately thereafter, ^{1}H NMR spectroscopy showed little conversion. After keeping the sample at room temperature for 10 d, it was again investigated by NMR spectroscopy, which now revealed the complete conversion of [**B**]$^{2–}$ to [**B**H]$^–$. In turn, some [**1**]$^–$ had formed, but also some starting material **2** was still left. The NMR tube was opened inside the glove box and its content transferred to a new NMR tube, which was additionally charged with [*n*Bu$_4$N]$_2$[**B**] (0.054 g, 0.052 mmol). The tube was flame-sealed under vacuum and stored at room temperature for 24 h. An NMR-spectroscopic investigation showed an increase in the relative intensities of the signals of [**1**]$^–$ and [**B**H]$^–$; nevertheless, residual **2** and [**B**]$^{2–}$ were still detectable. After heating the sample to 50 °C for 19 h, the complete conversion of **2** to [**1**]$^–$ and the corresponding formation of [**B**H]$^–$ was confirmed by NMR spectroscopy.[S1]

Note: Attempts at the deprotonation of **2** with the bulky bases lithium 2,2,6,6-tetramethylpiperidide, Li[(Me$_3$Si)$_3$C], or Li[(Me$_3$Si)CH$_2$] furnished only trace amounts of [**1**]$^–$ and were accompanied by decomposition reactions.

Methylation of [*n*Bu$_4$N][1].

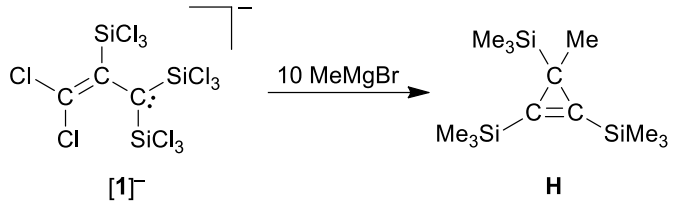

[**1**]$^-$ **H**

In the glove box, neat Si_2Cl_6 (0.115 g, 0.428 mmol) was added via syringe dropwise at room temperature to an NMR tube charged with a solution of [*n*Bu$_4$N]Cl (0.028 g, 0.101 mmol) and C_3Cl_6 (0.023 g, 0.092 mmol) in CH_2Cl_2 (0.5 mL). After the sample had been stored for 2 h at room temperature, it was removed from the glove box and attached to a Schlenk line. All volatiles were removed under reduced pressure. The residue was dissolved in THF (0.2 mL) and a solution of MeMgBr in Et_2O (3 M, 0.40 mL, 1.20 mmol) was added dropwise via syringe. The tube was flame-sealed under vacuum and heated to 60 °C for 21 h. The reaction mixture was subsequently added to a saturated aqueous solution of NH_4Cl (4 mL). The organic layer was separated, and the aqueous layer extracted with Et_2O (3 × 4 mL). The combined organic phases were dried over anhydrous $MgSO_4$, filtered, and all volatiles were removed under reduced pressure. 3-Methyl-1,2,3-tris(trimethylsilyl)cyclopropene (**H**) was obtained as a pale yellow oil. Yield: 0.020 g (0.074 mmol, 80%). ^{1}H and ^{13}C{^{1}H} NMR data of **H** were in accord with values from the literature;[S9] ^{29}Si{^{1}H} NMR data have not been published previously and are now given below.

^{1}H NMR (500.2 MHz, CDCl$_3$, 298 K): δ = 0.93 (s, 3H; C(*Me*)SiMe$_3$), 0.16 (s, 18H; 2 × =C(Si*Me*$_3$)), 0.11 ppm (s, 9H; C(Me)Si*Me*$_3$).

^{13}C{^{1}H} NMR (125.8 MHz, CDCl$_3$, 298 K): δ = 142.0 (=*C*(SiMe$_3$)), 25.2 (C(*Me*)SiMe$_3$), 11.0 (*C*(Me)SiMe$_3$), –0.5 (2 × =C(Si*Me*$_3$)), –1.8 ppm (C(Me)Si*Me*$_3$).[9]

^{29}Si{^{1}H} NMR (99.4 MHz, CDCl$_3$, 298 K): δ = 1.2 (C(Me)*Si*Me$_3$), –9.9 ppm (=C(*Si*Me$_3$)).

GC-MS (EI, method B): rt = 13.2 min, *m*/*z* = 270.10 ([M$^\bullet$]$^+$).

Methylation of 2.

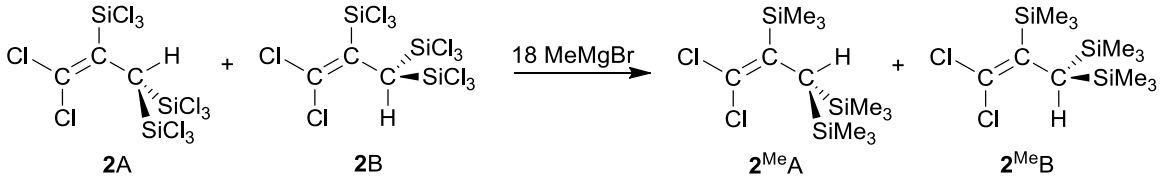

Neat Si_2Cl_6 (4.19 mL, 6.54 g, 24.3 mmol) was added dropwise with stirring at room temperature to a Schlenk flask containing a solution of [*n*Bu_4N]Cl (1.68 g, 6.04 mmol) and C_3Cl_6 (1.50 g, 6.03 mmol) in CH_2Cl_2 (50 mL). After further stirring for 5 h at room temperature, HOTf (0.59 mL, 1.0 g, 6.7 mmol) was added via syringe at room temperature, whereupon the dark red-brown reaction mixture adopted a pale yellow color. After stirring for 12 h, all volatiles were removed under reduced pressure. The orange, viscous residue was extracted with *n*-hexane (5 × 25 mL), and the combined extracts were evaporated under reduced pressure to furnish crude **2**A/**2**B (2.99 g, 5.84 mmol). **2**A/**2**B were dissolved in THF (10 mL) and a solution of MeMgBr in Et_2O (3 M, 24.0 mL, 72.0 mmol) was added with stirring at room temperature. After further stirring for 1.5 h, the reaction mixture was kept at reflux temperature for 1 d. The mixture was cooled to room temperature and added to a saturated aqueous solution of NH_4Cl (150 mL). The organic layer was separated, and the aqueous layer extracted with Et_2O (3 × 100 mL). The combined organic phases were dried over anhydrous $MgSO_4$. After filtration, all volatiles were removed from the filtrate under reduced pressure. The oily crude product was placed on top of a short plug of silica gel and eluted with *c*-hexane. The solvent was removed from the eluate under reduced pressure. $\mathbf{2}^{Me}$ was isolated as a colorless liquid, which partly solidified upon standing. Yield: 1.05 g (3.20 mmol, 53 %). Conformer ratio $\mathbf{2}^{Me}$A: $\mathbf{2}^{Me}$B ≈ 2:1 (determined by ^{1}H NMR spectroscopy).

$\mathbf{2}^{Me}$A:

^{1}H NMR (500.2 MHz, $CDCl_3$, 298 K): δ = 1.42* (s, $^2J_{HSi}$ = 11.1 Hz, $^3J_{HSi}$ = 6.8 Hz, 1H; C*H*($SiMe_3$)$_2$), 0.24* (s, $^2J_{HSi}$ = 6.5 Hz, 9H; C=CSi*Me*$_3$), 0.14 ppm (s, $^2J_{HSi}$ = 6.4 Hz, 18H; CH(Si*Me*$_3$)$_2$).

^{13}C{^{1}H} NMR (125.8 MHz, $CDCl_3$, 298 K): δ = 142.0 (C=*C*$SiMe_3$), 118.7 (Cl_2*C*=C), 27.2 (*C*H($SiMe_3$)$_2$), 1.9 (CH(Si*Me*$_3$)$_2$), –0.1 ppm (C=CSi*Me*$_3$).

^{29}Si{^{1}H} NMR (99.4 MHz, $CDCl_3$, 298 K): δ = 2.3 (CH(*Si*Me_3)$_2$), 1.4 (C=C*Si*Me_3).

$\mathbf{2}^{Me}$B:

^{1}H NMR (500.2 MHz, $CDCl_3$, 298 K): δ = 2.34** (s, $^2J_{HSi}$ = 12.0 Hz, $^3J_{HSi}$ = 10.4 Hz, 1H; C*H*($SiMe_3$)$_2$), 0.32** (s, $^2J_{HSi}$ = 6.6 Hz, 9H; C=CSi*Me*$_3$), 0.12 ppm (s, $^2J_{HSi}$ = 6.4 Hz, 18H; CH(Si*Me*$_3$)$_2$).

^{13}C{^{1}H} NMR (125.8 MHz, $CDCl_3$, 298 K): δ = 140.9 (C=*C*$SiMe_3$), 118.8 (Cl_2*C*=), 30.9 (*C*H($SiMe_3$)$_2$), 1.7 (CH(Si*Me*$_3$)$_2$), 1.4 ppm (C=CSi*Me*$_3$).

^{29}Si{^{1}H} NMR (99.4 MHz, $CDCl_3$, 298 K): δ = 1.3 (CH(*Si*Me_3)$_2$), –1.9 ppm (C=C*Si*Me_3).

Note: The assignment of the individual signal sets to the conformers $\mathbf{2}^{Me}$A/ $\mathbf{2}^{Me}$B is based on the relative values of the $^3J_{SiH}$ coupling constants (see **2**A/**2**B above)[S7,S8] and on selective NOESY experiments. The two signals marked with (*) show a cross-peak in the NOESY spectrum, which is absent in the case of the signals marked with (**).

EA (%): Found: C, 44.19; H, 8.28. Calc. for $C_{12}H_{28}Cl_2Si_3$: C, 44.01; H, 8.62%.

GC-MS (EI, method A): A: rt = 12.8 min, *m*/*z* = 326.05 ($[M^{\bullet}]^+$); **B**: rt = 13.0 min, *m*/*z* = 326.10 ($[M^{\bullet}]^+$).

Methoxylation of [*n*Bu$_4$N][1].

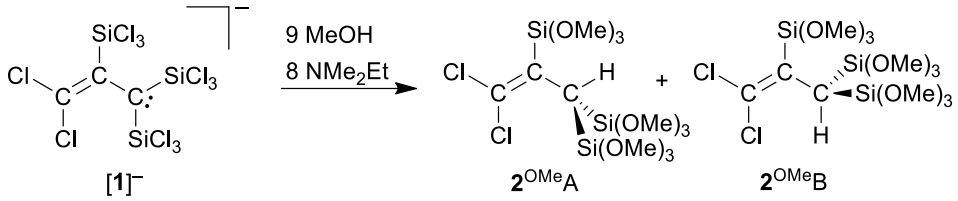

In the glove box, neat Si_2Cl_6 (0.17 mL, 0.27 g, 1.00 mmol) was added dropwise via syringe at room temperature to a small glass vessel charged with a solution of [*n*Bu$_4$N]Cl (0.048 g, 0.172 mmol) and C_3Cl_6 (0.049 g, 0.197 mmol) in CH_2Cl_2 (0.5 mL). After 24 h at room temperature, all volatiles were removed from the reaction mixture under reduced pressure to get rid of $SiCl_4$. The residue was re-dissolved in CH_2Cl_2 (4 mL), and MeOH (0.10 mL, 0.08 g, 2.5 mmol) and NMe_2Et (0.25 mL, 0.17 g, 2.3 mmol) were added simultaneously via two syringes with stirring at room temperature. After stirring had been continued for 3 h, all volatiles were removed under reduced pressure. The residue was extracted with *n*-pentane (1 × 4 mL, 10 × 1 mL). The combined extracts were evaporated under reduced pressure to furnish the conformers **2**^{OMe}A/**2**^{OMe}B in equimolar ratio as a yellow oil (determined by ^{1}H NMR spectroscopy; the sample still contained unknown minor impurities).

A:

^{1}H NMR (500.2 MHz, CD_2Cl_2, 298 K): δ = 3.59* (s, 9H; C=C(Si(O*Me*)$_3$)), 3.56 (s, 18H; CH(Si(O*Me*)$_3$)$_2$), 2.14* ppm (s, $^2J_{HSi}$ = 14.5 Hz, $^3J_{HSi}$ = 8.0 Hz, 1H; C*H*(Si(OMe)$_3$)$_2$).

^{13}C{^{1}H} NMR (125.8 MHz, CD_2Cl_2, 298 K): δ = 129.9 (C=*C*(Si(OMe)$_3$)), 125.2 (Cl_2*C*=C), 51.1 (C=C(Si(O*Me*)$_3$)), 51.1 (CH(Si(O*Me*)$_3$)$_2$), 17.9 ppm (*C*H(Si(OMe)$_3$)$_2$).

^{29}Si{^{1}H} NMR (99.4 MHz, CD_2Cl_2, 298 K): δ = –51.5 (CH(*Si*(OMe)$_3$)$_2$), –60.7† ppm (C=C(*Si*(OMe)$_3$)).

†This signal was only detectable in the ^{Si,H}HMBC-spectrum.

B:

^{1}H NMR (500.2 MHz, CD_2Cl_2, 298 K): δ = 3.59** (s, 9H; C=C(Si(*Me*O)$_3$)) 3.56 (s, 18H; CH(Si(*Me*O)$_3$)$_2$), 2.21** ppm (s, $^2J_{HSi}$ = 13.9 Hz, $^3J_{HSi}$ = 10.8 Hz, 1H; C*H*(Si(MeO)$_3$)$_2$).

^{13}C{^{1}H} NMR (125.8 MHz, CD_2Cl_2, 298 K): δ = 130.8 (C=*C*(Si(OMe)$_3$)), 123.4 (Cl_2*C*=C), 51.1 (C=C(Si(O*Me*)$_3$)), 51.1 (CH(Si(*Me*O)$_3$)$_2$), 21.9 ppm (*C*H(Si(MeO)$_3$)$_2$).

^{29}Si{^{1}H} NMR (99.4 MHz, CD_2Cl_2, 298 K): δ = –51.7 (CH(*Si*(MeO)$_3$)$_2$), –61.5 ppm (C=C(*Si*(OMe)$_3$)).

The assignment of the individual signal sets to the conformers **2**^{OMe}A/**2**^{OMe}B is based on selective NOESY experiments. The two signals marked with (*) show a cross-peak in the NOESY spectrum, which is absent in the case of the signals marked with (**).

GC-MS (EI, method C): rt = 20.8 min, *m*/*z* = 438.95 ([M–OMe]$^+$); rt = 21.0 min, *m*/*z* = 438.95 ([M–OMe]$^+$). An unambiguous assignment of structures **2**^{OMe}A/**2**^{OMe}B to the GC signals was not possible.

Synthesis of 2^{OMe}A/2^{OMe}B through methoxylation of 2.

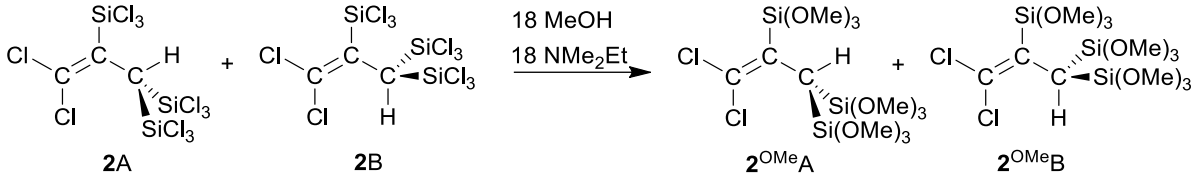

MeOH (0.16 mL, 0.13 g, 4.1 mmol) and NMe_2Et (0.42 mL, 0.28 g, 3.8 mmol) were added simultaneously via two syringes with stirring at 0 °C to **2**A/**2**B (0.201 g, 0.393 mmol) in CH_2Cl_2 (8 mL). Stirring was continued for 5 min at 0 °C and 2.5 h at room temperature. After removal of all volatiles under reduced pressure, the solid residue was extracted with *n*-hexane (8 × 1 mL). The combined extracts were evaporated to dryness under reduced pressure to afford $\mathbf{2}^{OMe}$A/$\mathbf{2}^{OMe}$B as a colorless gelatinous mass. Yield: 0.153 g (0.324 mmol, 82%). Conformer ratio $\mathbf{2}^{OMe}$A:$\mathbf{2}^{OMe}$B ≈ 1:1 (determined by ^{1}H NMR spectroscopy).

See above for characterization details of $\mathbf{2}^{OMe}$. *Note*: The methoxylation of **2** was much more selective than the direct methoxylation of [**1**]$^-$, which greatly facilitates the isolation of $\mathbf{2}^{OMe}$.

Reaction of [*n*Bu$_4$N][1] with eth. HCl.

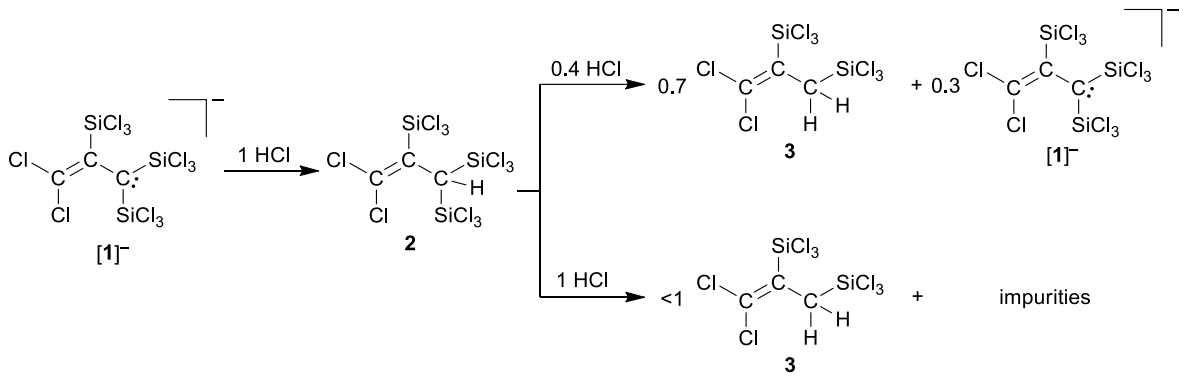

Neat Si_2Cl_6 (2.21 mL, 3.45 g, 12.8 mmol) was added dropwise with stirring at room temperature to a Schlenk flask containing a solution of [*n*Bu$_4$N]Cl (0.895 g, 3.22 mmol) and C_3Cl_6 (0.46 mL, 0.81 g, 3.26 mmol) in CH_2Cl_2 (40 mL). After stirring for 12 h, a solution of HCl in Et_2O (2 M, 2.25 mL, 4.50 mmol) was added with stirring at room temperature, whereupon the initially red-brown reaction mixture adopted an orange color. NMR-spectroscopic control at this point revealed the quantitative consumption of [**1**]$^-$ and the concomitant formation of **2** with negligible side products. To achieve further protodesilylation, the reaction mixture was transferred to a glass ampoule. The ampoule was flame-sealed under vacuum and placed into an explosion-proof metal container. The container was put in an oven and heated to 60 °C for 19 h. After cooling to room temperature again, the ampoule was opened inside a glove box and its content was transferred to a Schlenk flask. All volatiles were removed from the dark brown reaction solution under reduced pressure (the presence of $SiCl_4$ in the condensate and of [**1**]$^-$ in the residue was confirmed by NMR spectroscopy). The brown viscous residue was extracted with *n*-hexane (1 × 40 mL, 4 × 10 mL) and the combined clear yellow extracts were evaporated under reduced pressure to furnish the crude product as an orange oil. After distillation (10^{-3} mbar, bp: 45 °C), **3** was obtained as a colorless liquid, which still contained traces of an unknown impurity. Yield: 0.347 g (0.918 mmol, 41%, with respect to HCl and assuming that 2 eq of HCl are consumed to generate 1 eq **3**).

Note: The use of more than 1.4 eq of HCl leads to a significantly less selective reaction, even though the balanced equation requires 2 eq of HCl; the addition of catalytic amounts of [*n*Bu$_4$N]Cl did not improve the situation. The byproduct [**1**]$^-$ in the first case is easier to remove from **3** than the unknown side products in the second case.

^{1}H NMR (500.2 MHz, CD_2Cl_2, 298 K): δ = 3.00 ppm (s, $^2J_{HSi}$ = 12.6 Hz, $^3J_{HSi}$ = 10.4 Hz, 2H; $CH_2(SiCl_3)$).

^{13}C{^{1}H} NMR (125.8 MHz, CD_2Cl_2, 298 K): δ = 136.8 (C=CSiCl$_3$), 126.4 (Cl_2C=C), 32.2 ppm (CH_2(SiCl$_3$)).

^{29}Si NMR (99.4 MHz, CD_2Cl_2, 298 K): δ = –4.2 (t, $^2J_{SiH}$ = 12.6 Hz; $CH_2(SiCl_3)$), –8.1 ppm (t, $^3J_{SiH}$ = 10.4 Hz; =CSiCl$_3$).

GC-MS (EI, method B): rt = 18.9 min, *m*/*z* = 377.70 ([M$^•$]$^+$).

Reactivity of 2 toward [*n*Bu$_4$N]Cl and relative acidities of 2 and 3.

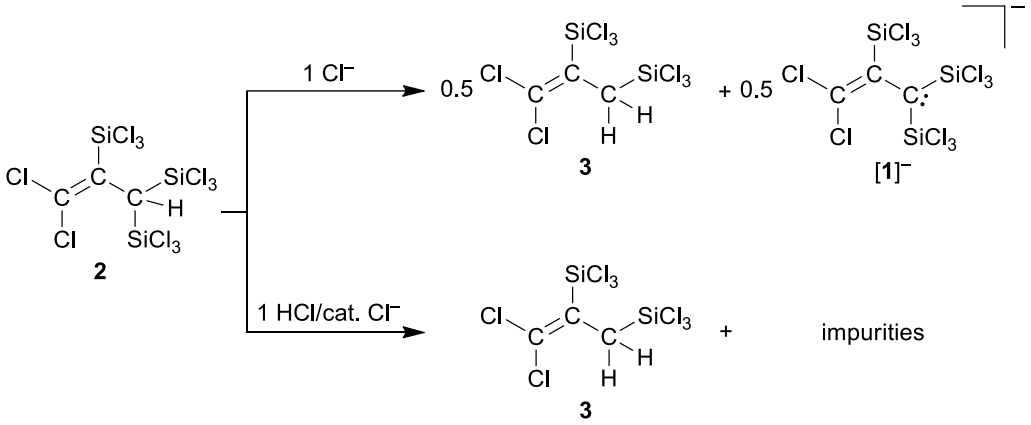

In the glove box, an NMR tube was charged with **2** (0.053 g, 0.104 mmol), [*n*Bu$_4$N]Cl (0.030 g, 0.108 mmol), and CD_2Cl_2 (0.5 mL). The tube was flame-sealed under vacuum. According to NMR spectroscopy, the slightly yellow solution still contained mainly the starting material **2** and only a small amount of **3**. The tube was heated at 60 °C for 3 d, whereupon the solution turned dark brown. An NMR-spectroscopic investigation of the sample revealed the conversion of **2** to a mixture of **3** and [*n*Bu$_4$N][**1**] (plus the formation of the byproduct $SiCl_4$).

See above for characterization details of **3** and [*n*Bu$_4$N][**1**].

Reaction of 2^{Me} with 1 eq *t*-BuLi.

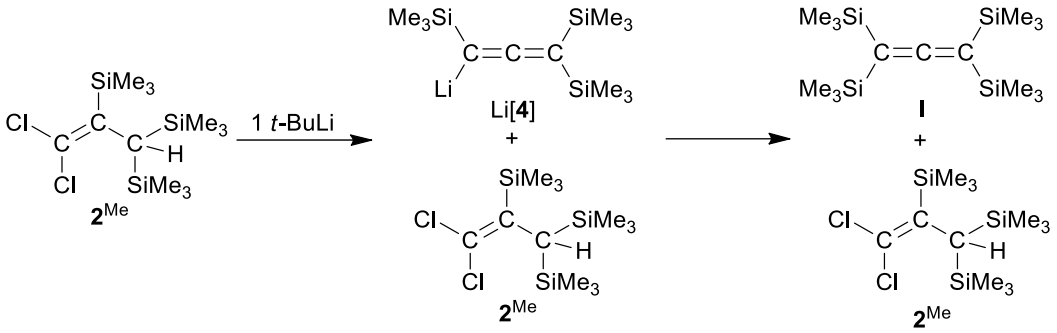

An NMR tube was charged with $\mathbf{2}^{Me}$ (0.065 g, 0.198 mmol) and THF (0.4 mL). A solution of *t*-BuLi in *n*-pentane (1.6 M, 0.12 mL, 0.19 mmol) was added dropwise via syringe at room temperature, whereupon the clear colorless solution adopted a dark brown color. The tube was flame-sealed under vacuum. An NMR-spectroscopic investigation revealed the formation of tetrakis(trimethylsilyl)allene (**G**) and the presence of unconsumed starting material $\mathbf{2}^{Me}$, whereas Li[**4**] (see below) was not detected in the reaction mixture. The sample was stored for 7 d at room temperature, the NMR tube was carefully opened, and the reaction mixture added to a saturated aqueous solution of NH_4Cl (4 mL). The organic layer was separated, and the aqueous layer extracted with Et_2O (3 × 5 mL). The combined organic phases were dried over anhydrous $MgSO_4$, filtered, and the solvent was removed from the filtrate under reduced pressure. The yellow oily residue was identified as a mixture of unconsumed $\mathbf{2}^{Me}$ and $\mathbf{I}^{S10}$ (ratio $\mathbf{2}^{Me}$:**I** ≈ 1:0.5; determined by ^{1}H NMR spectroscopy).

See above for characterization details of $\mathbf{2}^{Me}$ and below for those of **I**.

Reaction of 2^{Me} with 2 eq *t*-BuLi.

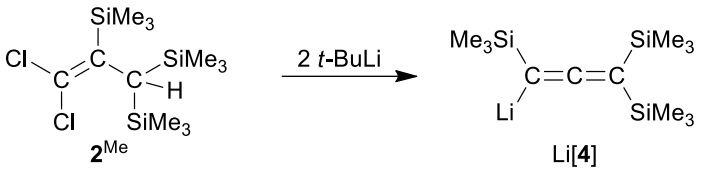

$\mathbf{2}^{Me}$ Li[**4**]

An NMR tube was charged with $\mathbf{2}^{Me}$ (0.028 g, 0.085 mmol) and THF (0.4 mL). A solution of *t*-BuLi in *n*-pentane (1.6 M, 0.12 mL, 0.19 mmol) was added dropwise via syringe at room temperature, whereupon the clear colorless solution adopted a dark brown color. The tube was flame-sealed under vacuum. An NMR-spectroscopic investigation revealed the quantitative consumption of $\mathbf{2}^{Me}$ and the formation of the known tris(trimethylsilyl)allenyllithium (Li[**4**]),[S10] together with the by-products *t*-BuCl,[S11] *iso*-butane,[S11] and *iso*-butene.[S12]

^{1}H NMR (500.2 MHz, THF, 298 K): δ = –0.09 (C=C(Si*Me*$_3$)$_2$), –0.10 ppm ((*Me*$_3$Si)LiC=C).

^{13}C{^{1}H} NMR (125.8 MHz, THF, 298 K): δ = 175.7 (C=*C*=C), 69.6 (C=*C*(SiMe$_3$)$_2$), 27.9 ((Me$_3$Si)Li*C*=C), 2.2 ((*Me*$_3$Si)LiC=C), 2.0 ppm (C=C(Si*Me*$_3$)$_2$).

^{29}Si{^{1}H} NMR (99.4 MHz, THF, 298 K): δ = –6.8 (C=C(*Si*Me$_3$)$_2$), –14.1 ppm ((Me$_3$*Si*)LiC=C).

Note: THF cleavage by *t*-BuLi occurs as a side reaction.[S13,S14] The lithium enolate of acetaldehyde[S15] and ethene[S2] were detected as the cleavage products in the NMR spectra of the reaction solution. The lithium enolate also reacted with MeI, Me$_3$SiCl, or Me$_3$SnCl in subsequent derivatization reactions of Li[**4**], but the corresponding products could easily be removed during purification.

Reaction of *in situ* generated Li[4] with 2^{Me}.

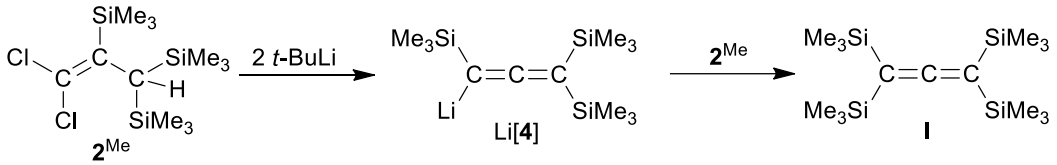

An NMR tube was charged with $\mathbf{2}^{Me}$ (0.030 g, 0.092 mmol) and THF (0.4 mL). A solution of *t*-BuLi in *n*-pentane (2.3 M, 0.10 mL, 0.23 mmol) was added dropwise via syringe at room temperature, whereupon the clear colorless solution adopted a dark brown color. The tube was flame-sealed under vacuum. An NMR-spectroscopic investigation revealed the consumption of $\mathbf{2}^{Me}$ and the formation of Li[**4**] (together with the above mentioned by-products/side products). The NMR tube was opened inside the glove box and its content was transferred into a new NMR tube charged with $\mathbf{2}^{Me}$ (0.031 g, 0.095 mmol). The tube was flame-sealed under vacuum and the $^{13}C\{^{1}H\}$ NMR spectrum of the remaining brown solution showed the signals of both Li[**4**] and $\mathbf{2}^{Me}$. After the sample had been stored for 5 d at room temperature an NMR-spectroscopic investigation revealed complete consumption of Li[**4**] and formation of **I**, as well as remaining $\mathbf{2}^{Me}$.

See above for characterization details of $\mathbf{2}^{Me}$ and below for those of **I**.

Reaction of *in situ* generated Li[4] with Me_3SiCl.

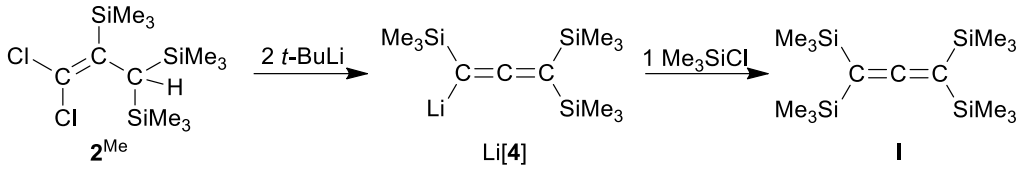

An NMR tube was charged with **2**^{Me} (0.026 g, 0.079 mmol) and THF (0.4 mL). A solution of *t*-BuLi in *n*-pentane (1.6 M, 0.15 mL, 0.24 mmol) was added dropwise via syringe at room temperature, whereupon the clear colorless solution adopted a dark brown color. The tube was flame-sealed under vacuum. An NMR-spectroscopic investigation revealed the quantitative consumption of **2**^{Me} and the formation of Li[**4**] (together with the above mentioned by-products/side products). The NMR tube was opened inside the glove box, its content was transferred into a new NMR tube, and Me_3SiCl (0.063 g, 0.580 mmol) was added. The solution immediately turned yellow and a colorless precipitate was formed. The tube was flame-sealed under vacuum and the $^{13}C\{^1H\}$ NMR spectrum revealed the complete consumption of Li[**4**]. The tube was carefully opened, and the reaction mixture was added to a saturated aqueous solution of NH_4Cl (4 mL). The organic layer was separated, and the aqueous layer extracted with Et_2O (3 × 4 mL). The combined organic phases were dried over anhydrous $MgSO_4$, filtered, and all volatiles were removed from the filtrate under reduced pressure. The yellow oily residue was identified as **I**. NMR-spectroscopic data and IR data were in accord with values from the literature.[S10,16]

^{1}H NMR (300.0 MHz, $CDCl_3$, 298 K): δ = 0.10 ppm (s, 38H; 4 × Si*Me*$_3$).

$^{13}C\{^1H\}$ NMR (75.5 MHz, $CDCl_3$, 298 K): δ = 204.0 (C=*C*=C), 64.4 (C=*C*(SiMe$_3$)$_2$), 0.8 ppm (C=C(Si*Me*$_3$)$_2$).

$^{29}Si\{^1H\}$ NMR (59.6 MHz, $CDCl_3$, 298 K): δ = –4.0 ppm (C=C(*Si*Me$_3$)$_2$).

GC-MS (EI, method B): rt = 17.1 min, *m*/*z* = 328.15 ([M$^{\bullet}$]$^+$).

IR (ATR, neat): ν = 2954.4 (w), 2898.5 (w), 1877.4 (s, C=C=C), 1794.4 (w), 1401.0 (w), 1246.8 (s, SiMe$_3$), 1045.2 (w), 897.7 (m), 830.2 (s), 757.9 (m), 687.5 (m), 638.3 (m), 619.0 (m), 540.0 (m), 513.0 cm^{-1} (m).

Reaction of *in situ* generated Li[4] with MeI.

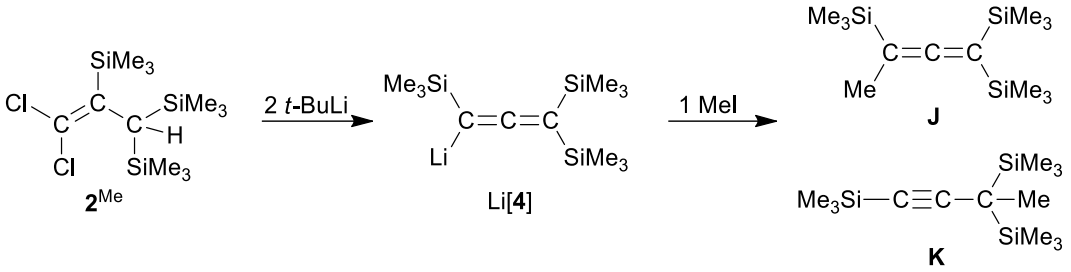

An NMR tube was charged with $\mathbf{2}^{Me}$ (0.062 g, 0.189 mmol) and THF (0.4 mL). A solution of *t*-BuLi in *n*-pentane (1.6 M, 0.35 mL, 0.56 mmol) was added dropwise at room temperature, whereupon the clear colorless solution adopted a dark brown color. The tube was flame-sealed under vacuum. An NMR-spectroscopic investigation revealed the quantitative consumption of $\mathbf{2}^{Me}$ and the formation of Li[**4**] (together with the above-mentioned by-products/side products). The NMR tube was opened inside the glove box, its content was transferred to a new NMR tube, and MeI (0.136 g, 0.958 mmol) was added. The solution immediately turned yellow. The tube was flame-sealed under vacuum and the $^{13}C\{^1H\}$ NMR spectrum revealed the quantitative consumption of Li[**4**]. The tube was carefully opened, and the reaction mixture was added to a saturated aqueous solution of NH_4Cl (4 mL). The organic layer was separated, and the aqueous layer extracted with Et_2O (3 × 4 mL). The combined organic phases were dried over anhydrous $MgSO_4$, filtered, and all volatiles were removed from the filtrate under reduced pressure. The orange-colored oily residue was identified by NMR spectroscopy and GC-MS measurements as a mixture of 1,1,3-tris(trimethylsilyl)-1,2-butadiene (**J**)[S10] and 1,3,3-tris(trimethylsilyl)-1-butyne (**K**;[S10] ratio **J**:**K** ≈1.2:1, determined by ^1H NMR spectroscopy). Traces of **I**[S10] were also present as side product. NMR-spectroscopic data were in accord with values from the literature.[S10,S17]

J:

^{1}H NMR (300.0 MHz, $CDCl_3$, 298 K): δ = 1.58 (s, 3H; $(Me_3Si)\mathit{Me}C{=}C$), 0.09 (s, 18H; $C{=}C(Si\mathit{Me}_3)_2$), 0.05 (s, 9H; $(\mathit{Me}_3Si)MeC{=}C$).

$^{13}C\{^1H\}$ NMR (75.5 MHz, $CDCl_3$, 298 K): δ = 208.0 ($C{=}\mathit{C}{=}C$), 77.8 ($C{=}\mathit{C}(SiMe_3)_2$), 70.9 ($(Me_3Si)Me\mathit{C}{=}C$), 13.5 ($(Me_3Si)\mathit{Me}C{=}C$), 0.6 ($C{=}C(Si\mathit{Me}_3)_2$), –1.5 ppm ($(\mathit{Me}_3Si)MeC{=}C$).

$^{29}Si\{^1H\}$ NMR (59.6 MHz, $CDCl_3$, 298 K): δ = –3.5 ($(Me_3\mathit{Si})MeC{=}C$), –3.9 ppm ($=C(\mathit{Si}Me_3)_2$).

K:

^{1}H NMR (300.0 MHz, $CDCl_3$, 298 K): δ = 1.18 (s, 3H; $C–C\mathit{Me}(SiMe_3)_2$), 0.11 (s, 9H; $(\mathit{Me}_3Si)C{\equiv}C$), 0.09 (s, 18H; $–CMe(Si\mathit{Me}_3)_2$).

$^{13}C\{^1H\}$ NMR (75.5 MHz, $CDCl_3$, 298 K): δ = 114.0 ($C{\equiv}\mathit{C}–C$), 82.9 ($(Me_3Si)\mathit{C}{\equiv}\mathit{C}$), 17.2 ($C–C\mathit{Me}(SiMe_3)_2$), 11.2 ($C–\mathit{C}Me(SiMe_3)_2$), 0.7 ($(\mathit{Me}_3Si)C{\equiv}C$), –2.1 ppm ($C–CMe(Si\mathit{Me}_3)_2$).

$^{29}Si\{^1H\}$ NMR (59.6 MHz, $CDCl_3$, 298 K): δ = 6.6 ($C–CMe(\mathit{Si}Me_3)_2$), –20.4 ppm ($(Me_3\mathit{Si})C{\equiv}C$).

GC-MS (EI, method B): rt = 13.8 min, *m*/*z* = 270.10 ($[M^\bullet]^+$; **J**); rt = 14.1 min, *m*/*z* = 270.10 ($[M^\bullet]^+$; **K**); rt = 17.1 min, *m*/*z* = 328.15 ($[M^\bullet]^+$; **I**).

Synthesis of 5 through the reaction of *in situ* generated Li[4] with Me_3SnCl.

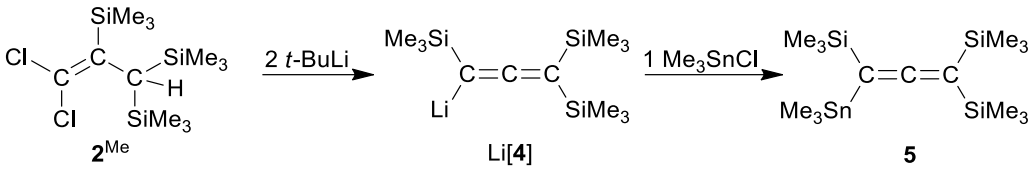

A Schlenk flask was charged with **2**^{Me} (0.205 g, 0.626 mmol) and THF (5 mL). A solution of *t*-BuLi in *n*-pentane (2.3 M, 0.67 mL, 1.54 mmol) was added dropwise via syringe with stirring at room temperature, whereupon the reaction mixture adopted a dark brown color. After stirring for 1 h, a solution of Me_3SnCl in THF (0.5 M, 3.10 mL, 1.55 mmol) was added via syringe to give a clear yellow solution. After further stirring for 1 h at room temperature, all volatiles were removed under reduced pressure. The dark yellow residue was extracted with *n*-hexane (1 × 5 mL, 3 × 3 mL). The combined clear yellow extracts were evaporated under reduced pressure to furnish the crude product as a yellow oil. After distillation (10^{-3} mbar, oil bath: 80 °C) 1,3,3-tris(trimethylsilyl)-1-trimethylstannylallene (**5**) was obtained as a colorless oil. Yield: 0.184 g (0.439 mmol, 70%).

^{1}H NMR (500.2 MHz, $CDCl_3$, 298 K): δ = 0.19 (s, 9H; (Sn*Me*$_3$)(Si)C=C), 0.08 (s, 18H; C=C(*Si*Me_3)$_2$), 0.07 ppm (s, 9H; (Si*Me*$_3$)(Sn)C=C).

^{13}C{^{1}H} NMR (125.8 MHz, $CDCl_3$, 298 K): δ = 200.3 (C=*C*=C), 60.4 (C=*C*(SiMe$_3$)$_2$), 60.2 ((SiMe$_3$)(SnMe$_3$)*C*=C), 0.8 (=C(Si*Me*$_3$)$_2$), 0.7 ((Si*Me*$_3$)(SnMe$_3$)C=C), –7.9 ppm ((SiMe$_3$)(Sn*Me*$_3$)C=C).

^{29}Si{^{1}H} NMR (99.4 MHz, $CDCl_3$, 298 K): δ = –3.8 ((*Si*Me$_3$)(SnMe$_3$)C=C), –4.1 ppm (C=C(*Si*Me$_3$)$_2$).

^{119}Sn{^{1}H} NMR (186.5 MHz, $CDCl_3$, 298 K): δ = 1.5 ppm ((SiMe$_3$)(*Sn*Me$_3$)C=C).

GC-MS (EI, method B): rt = 18.5 min, *m*/*z* = 420.05 ([M$^{\bullet}$]$^+$).

IR (ATR, neat): *v* = 2953.5 (w, CH), 2896.6 (w, CH), 1868.7 (s, C=C=C), 1814.7 (w), 1400.1 (w), 1259.3 (m), 1245.8 (s, SiMe$_3$), 909.3 (m), 831.2 (s), 756.9 (s), 686.5 (m), 636.4 (m), 620.0 (m), 526.5 (m), 508.2 (m), 482.1 (m).

Note: **5** can be handled in ambient atmosphere but should be stored under inert conditions due to slow decomposition in ambient atmosphere.

Reaction of [*n*Bu$_4$N][1] with AlCl$_3$.

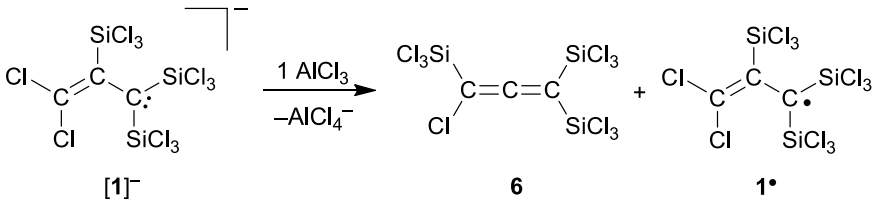

[**1**]$^-$ **6** **1**$^\bullet$

Neat Si_2Cl_6 (2.80 mL, 4.37 g, 16.3 mmol) was added dropwise with stirring at room temperature to a Schlenk flask containing a solution of [*n*Bu$_4$N]Cl (1.121 g, 4.03 mmol) and C_3Cl_6 (1.003 g, 4.03 mmol) in CH_2Cl_2 (50 mL). After further stirring for 1 h, all volatiles were removed under reduced pressure. The brown residue was re-dissolved in CH_2Cl_2 (20 mL) and neat $AlCl_3$ (0.536 g, 4.02 mmol) was added with stirring at room temperature. The reaction mixture was stirred for 12 h, whereupon it adopted a dark green color (the formation of $[AlCl_4]^-$ was confirmed by ^{27}Al NMR spectroscopy[S18]). *n*-Hexane (100 mL) was added and an off-white solid precipitated. After removal of the precipitate by filtration, the solvent was evaporated from the clear green filtrate to obtain the crude product mixture **6**/**1**$^\bullet$ as a dark green oil. Subsequent distillation (10^{-3} mbar, 70 °C) gave an intensely blue-colored liquid (yield: 0.772 g). The resonances of **6** were detectable in the ^{13}C{^{1}H} and ^{29}Si{^{1}H} NMR spectra, despite the presence of the radical **1**$^\bullet$, which was, in turn, detected by EPR spectroscopy.

See below for the NMR data of an authentic sample of **6**.

*Determination of the ratio **6**:**1**$^\bullet$ in the product mixture:* In the glove box, an NMR tube was charged with an aliquot of the above-mentioned blue liquid (0.061 g), 1,4-cyclohexadiene (0.043 g, 0.537 mmol), and CD_2Cl_2 (0.5 mL). The tube was flame-sealed under vacuum. After 2 h at room temperature, the blue color of the solution had completely vanished and, in addition to the NMR signals of **6**, the resonances of **2** and C_6H_6 had appeared. The NMR tube was opened inside the glove box and the reaction mixture was transferred to a new NMR tube. All volatiles were removed under reduced pressure. The colorless residue was dissolved in Et_2O (0.3 mL) and a solution of MeMgBr in Et_2O (3 M, 0.52 mL, 1.6 mmol) was slowly added via syringe at room temperature, whereupon the solution adopted a yellow color and a colorless solid precipitated. The tube was flame-sealed under vacuum and heated to 60 °C for 14 h. After cooling to room temperature, the NMR tube was carefully opened, and the reaction mixture was added to a saturated aqueous solution of NH_4Cl (4 mL). The organic layer was separated, and the aqueous layer extracted with Et_2O (3 × 4 mL). The combined organic phases were dried over anhydrous $MgSO_4$, filtered, and the solvent was removed from the filtrate under reduced pressure. NMR-spectroscopic investigation of the remaining pale yellow oil confirmed the complete conversion of **6** and **2** to the corresponding Me-substituted species 1,1,3-tris(trimethylsilyl)-3-chloroallene (**6**^{Me}) and **2**^{Me} (ratio **6**^{Me}:**2**^{Me} ≈ 4:1, as determined by ^{1}H NMR spectroscopy).

6^{Me}:

^{1}H NMR (500.2 MHz, $CDCl_3$, 298 K): δ = 0.16 (s, 18H; C=C(SiMe_3)$_2$), 0.15 ppm (s, 9H; (Me_3Si)ClC=C).

^{13}C{^{1}H} NMR (125.8 MHz, $CDCl_3$, 298 K): δ = 207.4 (C=*C*=C), 95.8 (C=*C*(SiMe$_3$)$_2$), 87.4 ((Me$_3$Si)Cl*C*=C), 0.1 ((Me_3Si)ClC=C), –1.8 ppm (C=C(SiMe_3)$_2$).

^{29}Si{^{1}H} NMR (99.4 MHz, $CDCl_3$, 298 K): δ = –2.1 ((Me$_3$*Si*)ClC=C), –2.9 ppm (C=C(*Si*Me$_3$)$_2$).

GC-MS (EI, method D): rt = 11.9 min, *m*/z = 290.10 ([M$^{\bullet}$]$^{+}$).

See above for characterization details of **2**^{Me}.

Synthesis of 6.

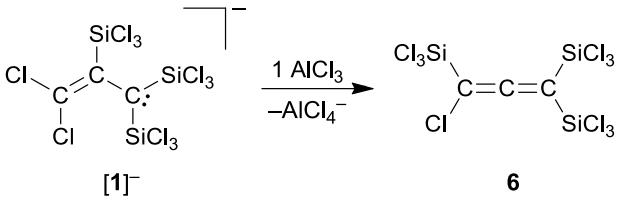

[**1**]$^-$ **6**

Neat Si_2Cl_6 (4.19 mL, 6.54 g, 24.3 mmol) was added dropwise with stirring at room temperature to a Schlenk flask containing a solution of [*n*Bu_4N]Cl (1.68 g, 6.04 mmol) and C_3Cl_6 (1.50 g, 6.03 mmol) in CH_2Cl_2 (50 mL). After further stirring for 3 h, all volatiles were removed under reduced pressure. The brown residue was re-dissolved in CH_2Cl_2 (50 mL) and neat $AlCl_3$ (1.00 g, 7.50 mmol) was added with stirring at room temperature. The reaction mixture was stirred for 12 h, whereupon the initially red-brown mixture adopted a dark green color. *n*-Hexane (150 mL) was added and an off-white solid precipitated. After removal of the precipitate by filtration, the solvent was evaporated from the clear green filtrate to obtain the crude product mixture **6**/**1**$^\bullet$ as a dark green oil. The oil was dissolved in *n*-pentane (2.5 mL) and 1,4-cyclohexadiene (0.770 g, 9.61 mmol) was added via syringe. After stirring for 6 h at room temperature, the green color had vanished and a clear, light brown solution had formed. After removal of all volatiles under reduced pressure, **6** and **2** were separated from each other by distillation. **6** was isolated as a colorless liquid (10 mmHg, bp: 85 °C). Yield: 0.685 g (1.44 mmol, 24%).

^{13}C{^{1}H} NMR (125.8 MHz, CD_2Cl_2, 298 K): δ = 216.7 (C=*C*=C), 98.1 (*C*=C=*), 92.7 ppm (*C*=C=*).

*An unambiguous assignment of the two terminal C atoms was not possible.

^{29}Si{^{1}H} NMR (99.4 MHz, CD_2Cl_2, 298 K): δ = –10.9 ((Cl_3*Si*)ClC=C), –11.2 ppm (C=C(*Si*Cl_3)$_2$).

GC-MS (EI, method D): rt = 16.6 min, *m*/*z* = 473.60 ([M$^\bullet$]$^+$).

IR (ATR, neat): ν = 1928.5 (s, C=C=C), 1262.2 (m), 909.3 (s), 644.1 (s), 600.7 (s), 550.6 (m), 535.2 (m), 512.0 (s), 477.3 (w), 455.1 (s), 446.4 (s), 419.4 cm^{-1} (w).

2. Plots of ^{1}H, $^{13}C\{^{1}H\}$, and ^{29}Si NMR spectra

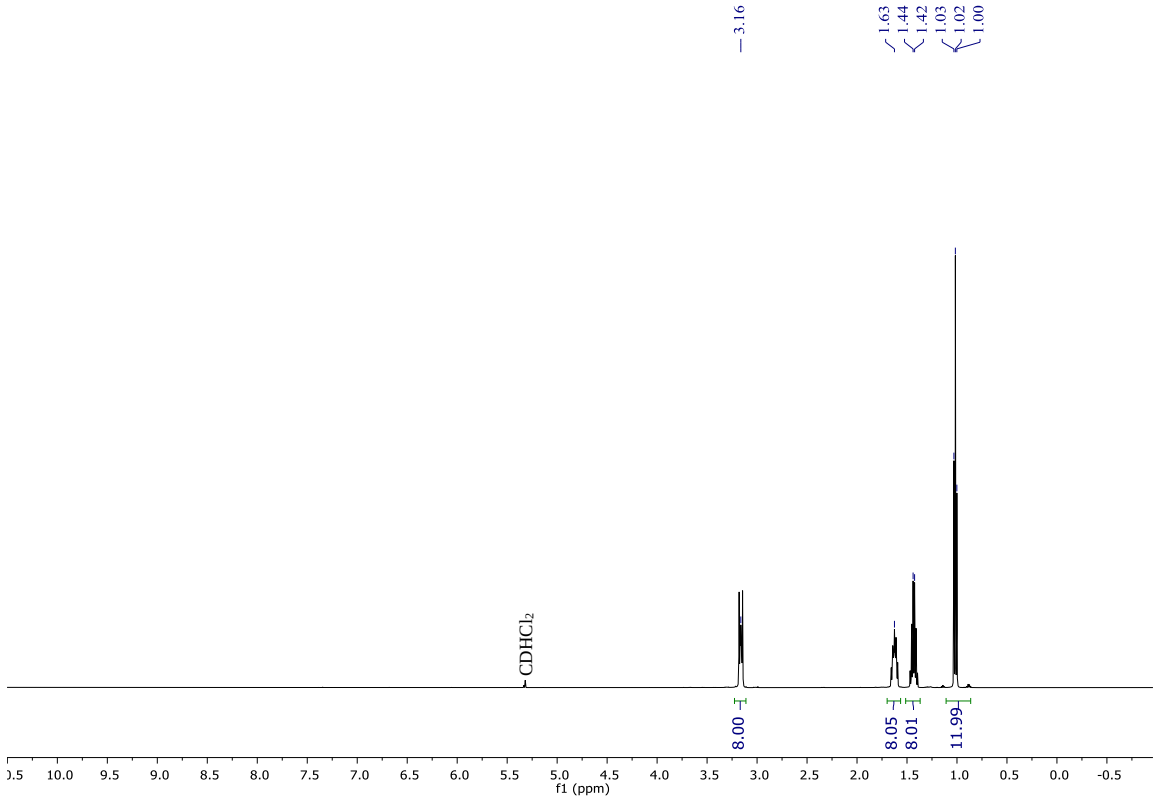

Figure S1: ^{1}H NMR spectrum of [*n*Bu$_4$N][**1**] (CD_2Cl_2, 500.2 MHz).

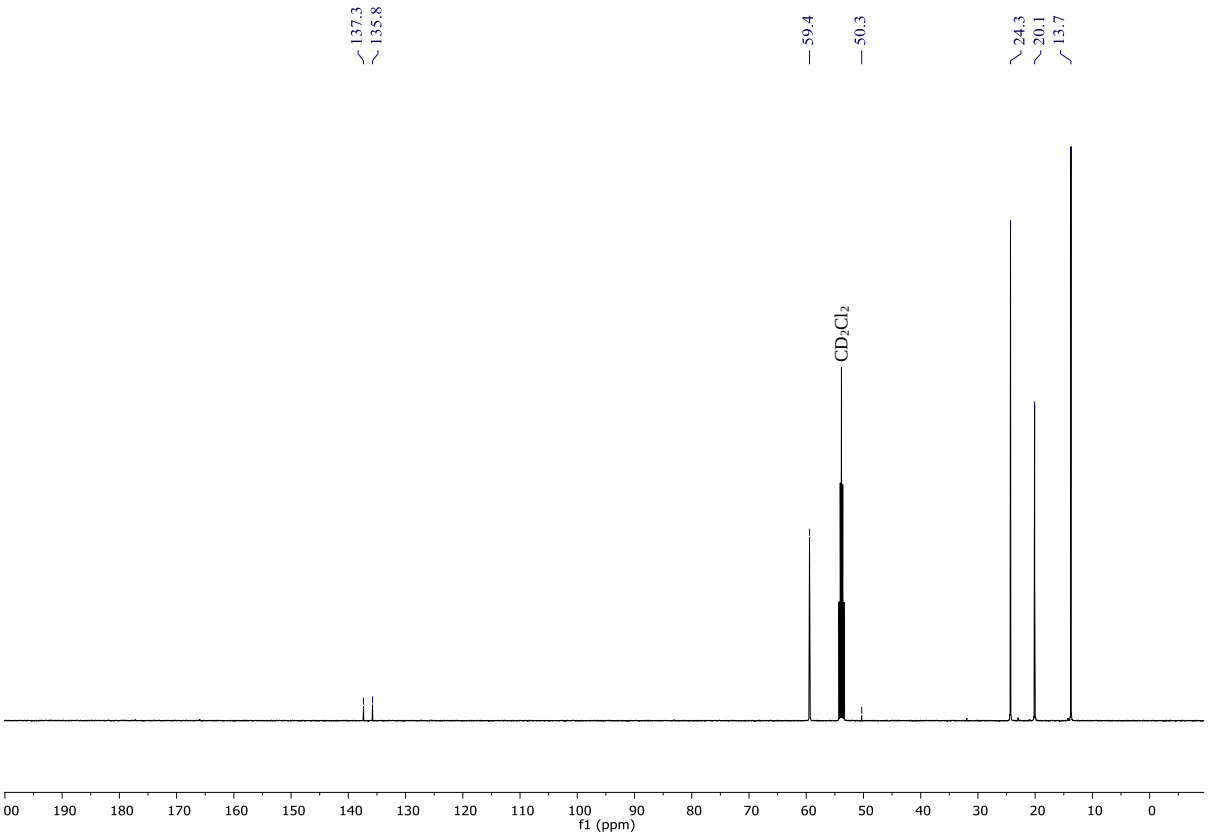

Figure S2: $^{13}C\{^{1}H\}$ NMR spectrum of [*n*Bu$_4$N][**1**] (CD_2Cl_2, 125.8 MHz).

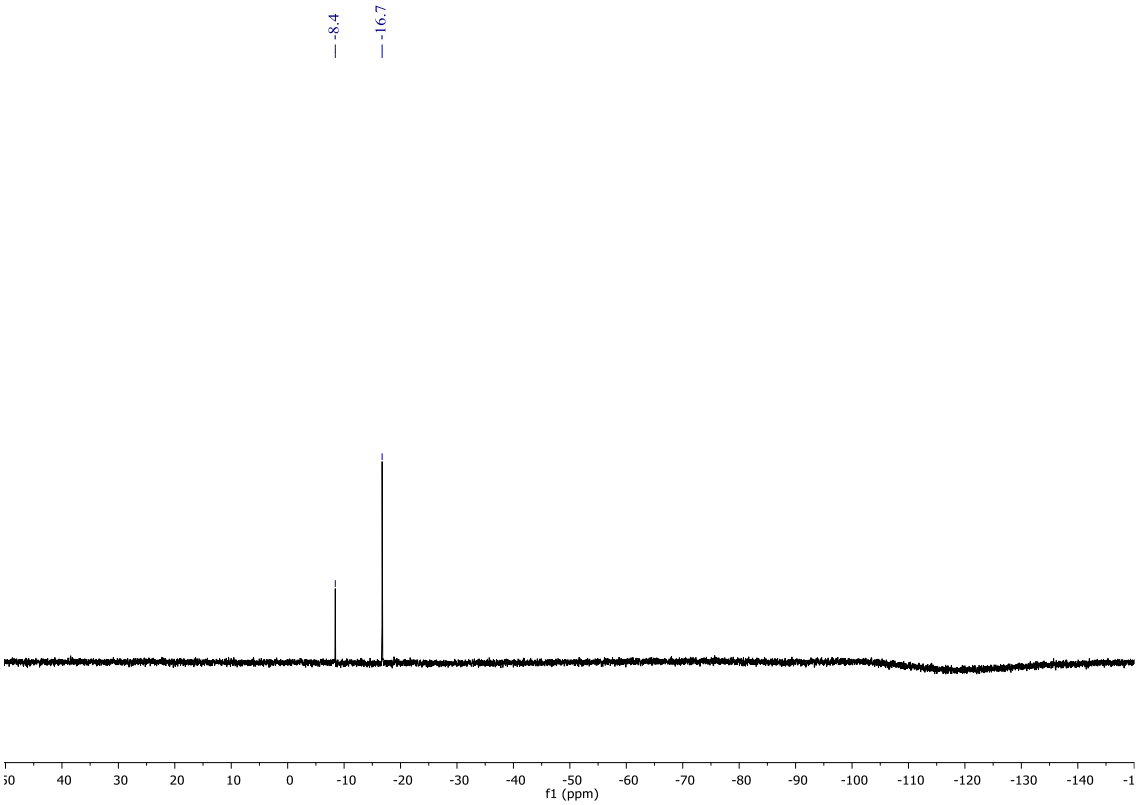

Figure S3: $^{29}Si\{^{1}H\}$ NMR spectrum of [*n*Bu$_4$N][**1**] (CD_2Cl_2, 99.4 MHz).

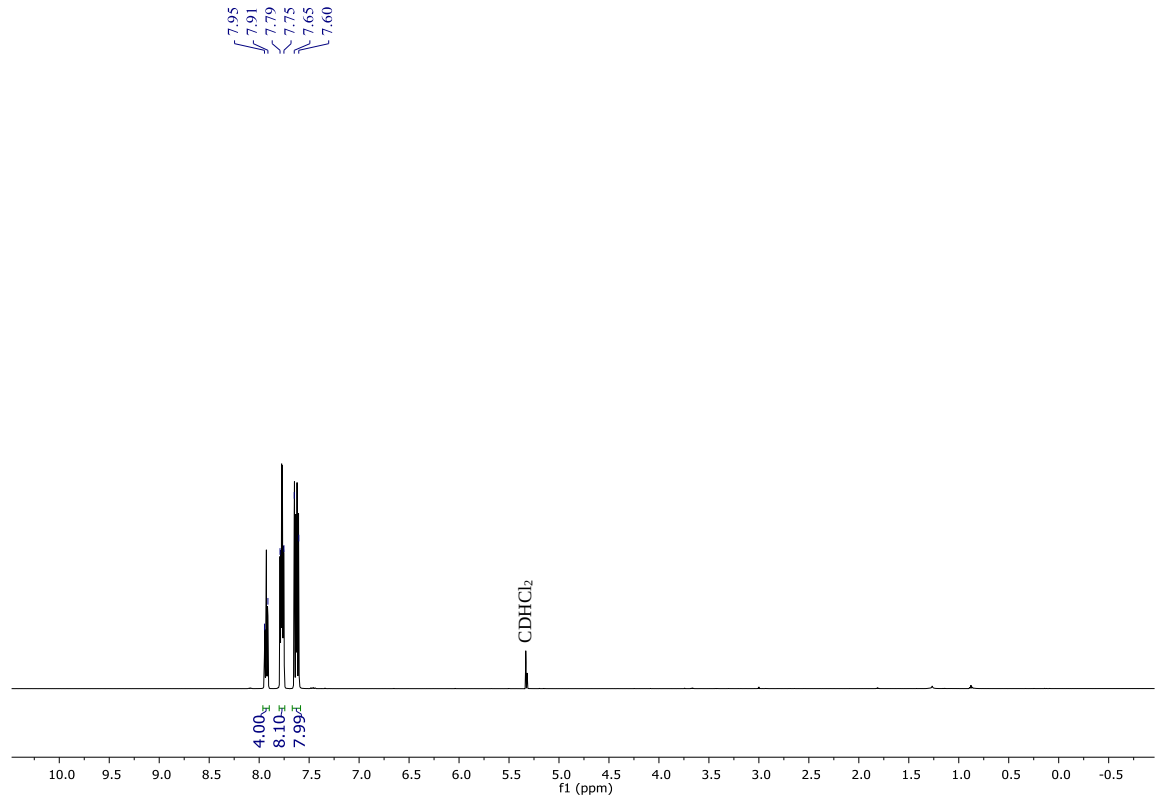

Figure S4: ^{1}H NMR spectrum of [Ph$_4$P][**1**] (CD_2Cl_2, 500.2 MHz).

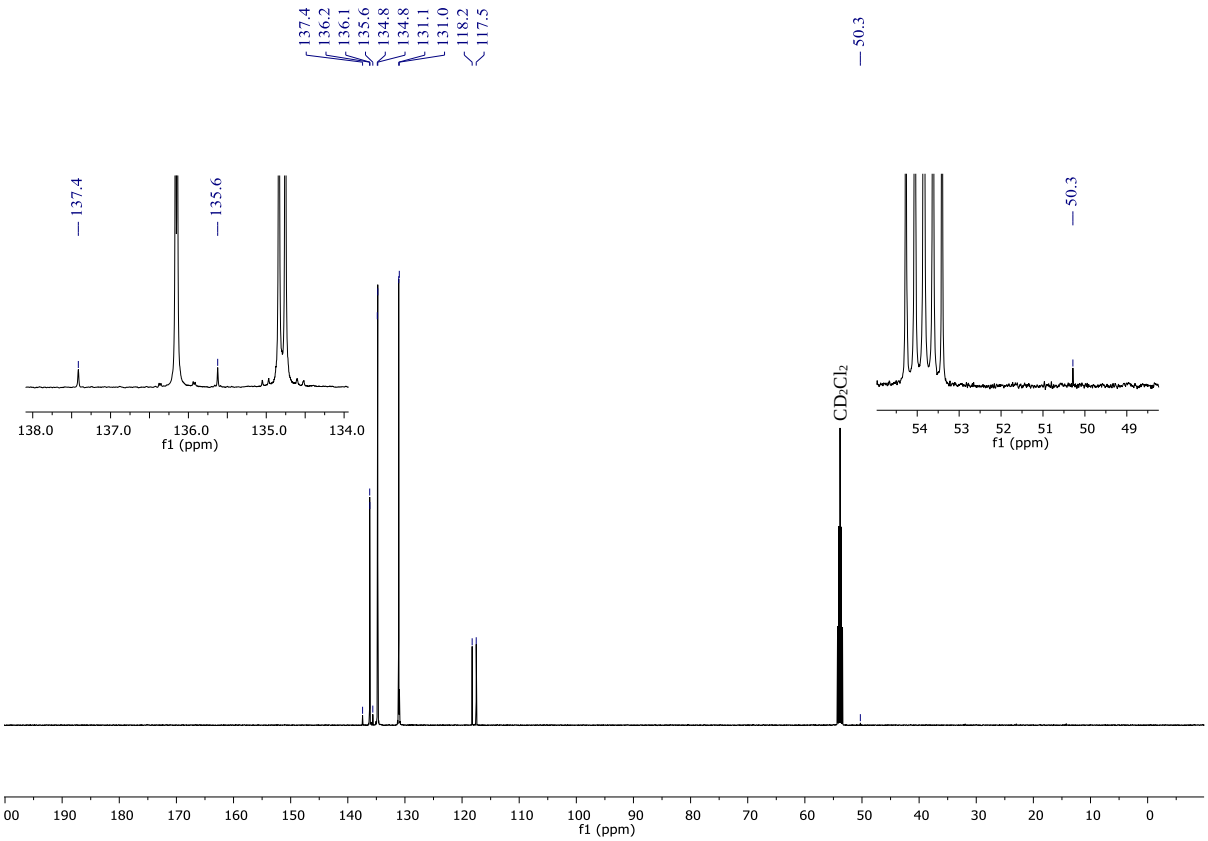

Figure S5: $^{13}C\{^{1}H\}$ NMR spectrum of [Ph_4P][**1**] (CD_2Cl_2, 125.8 MHz).

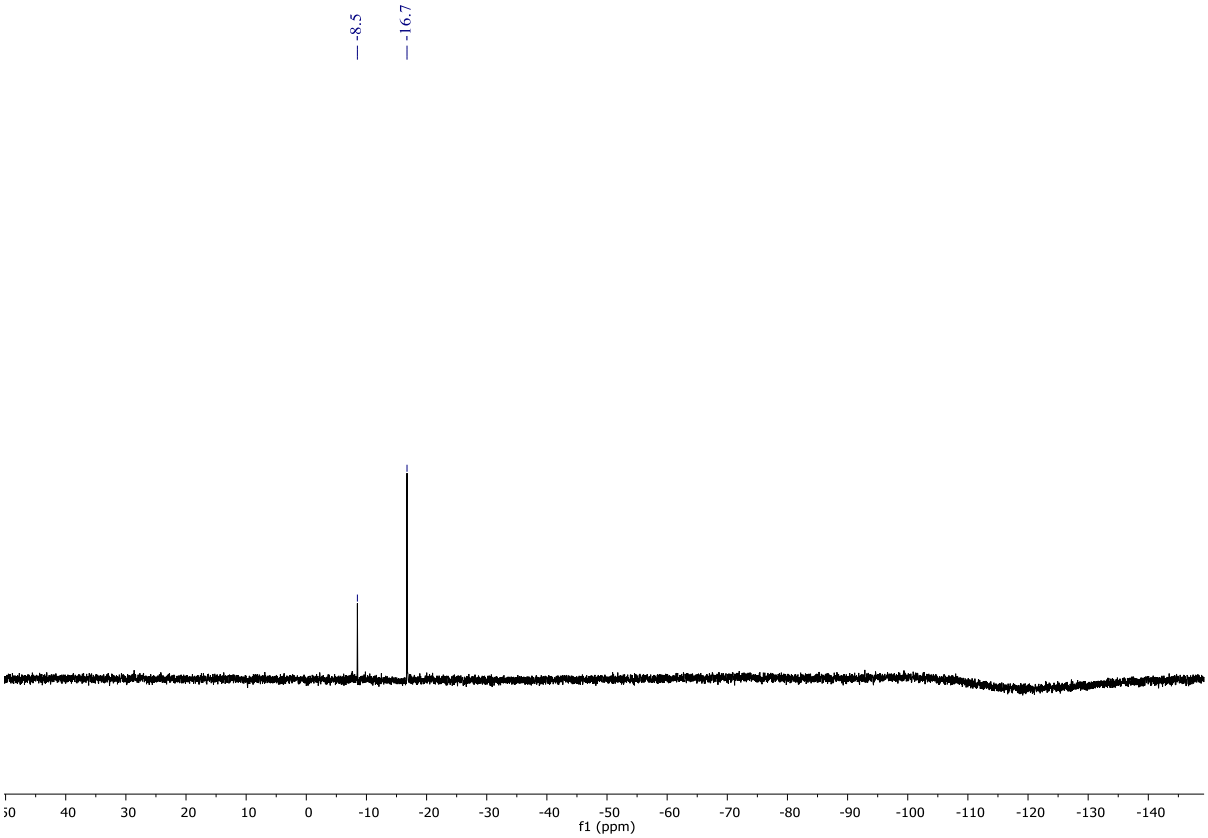

Figure S6: $^{29}Si\{^{1}H\}$ NMR spectrum of [Ph_4P][**1**] (CD_2Cl_2, 99.4 MHz).

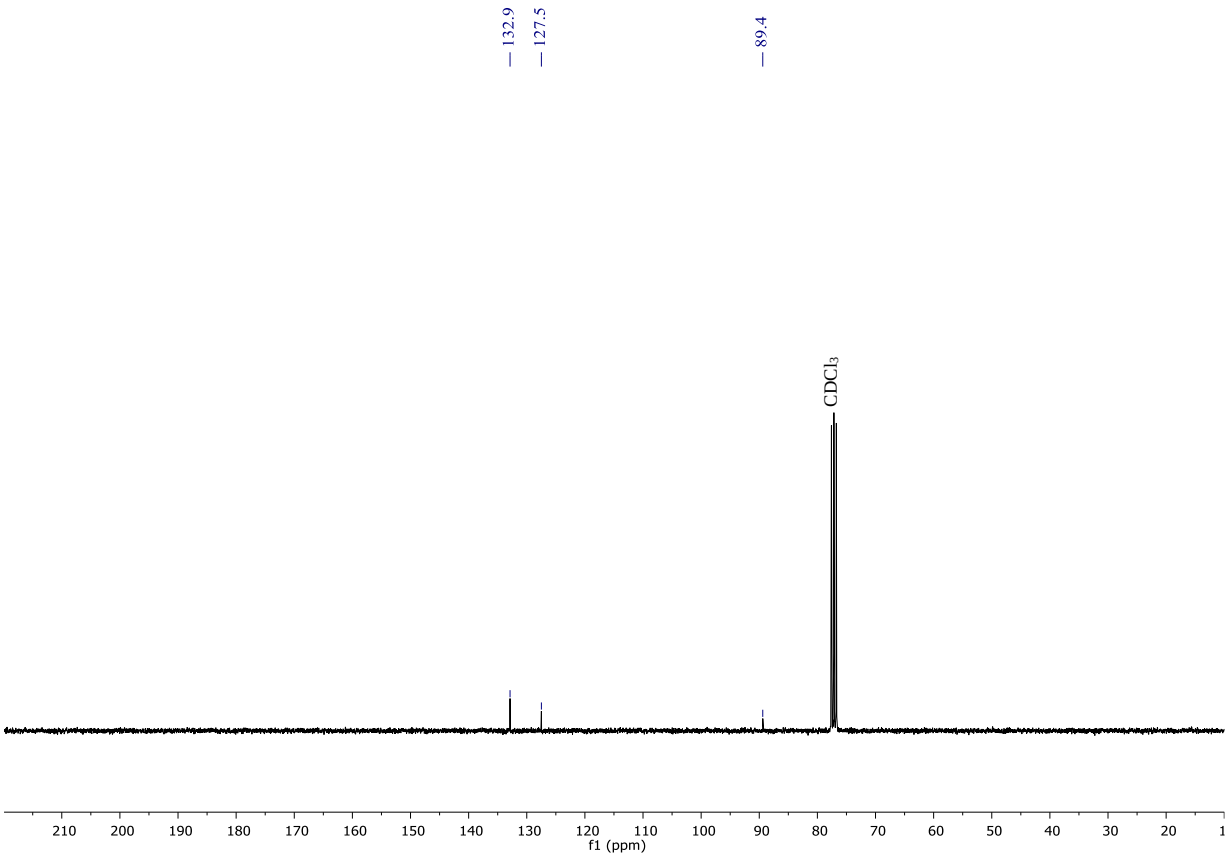

Figure S7: $^{13}C\{^{1}H\}$ NMR spectrum of **G** ($CDCl_3$, 75.5 MHz).

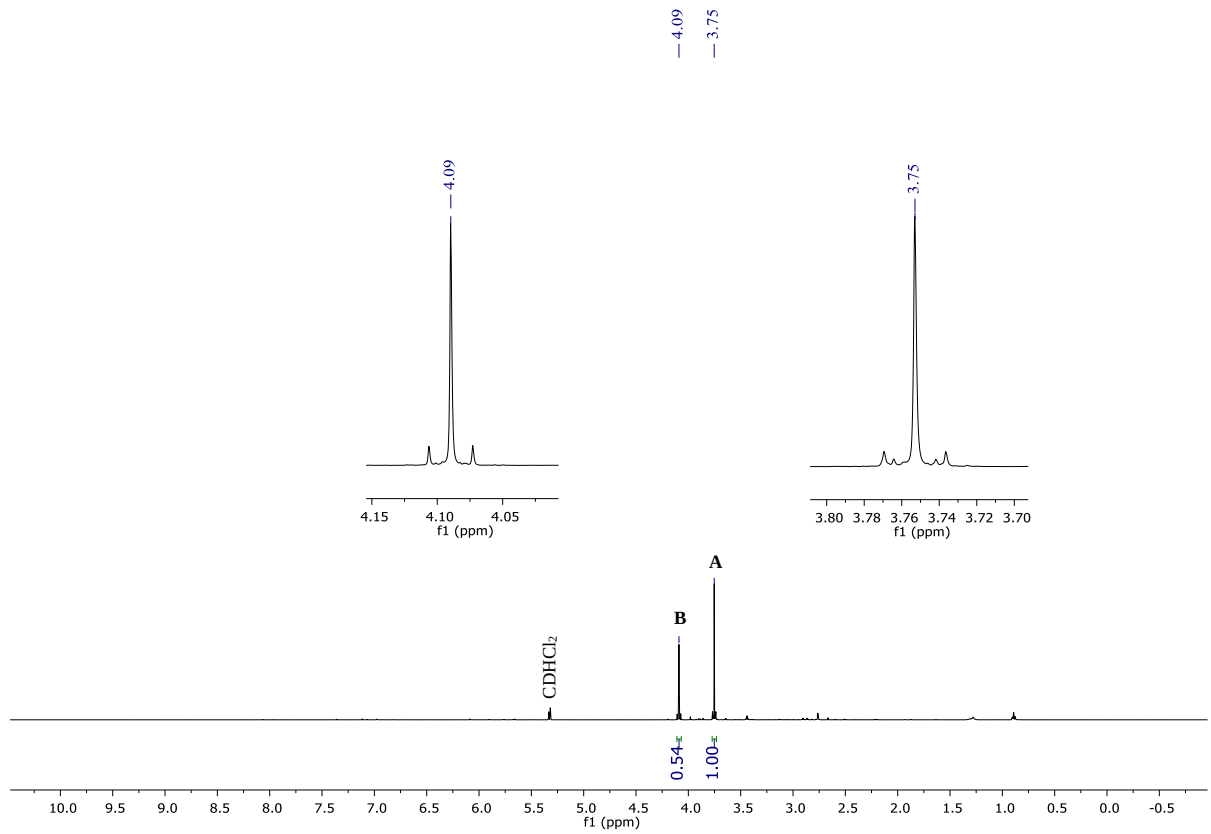

Figure S8: ^{1}H NMR spectrum of **2** (**2**A: **A**; **2**B: **B**) (CD_2Cl_2, 500.2 MHz).

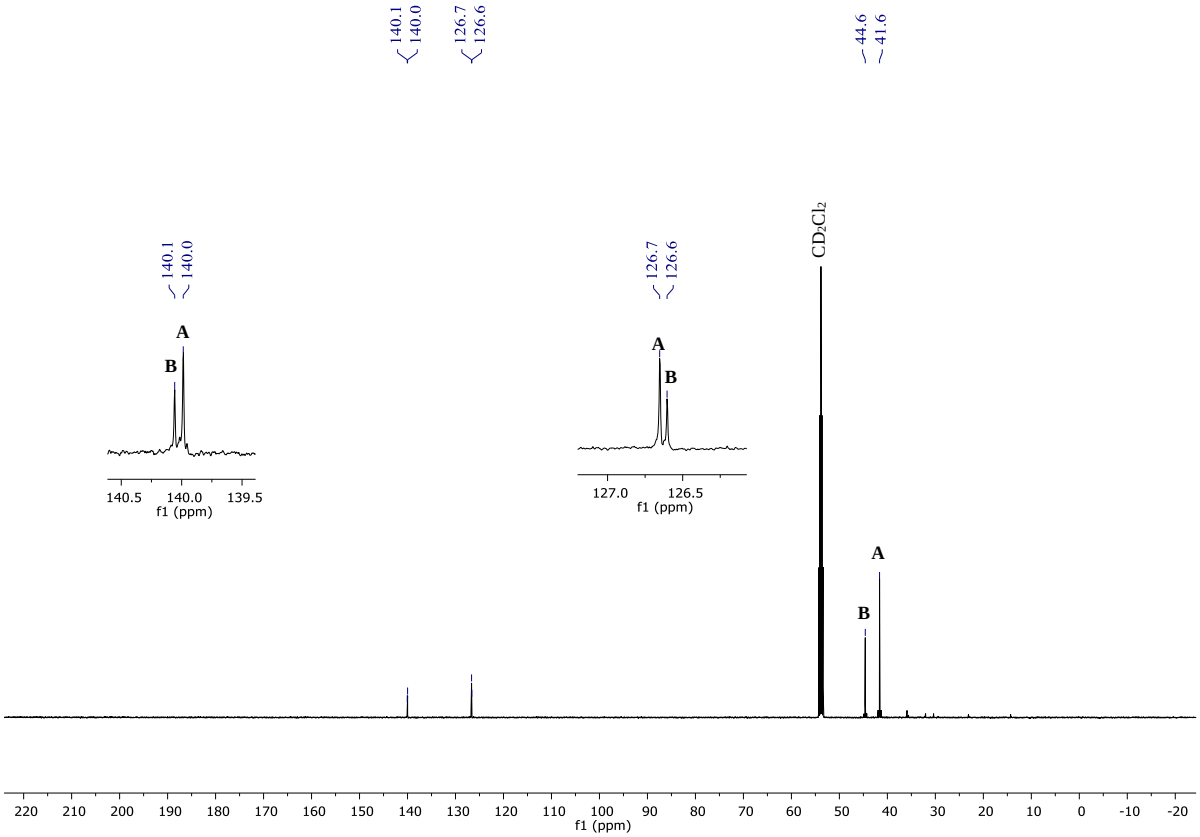

Figure S9: $^{13}C\{^{1}H\}$ NMR spectrum of **2** (**2**A: **A**; **2**B: **B**) (CD_2Cl_2, 125.8 MHz).

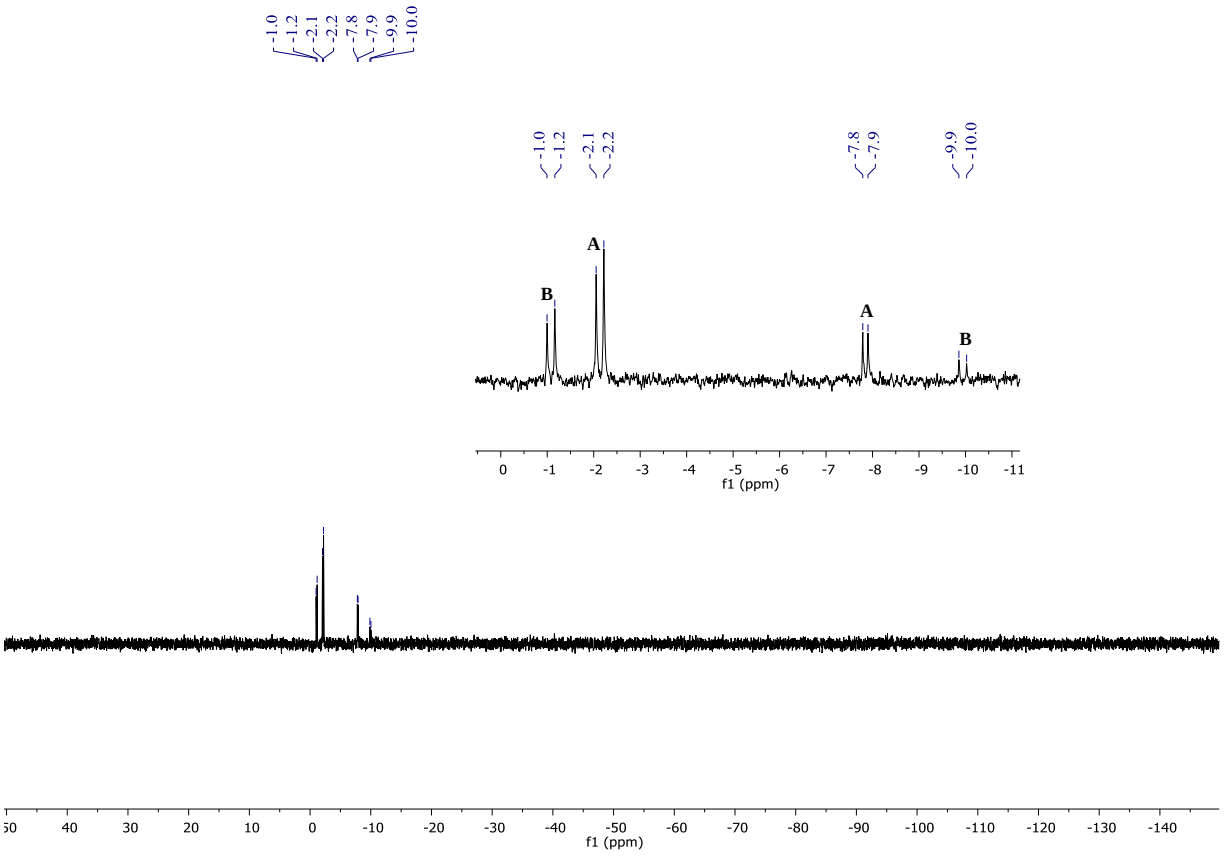

Figure S10: ^{29}Si NMR spectrum of **2** (**2**A: **A**; **2**B: **B**) (CD_2Cl_2, 99.4 MHz).

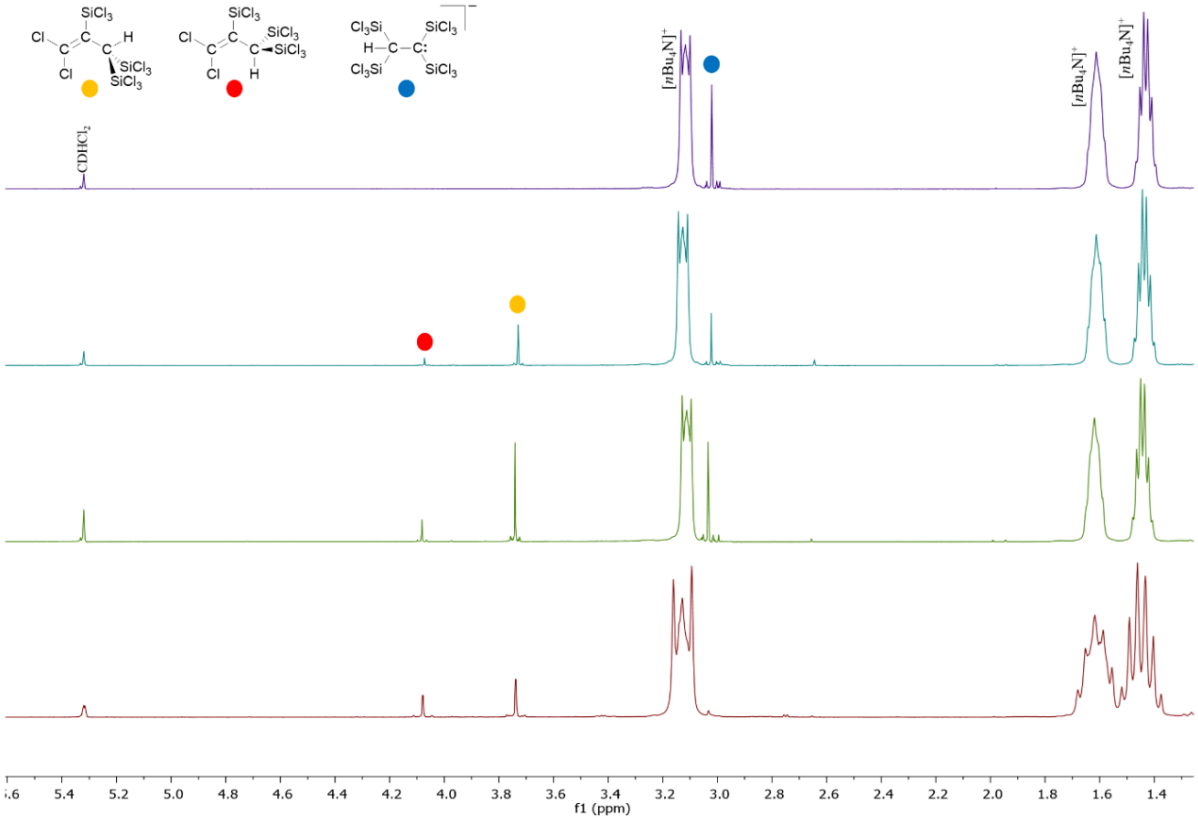

Figure S11: ^{1}H NMR spectra on the reaction mixture of **2** and 0.5 eq of [*n*Bu$_4$N]$_2$[**B**] in CD_2Cl_2 from below: directly after mixing the compounds (red, 250 MHz), after 10 d at room temperature (green, 500 MHz), after addition of another 0.5 eq of [*n*Bu$_4$N]$_2$[**B**] (blue, 500 MHz) and after heating to 50 °C for 19 h (purple, 500 MHz).

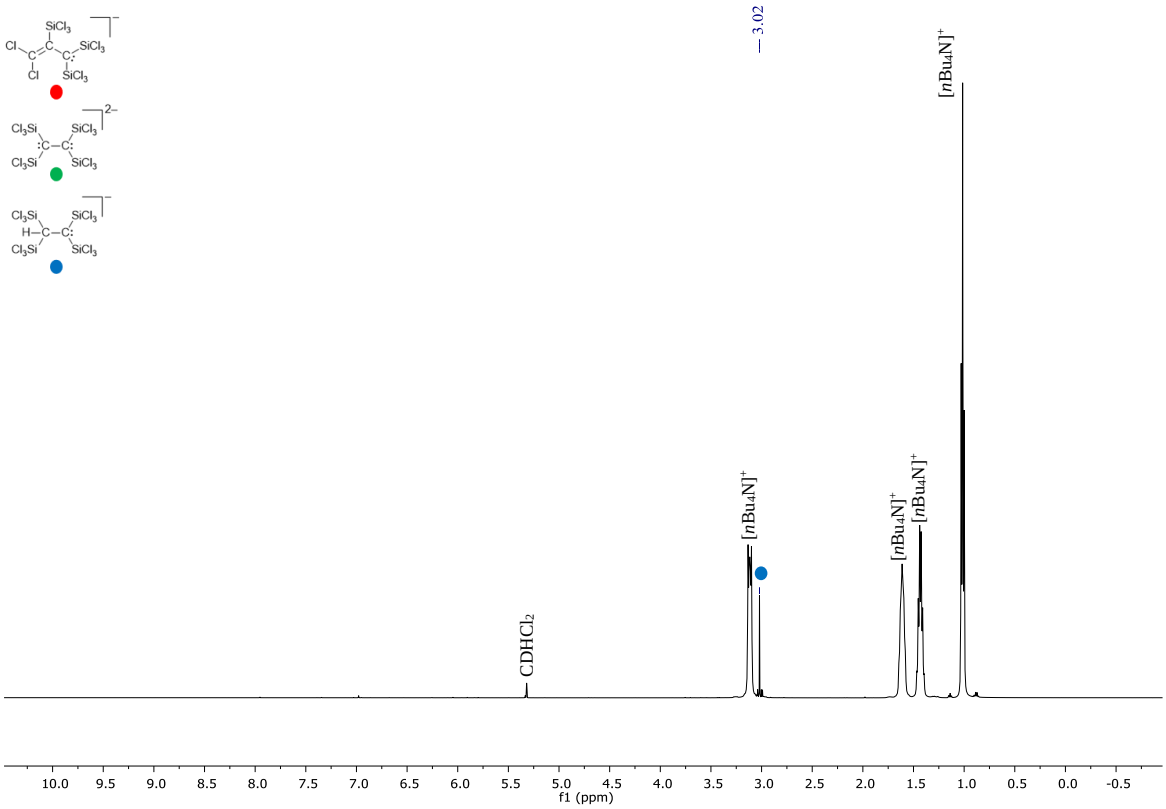

Figure S12: ^{1}H NMR spectrum of the reaction mixture of **2** and [*n*Bu$_4$N]$_2$[**B**] which furnishes [*n*Bu$_4$N][**1**] and the monoprotonated species [*n*Bu$_4$N][**B**H] (CD_2Cl_2, 500.2 MHz).

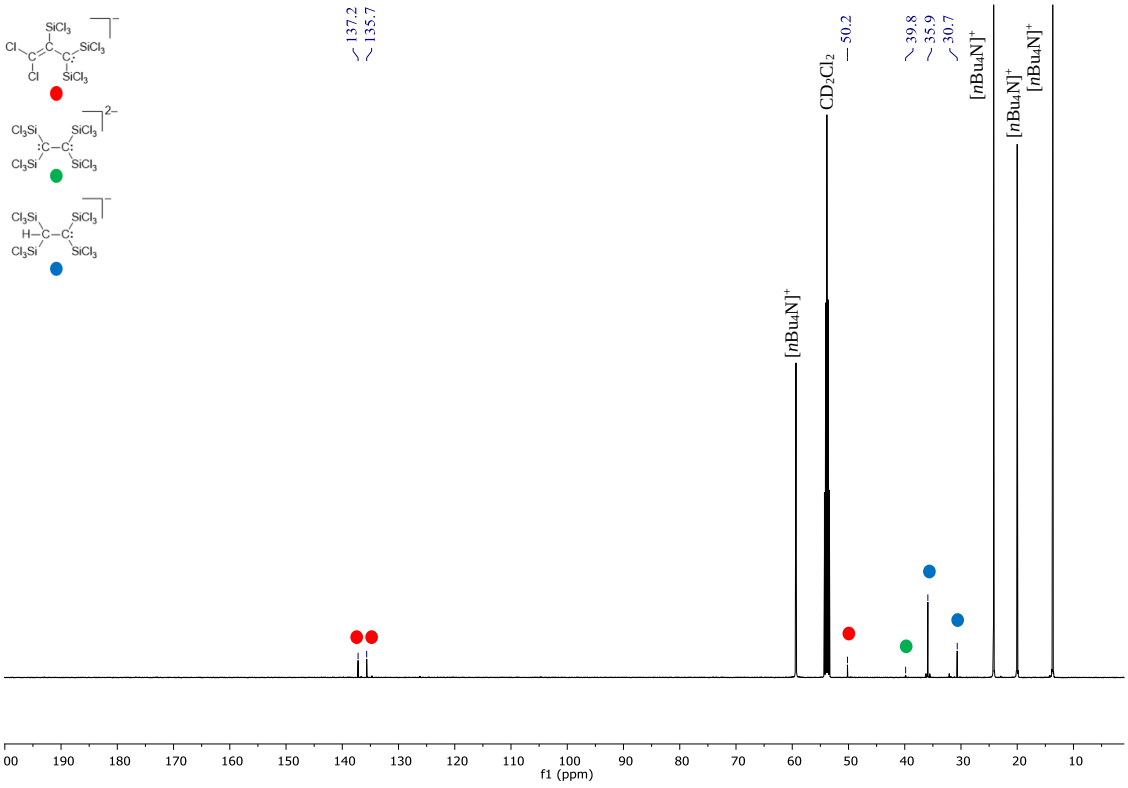

Figure S13: ^{13}C{^{1}H} NMR spectrum of the reaction mixture of **2** and [*n*Bu$_4$N]$_2$[**B**] which furnishes [*n*Bu$_4$N][**1**] and the monoprotonated species [*n*Bu$_4$N][**B**H] (CD_2Cl_2, 125.8 MHz).

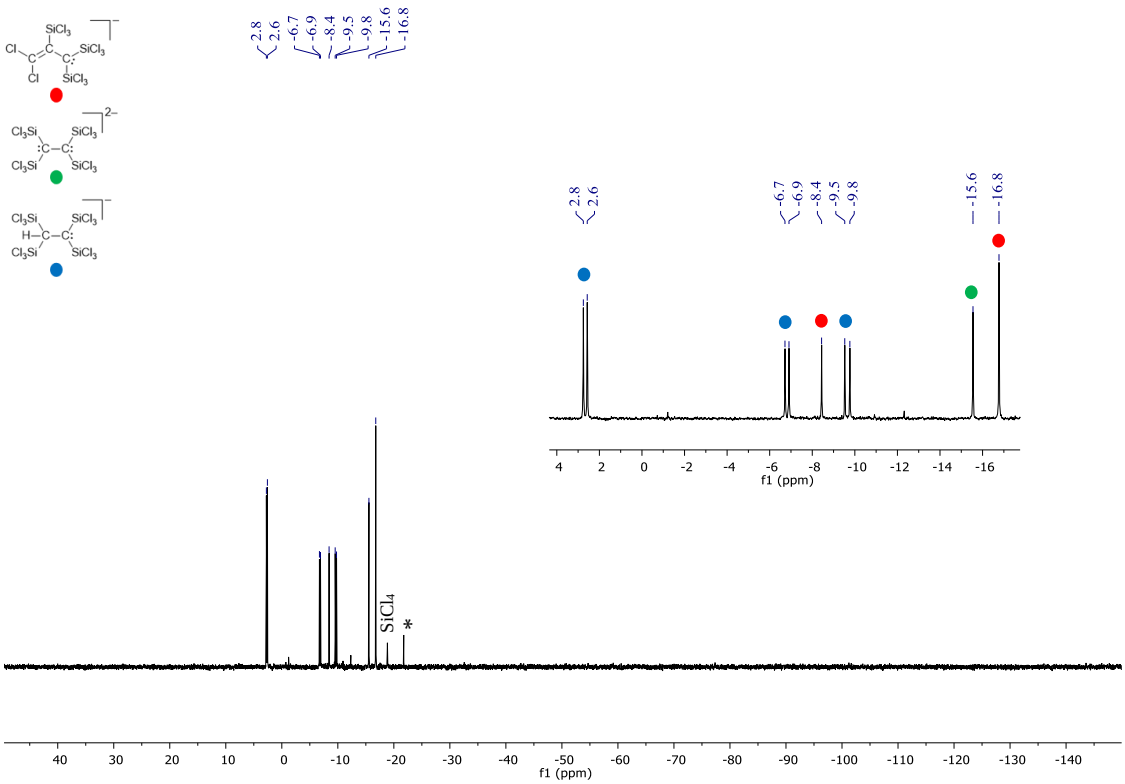

Figure S14: ^{29}Si NMR spectrum of the reaction mixture of **2** and [*n*Bu$_4$N]$_2$[**B**] which furnishes [*n*Bu$_4$N][**1**] and the monoprotonated species [*n*Bu$_4$N][**B**H] (CD_2Cl_2, 99.4 MHz). The signal marked with * corresponds to a minor impurity.

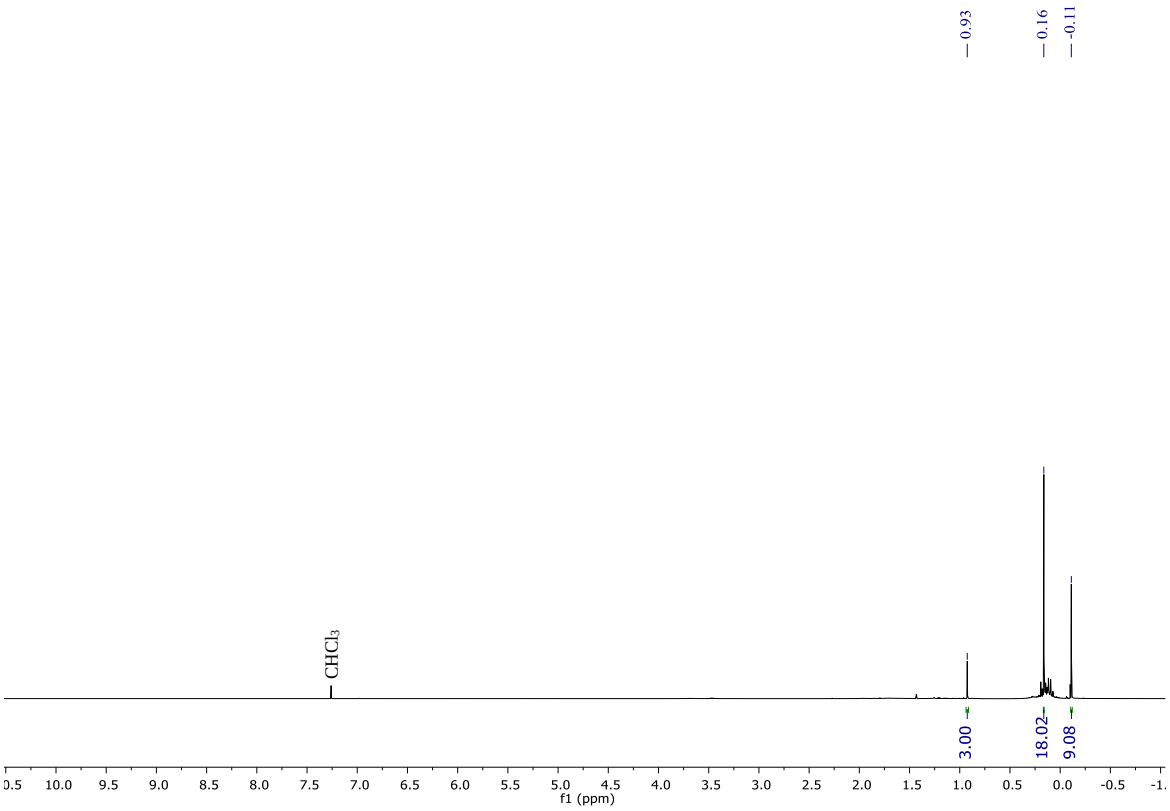

Figure S15: ^{1}H NMR spectrum of **H** ($CDCl_3$, 500.2 MHz).

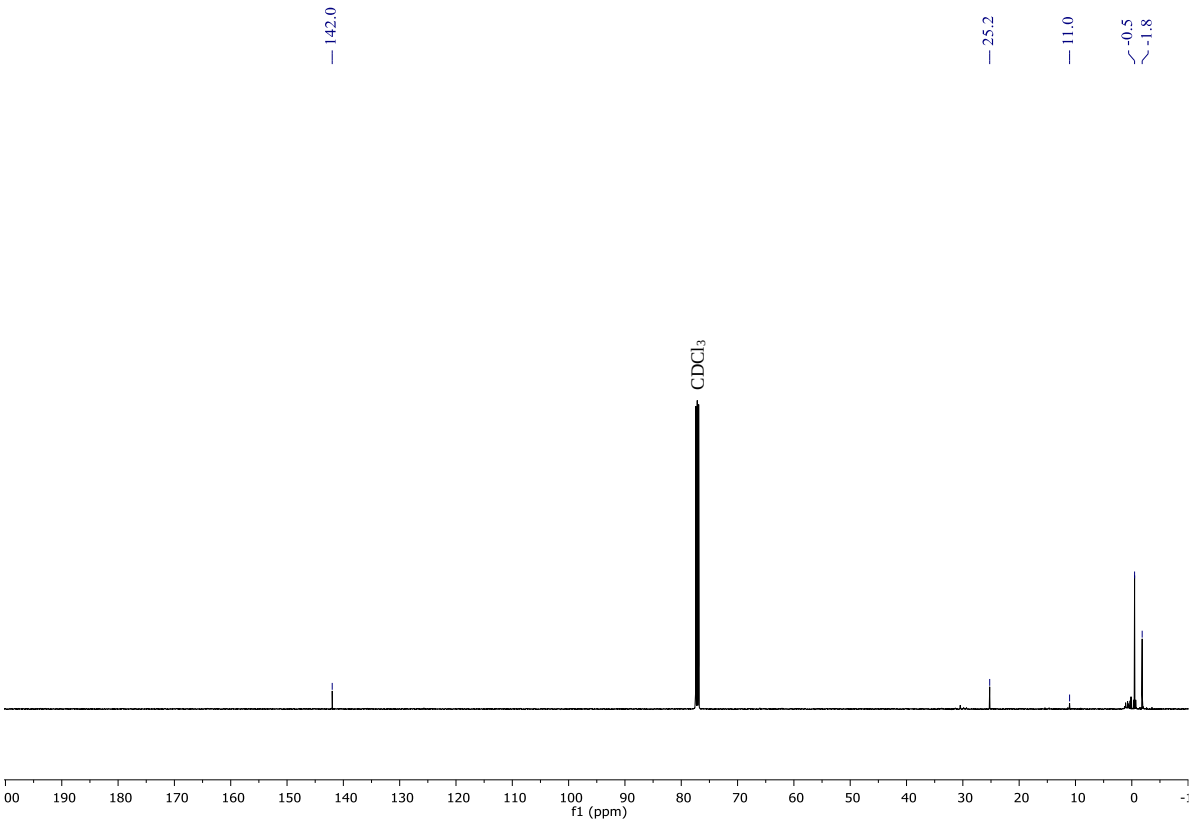

Figure S16: $^{13}C\{^{1}H\}$ NMR spectrum of **H** ($CDCl_3$, 125.8 MHz).

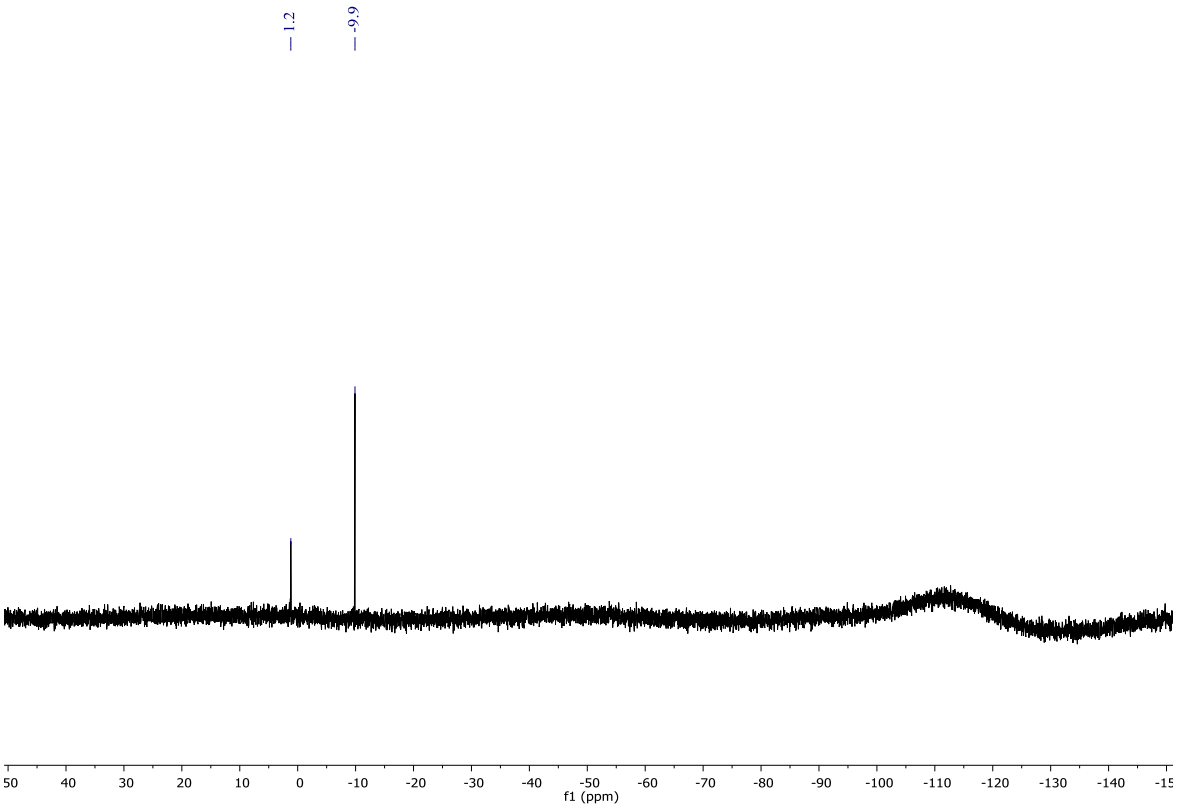

Figure S17: $^{29}Si\{^{1}H\}$ NMR spectrum of **H** ($CDCl_3$, 99.4 MHz).

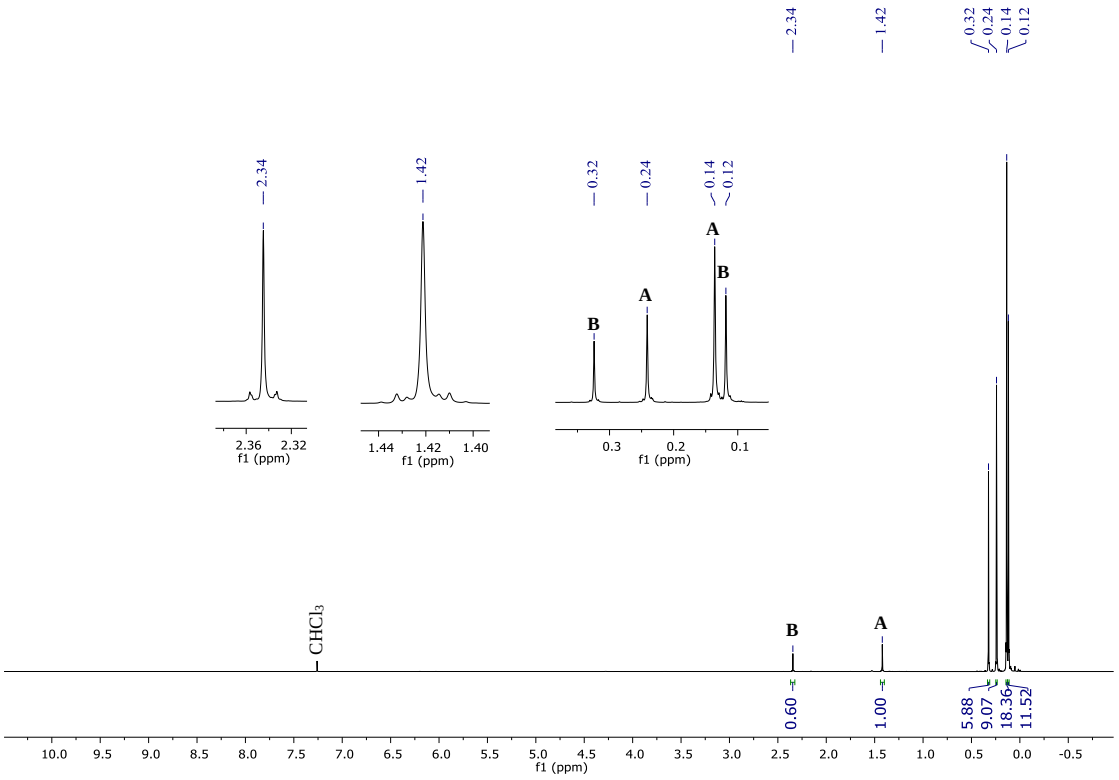

Figure S18: ^{1}H NMR spectrum of **2**Me (**2**^{Me}A: **A**; **2**^{Me}B: **B**) ($CDCl_3$, 500.2 MHz).

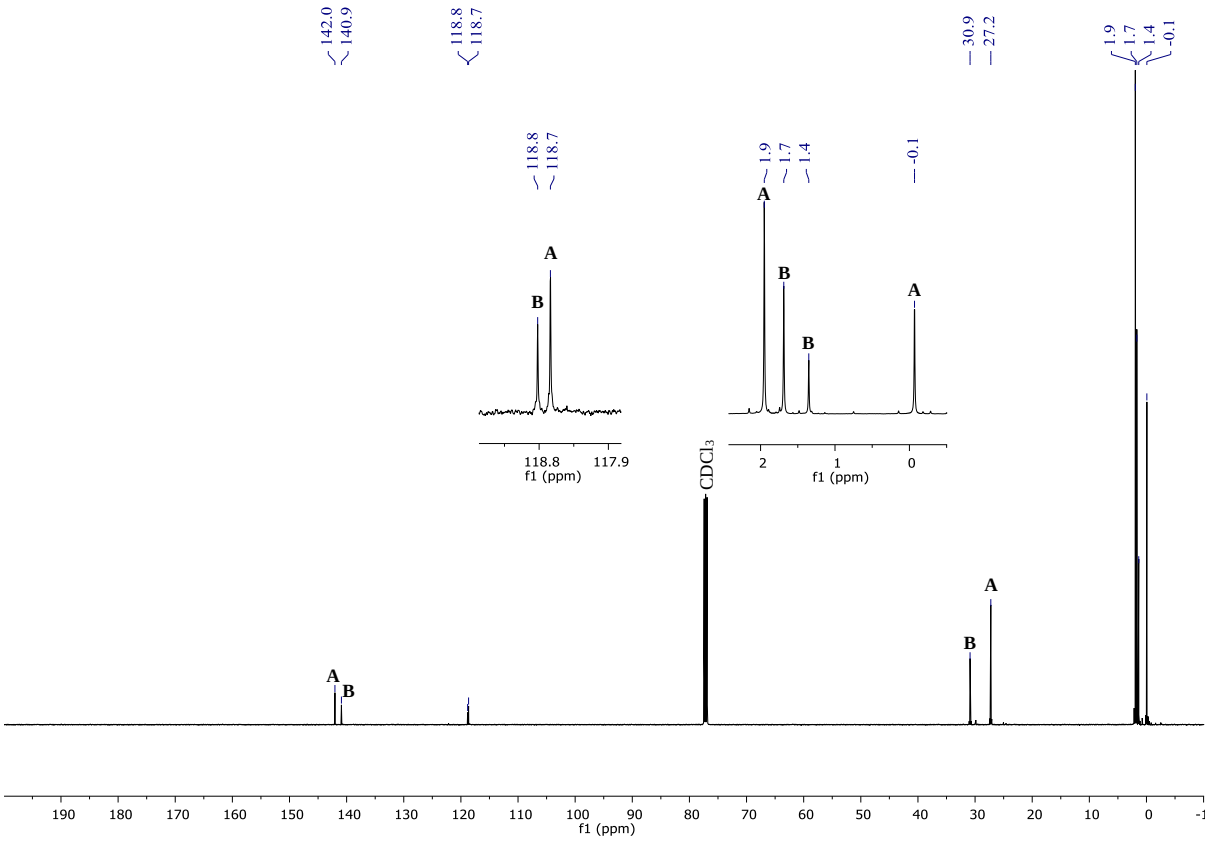

Figure S19: ^{13}C{^{1}H} NMR spectrum of **2**^{Me} (**2**^{Me}A: **A**; **2**^{Me}B: **B**) ($CDCl_3$, 125.8 MHz).

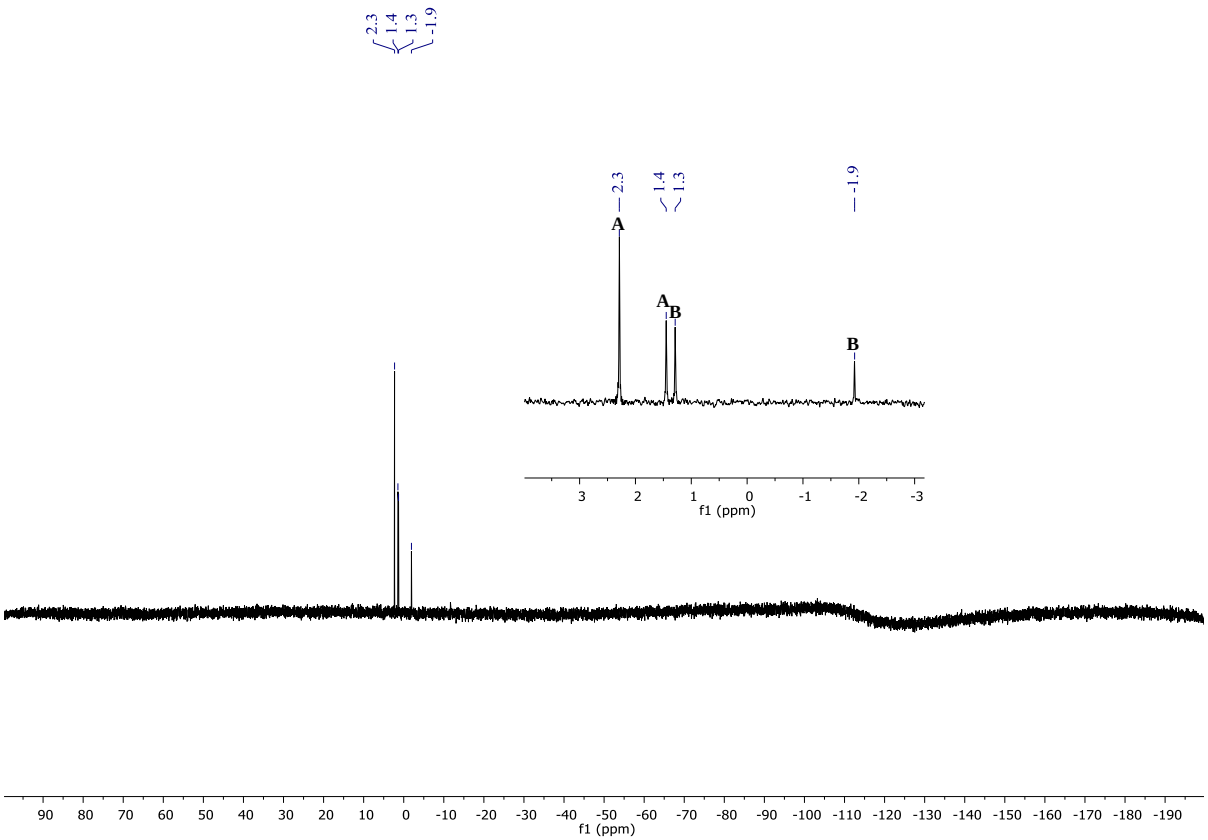

Figure S20: $^{29}Si\{^{1}H\}$ NMR spectrum of **2**^{Me} (**2**^{Me}A: **A**; **2**^{Me}B: **B**) ($CDCl_3$, 99.4 MHz).

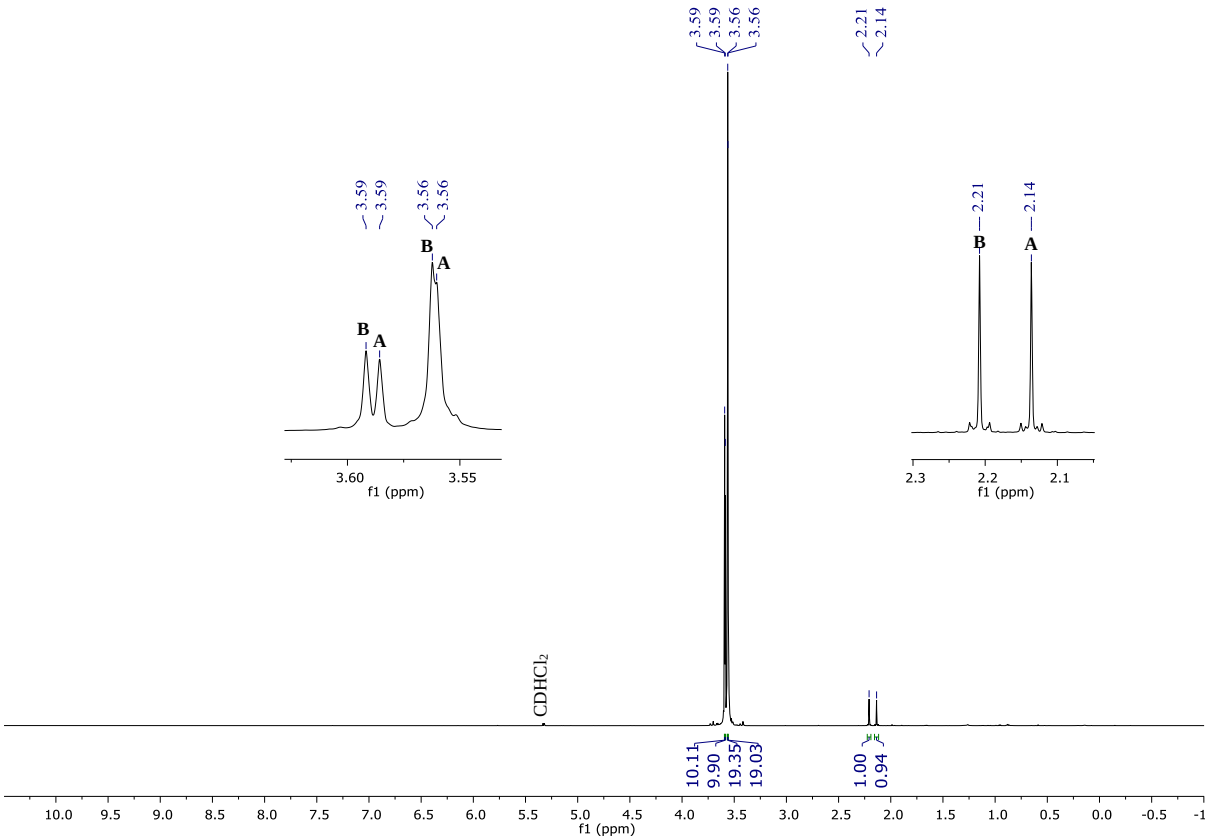

Figure S21: ^{1}H NMR spectrum of **2**^{OMe} (**2**^{OMe}A: **A**; **2**^{OMe}B: **B**) (CD_2Cl_2, 500.2 MHz).

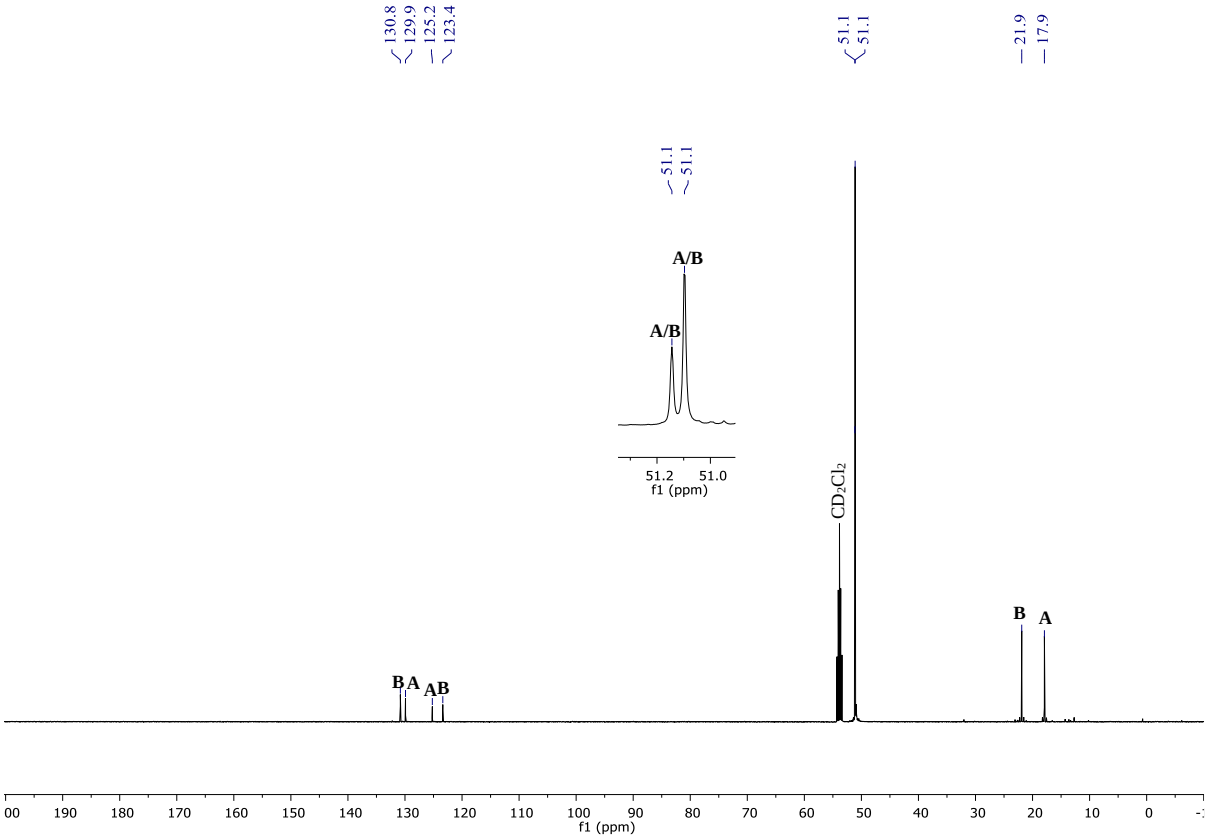

Figure S22: $^{13}C\{^{1}H\}$ NMR spectrum of **2**^{OMe} (**2**^{OMe}A: **A**; **2**^{OMe}B: **B**) (CD_2Cl_2, 125.8 MHz).

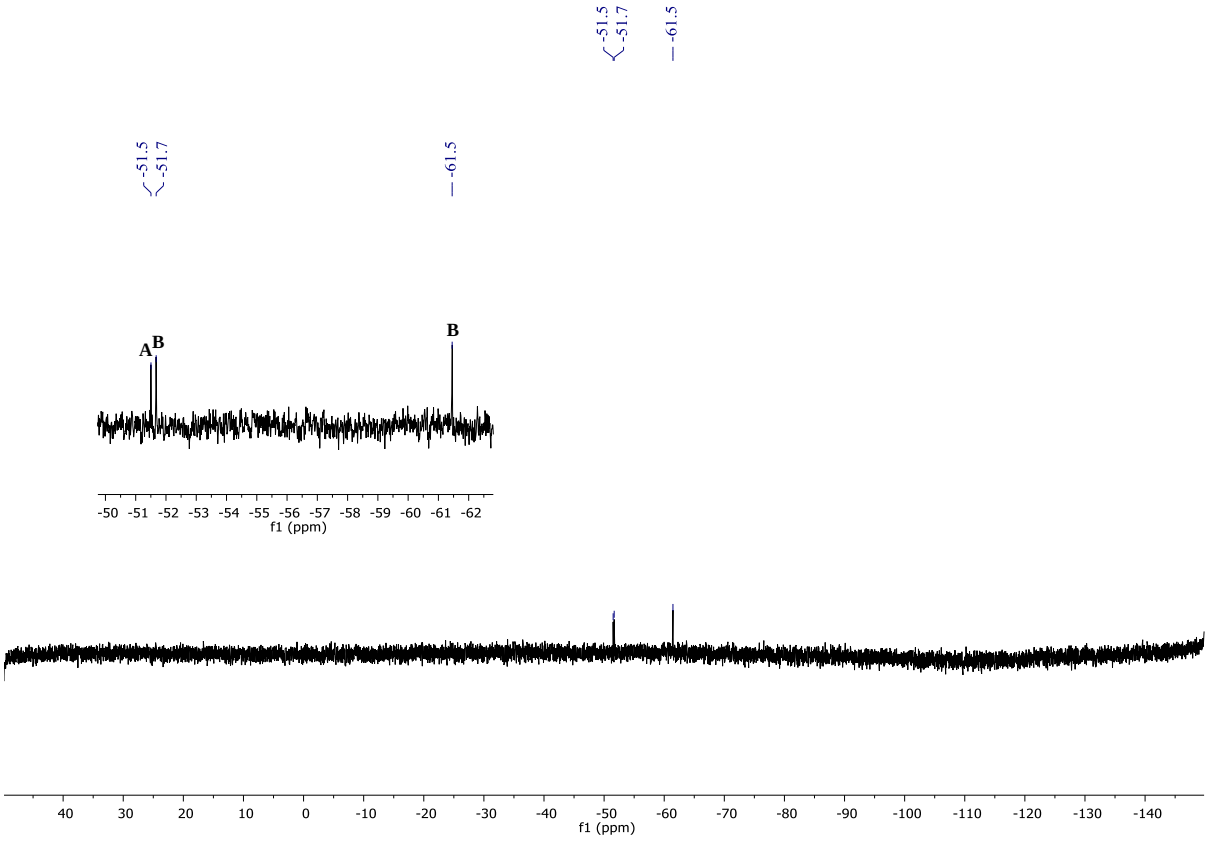

Figure S23: $^{29}Si\{^{1}H\}$ NMR spectrum of **2**^{OMe} (**2**^{OMe}A: **A**; **2**^{OMe}B: **B**) (CD_2Cl_2, 99.4 MHz).

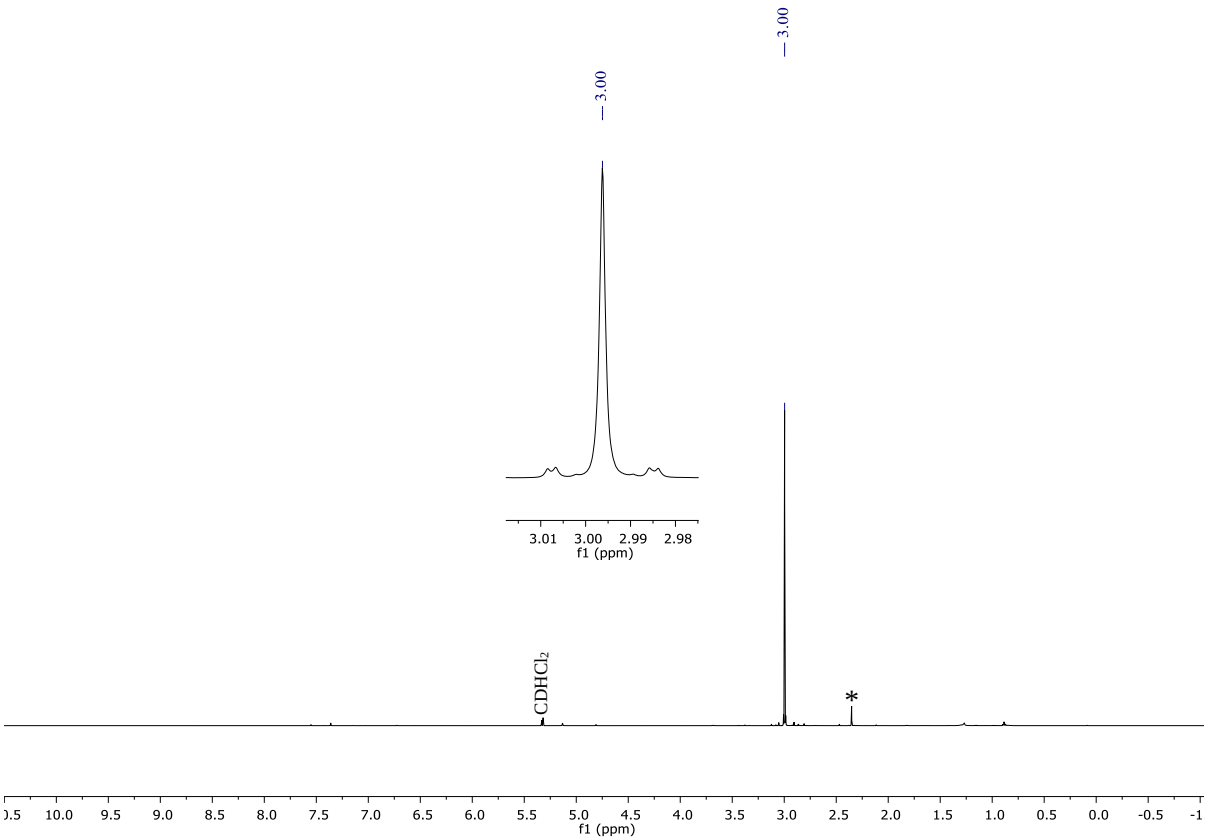

Figure S24: ^{1}H NMR spectrum of **3** (CD_2Cl_2, 500.2 MHz). The signal marked with * corresponds to a minor impuritiy.

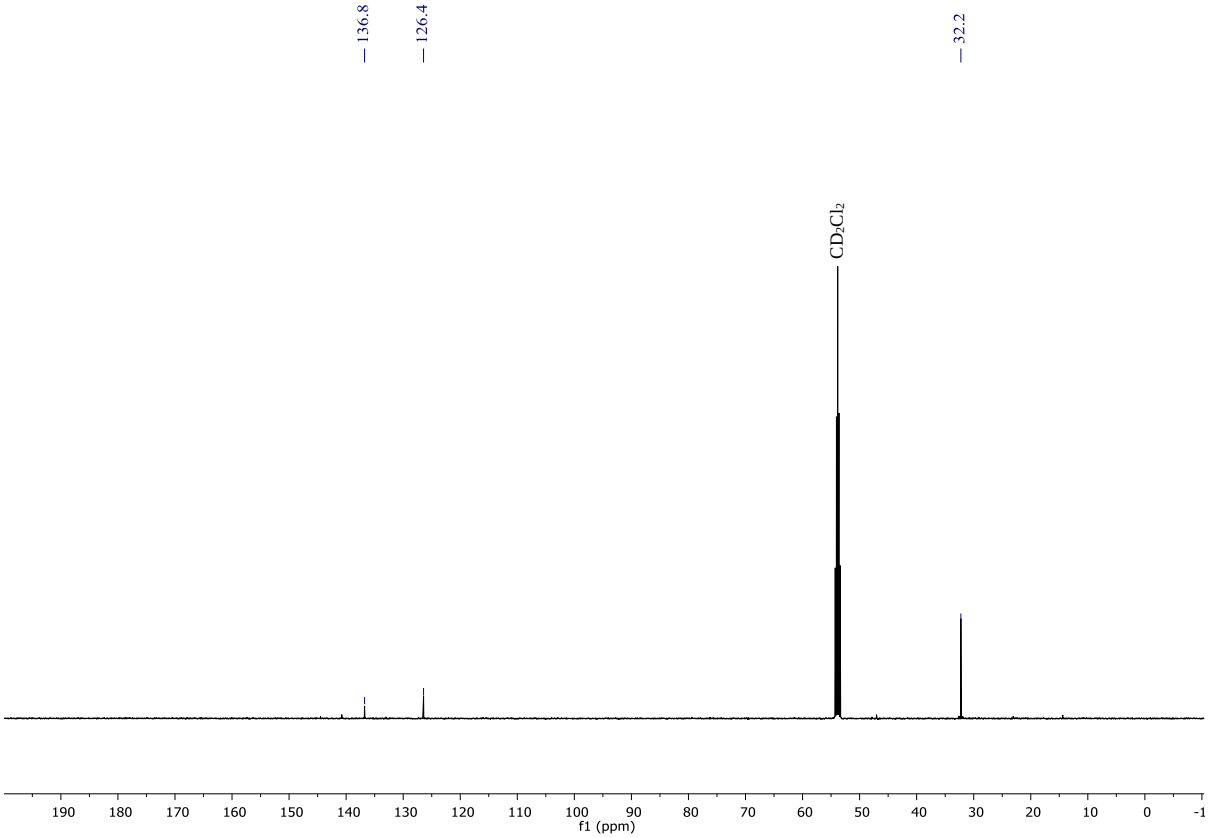

Figure S25: $^{13}C\{^{1}H\}$ NMR spectrum of **3** (CD_2Cl_2, 125.8 MHz).

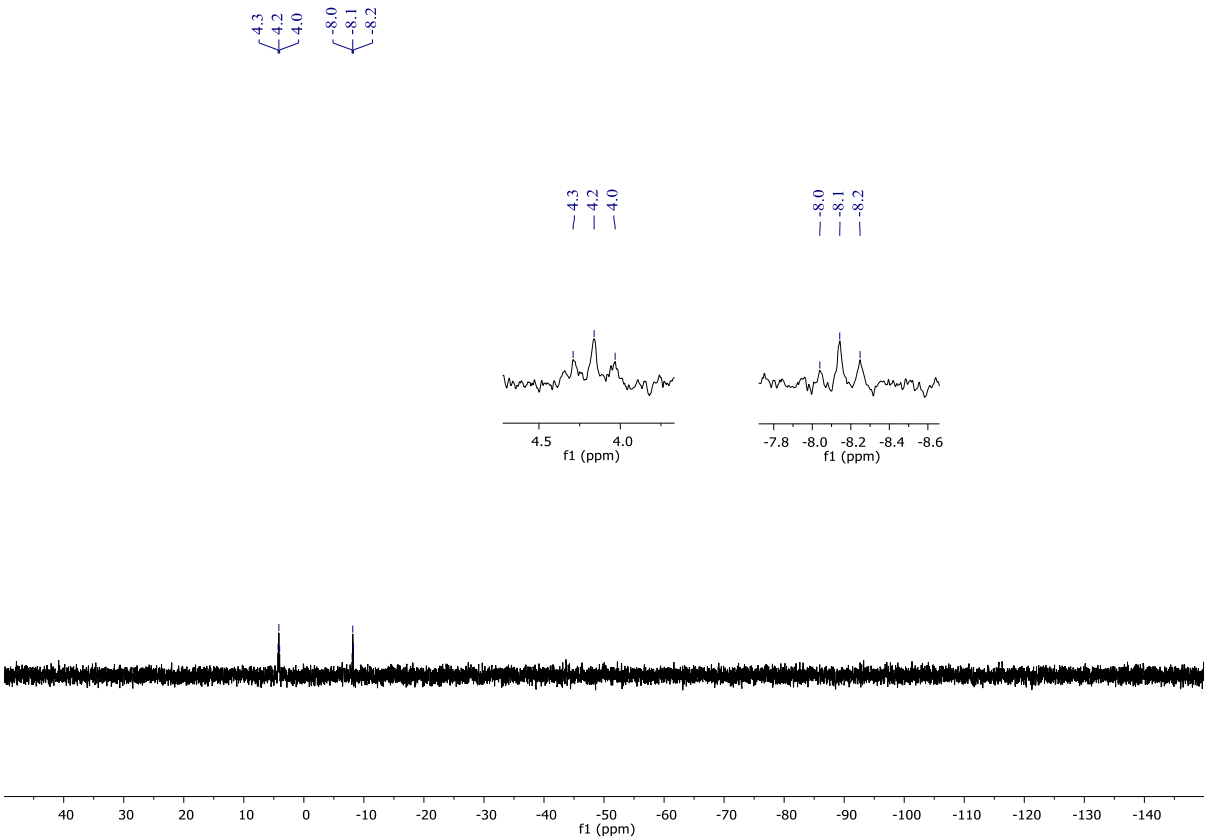

Figure S26: ^{29}Si NMR spectrum of **3** (CD_2Cl_2, 99.4 MHz).

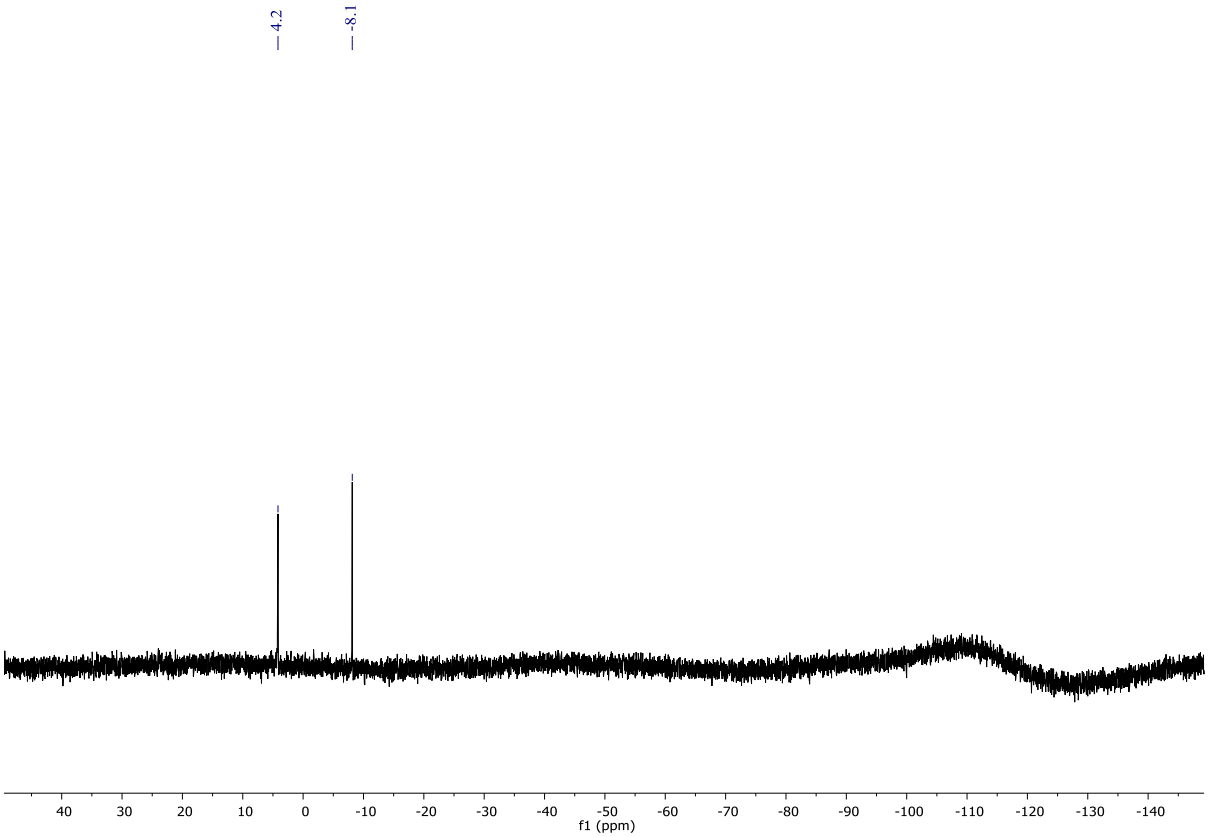

Figure S27: ^{29}Si{^{1}H} NMR spectrum of **3** (CD_2Cl_2, 99.4 MHz).

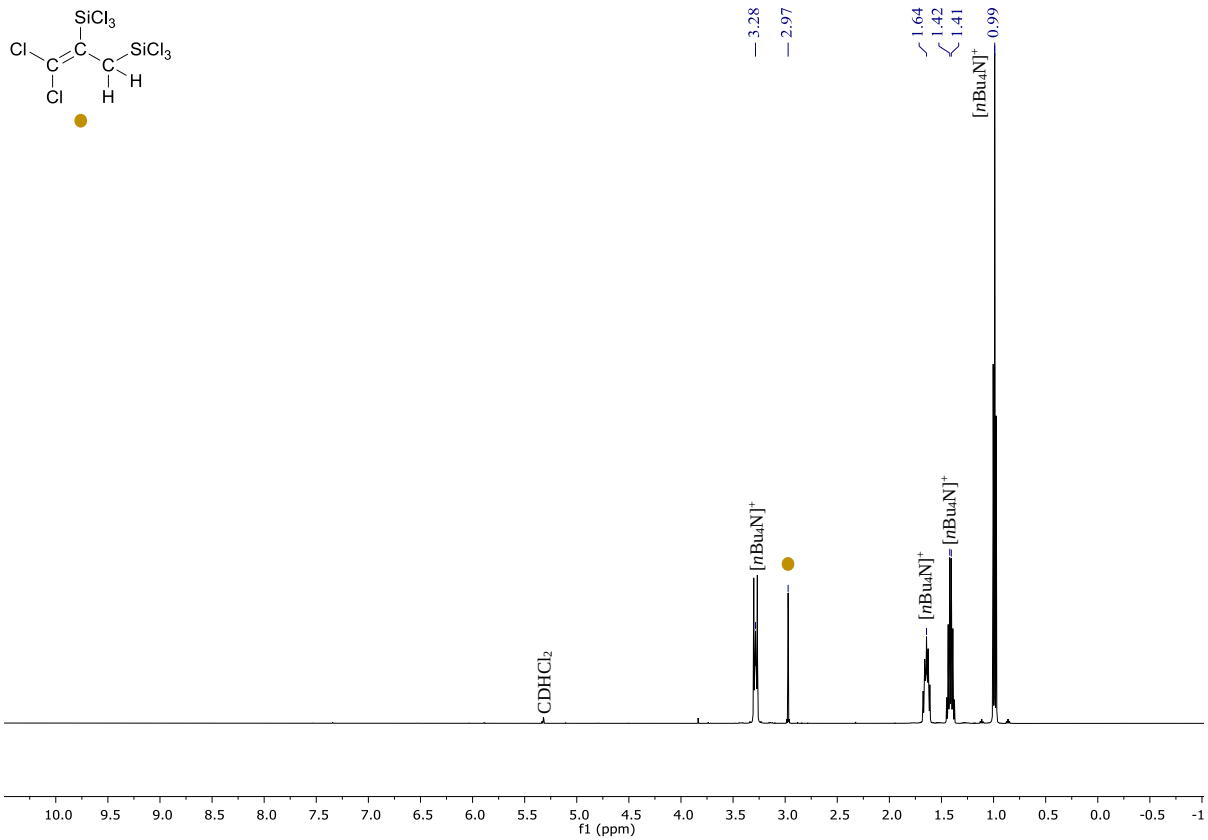

Figure S28: ^{1}H NMR spectrum of the reaction mixture of **2** and [*n*Bu$_4$N]Cl after heating to 60 °C for 3 d, which furnishes [*n*Bu$_4$N][**1**] and **3** (CD_2Cl_2, 500.2 MHz).

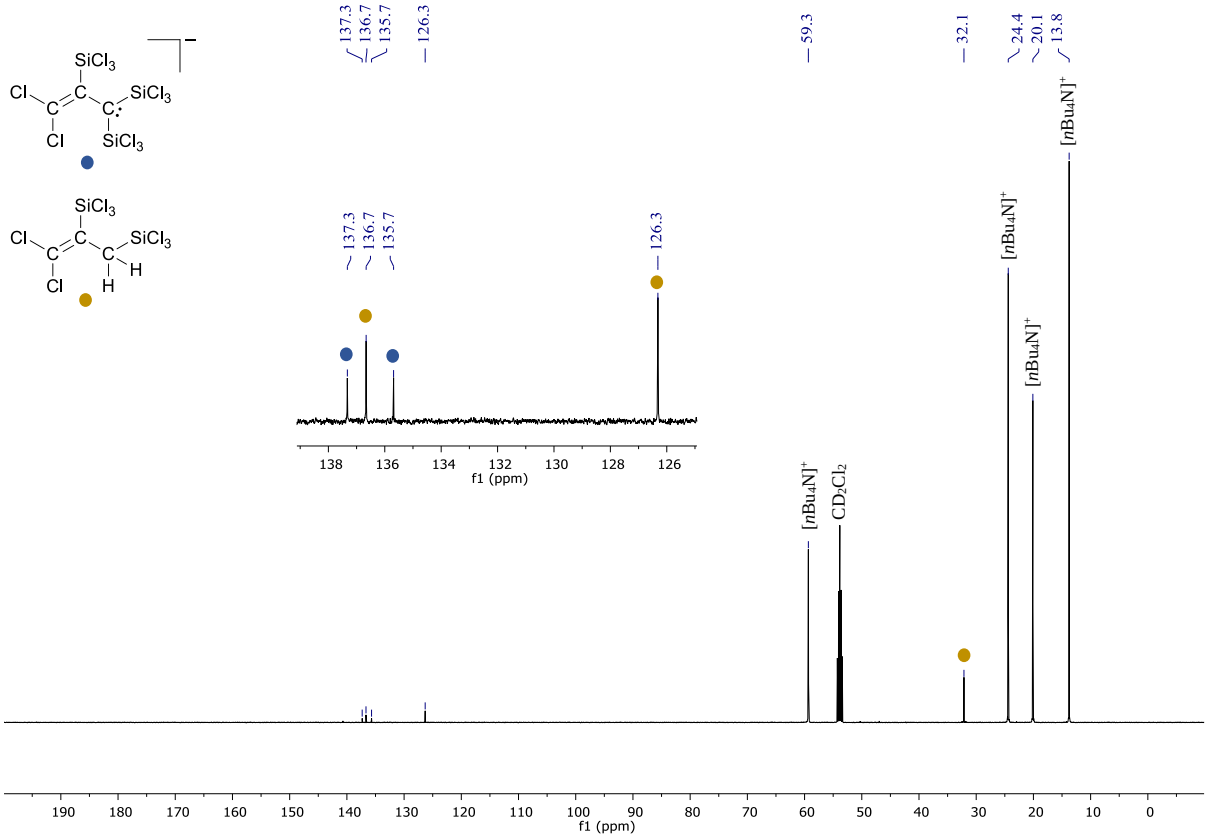

Figure S29: ^{13}C{^{1}H} NMR spectrum of the reaction mixture of **2** and [*n*Bu$_4$N]Cl after heating to 60 °C for 3 d, which furnishes [*n*Bu$_4$N][**1**] and **3** (CD_2Cl_2, 125.8 MHz).

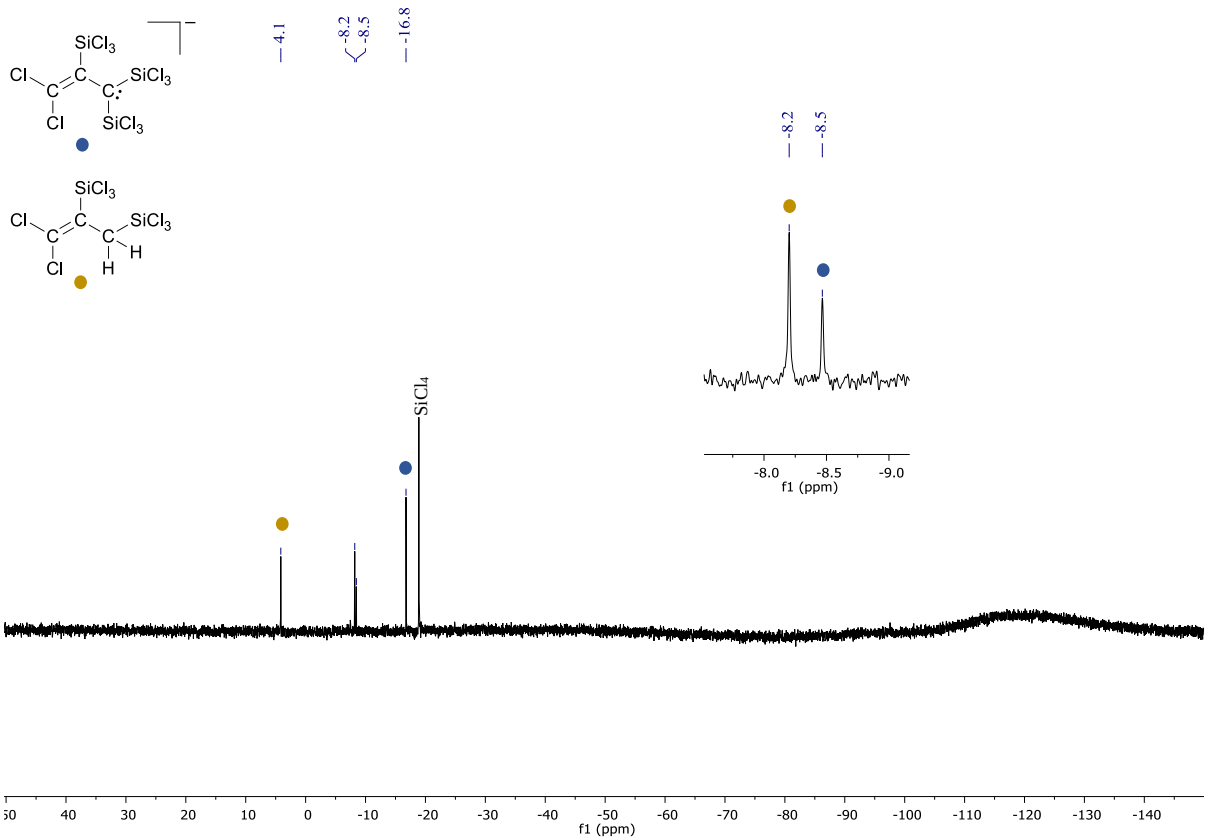

Figure S30: $^{29}Si\{^{1}H\}$ NMR spectrum of the reaction mixture of **2** and [*n*Bu$_4$N]Cl after heating to 60 °C for 3 d, which furnishes [*n*Bu$_4$N][**1**], **3,** and $SiCl_4$ (CD_2Cl_2, 99.4 MHz).

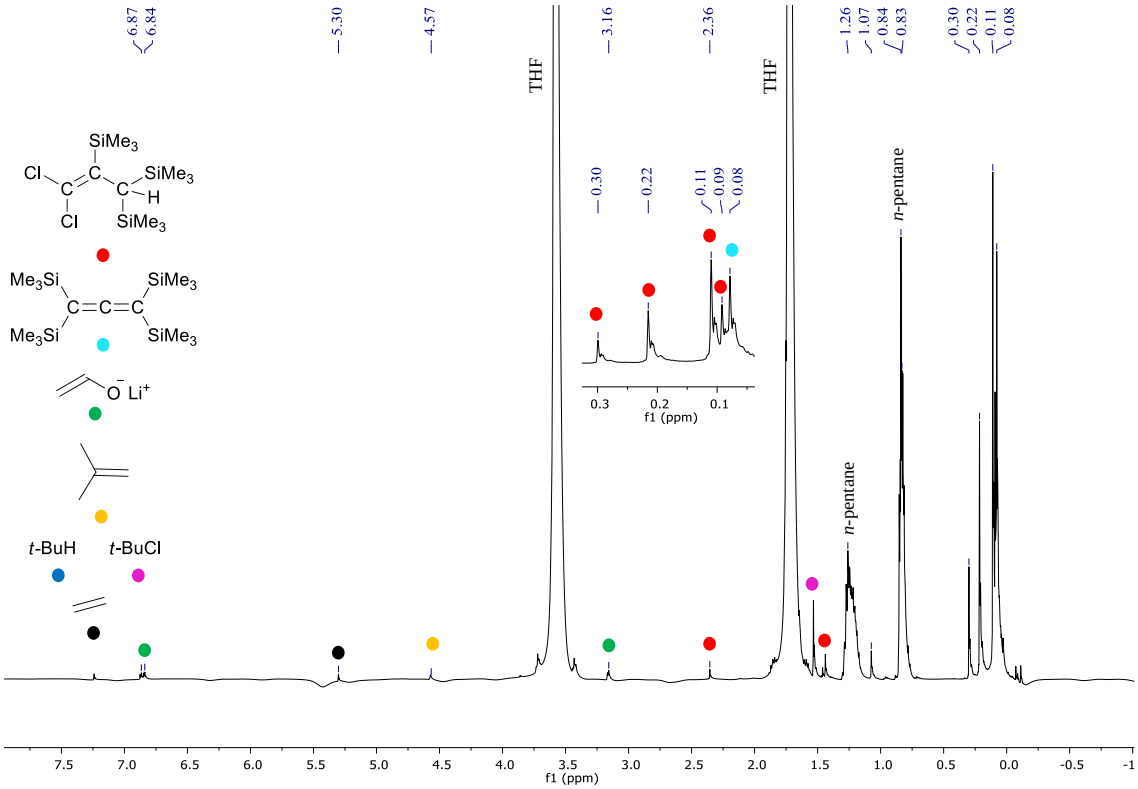

Figure S31: ^{1}H NMR spectrum of the reaction mixture of **2**^{Me} and 1 eq *t*-BuLi which furnishes **I** and the byproducts *t*-BuCl,[S11] *iso*-butane,[S11] and *iso*-butene,[S12] as well as the lithium enolate of acetaldehyde[S15] and ethene,[S2] which result from the side reaction of *t*-BuLi with THF (THF, 500.2 MHz).

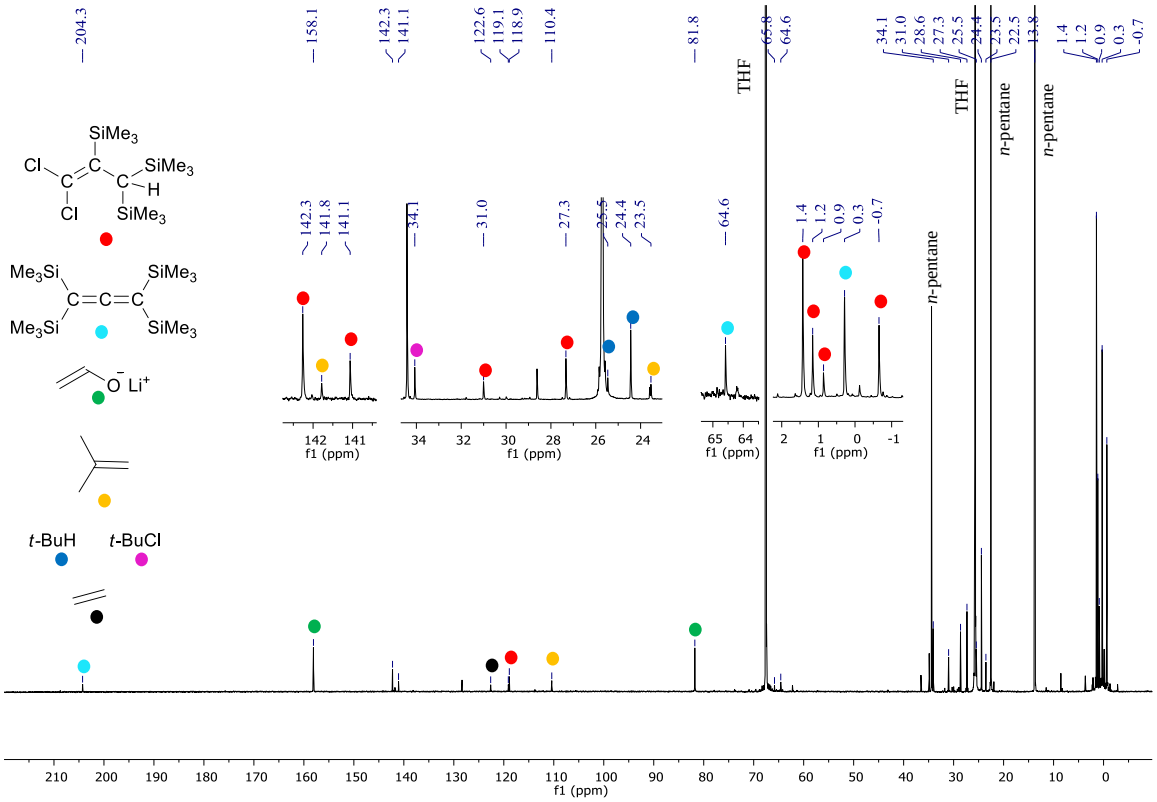

Figure S32: $^{13}C\{^{1}H\}$ NMR spectrum of the reaction mixture of **2**^{Me} and 1 eq *t*-BuLi which furnishes **I** and the byproducts *t*-BuCl,[S11] *iso*-butane,[S11] and *iso*-butene,[S12] as well as the lithium enolate of acetaldehyde[S15] and ethene,[S2] which result from the side reaction of *t*-BuLi with THF (THF, 125.8 MHz).

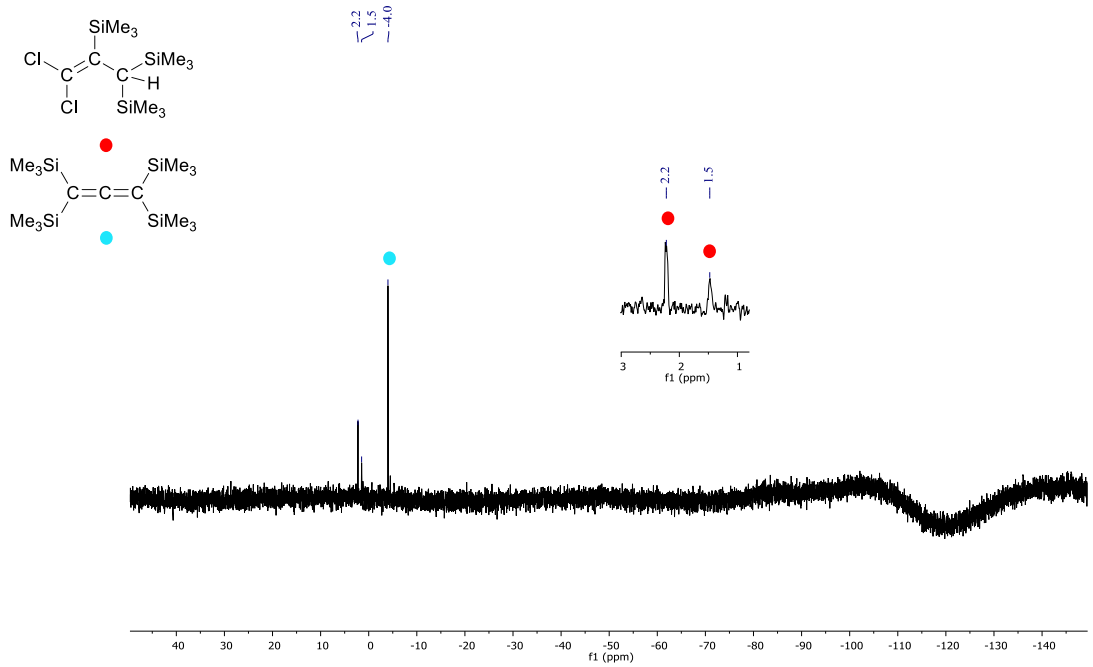

Figure S33: $^{29}Si\{^{1}H\}$ NMR spectrum of the reaction mixture of **2**^{Me} and 1 eq *t*-BuLi which furnishes **I** (due to the low concentration of remaining **2**^{Me} only two out of four signals can be detected, THF, 99.4 MHz).

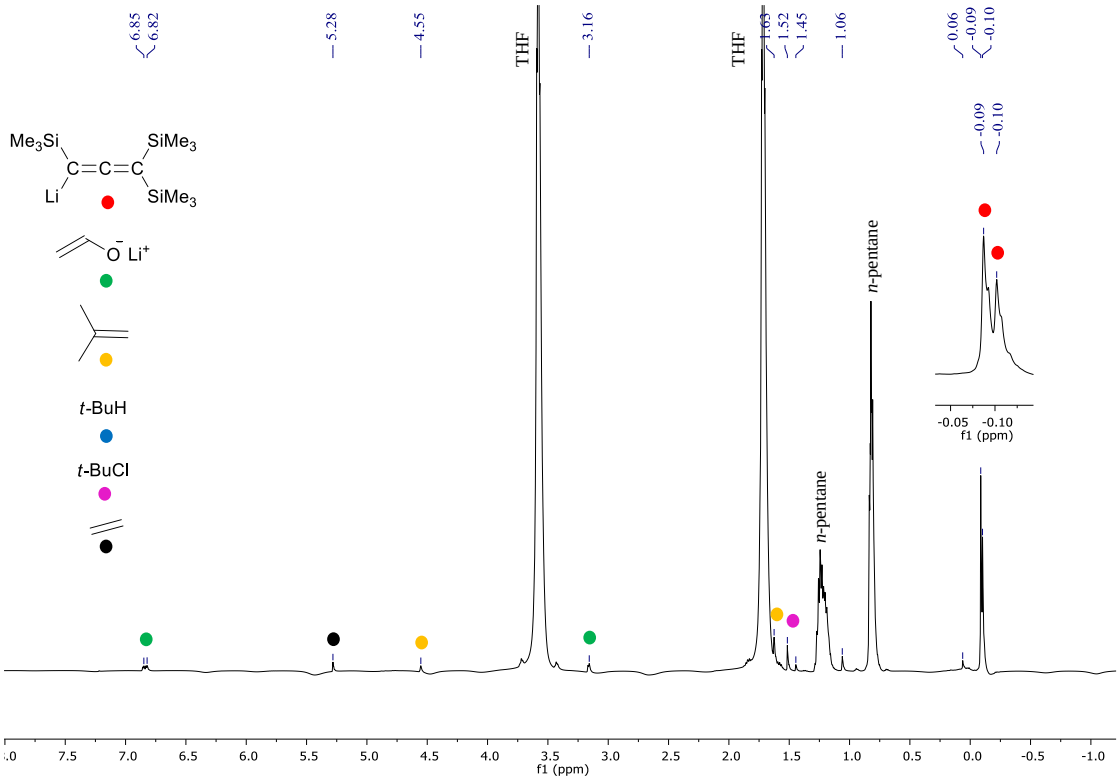

Figure S34: ^{1}H NMR spectrum of the reaction mixture of **2**^{Me} and 2 eq *t*-BuLi which furnishes Li[**4**], and the byproducts *t*-BuCl,[S11] *iso*-butane[S11] and *iso*-butene,[S12] as well as the lithium enolate of acetaldehyde[S15] and ethene,[S2] which result from the side reaction of *t*-BuLi with THF (THF, 500.2 MHz).

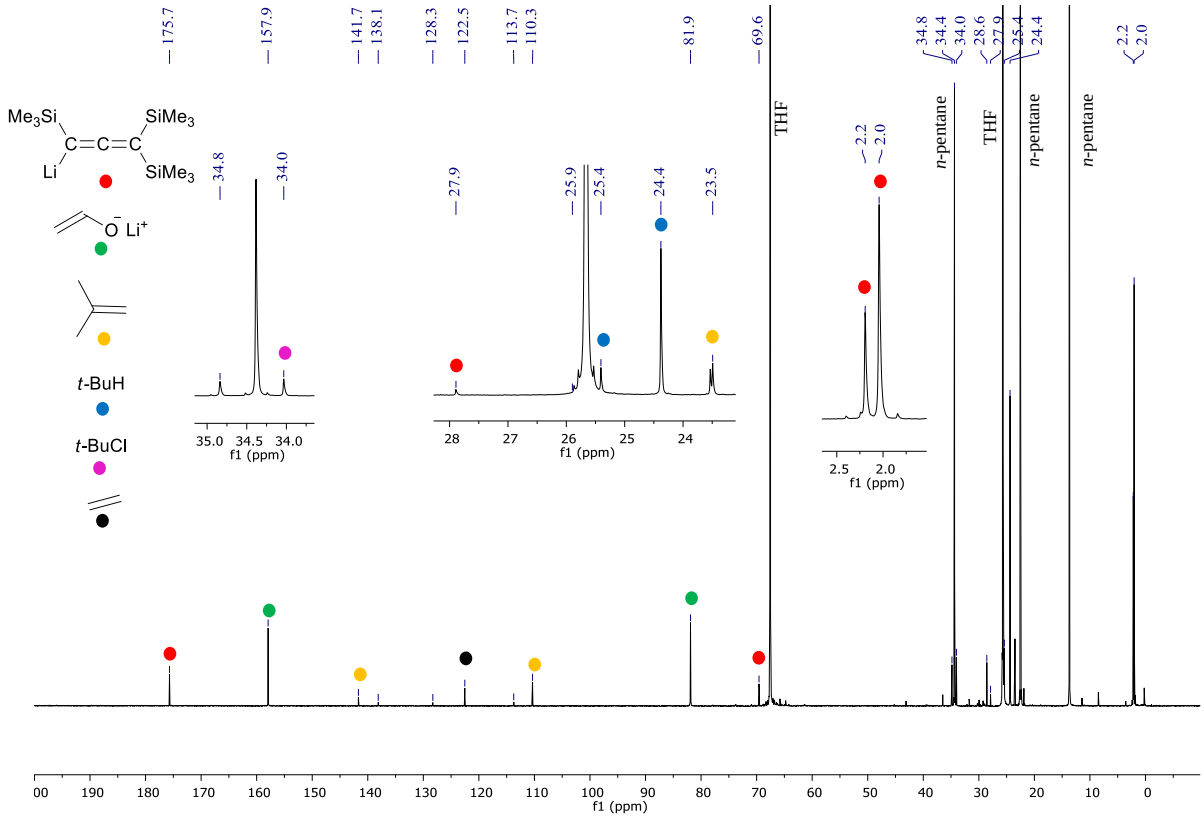

Figure S35: $^{13}C\{^{1}H\}$ NMR spectrum of the reaction mixture of **2**^{Me} and 2 eq *t*-BuLi which furnishes Li[**4**], and the byproducts *t*-BuCl,[S11] *iso*-butane,[S11] and *iso*-butene,[S12] as well as the lithium enolate of acetaldehyde[S15] and ethene,[S2] which result from the side reaction of *t*-BuLi with THF (THF, 125.8 MHz).

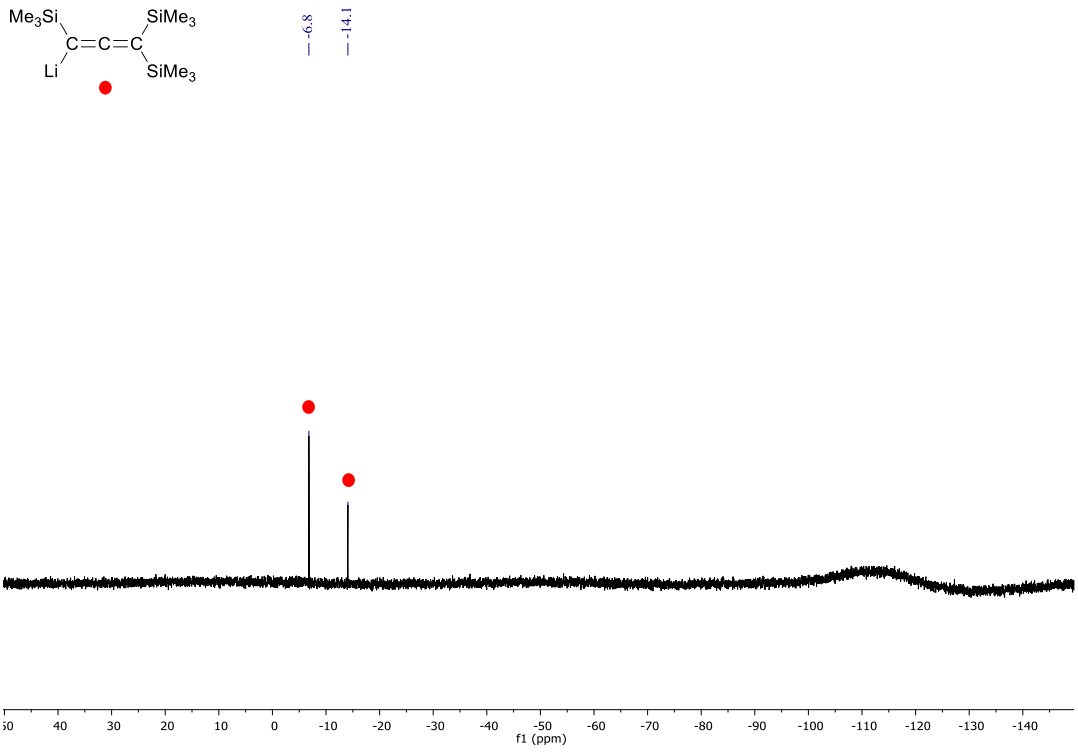

Figure S36: $^{29}Si\{^{1}H\}$ NMR spectrum of the reaction mixture of **2**^{Me} and 2 eq *t*-BuLi which furnishes Li[**4**] (THF, 99.4 MHz).

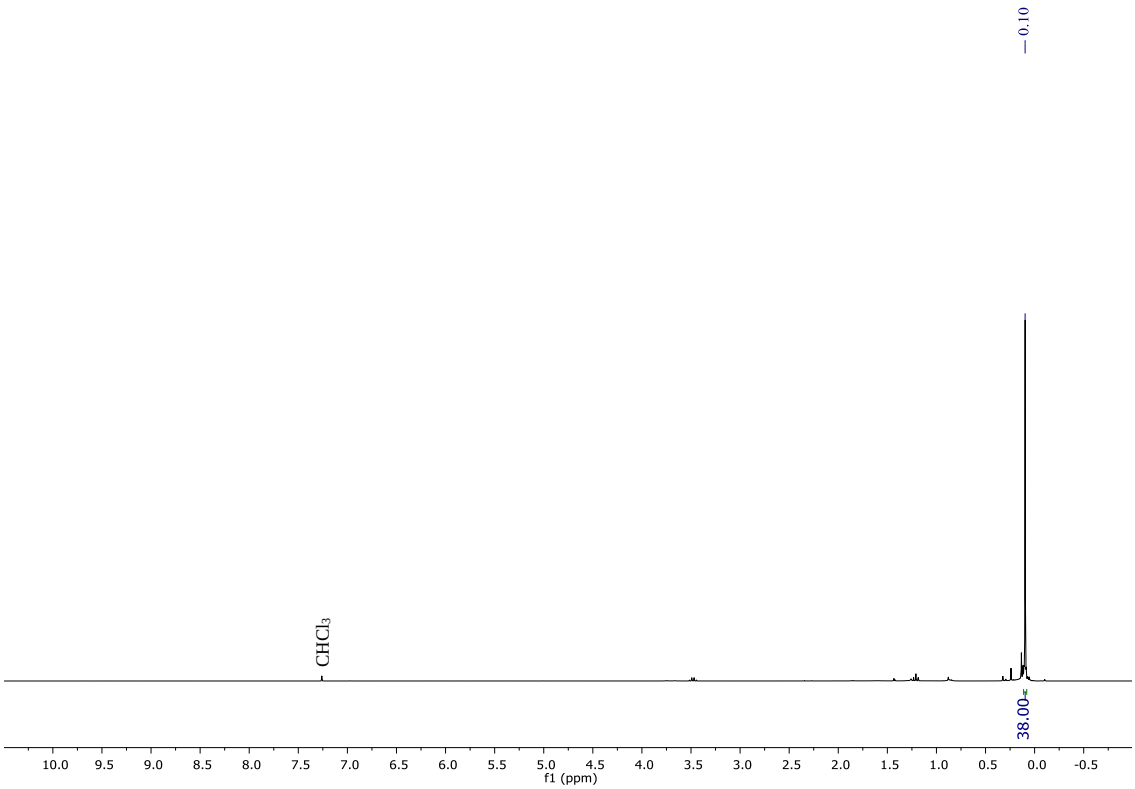

Figure S37: ^{1}H NMR spectrum of the product from the reaction of *in situ* generated Li[**4**] with Me_3SiCl, which could be identified as **I** ($CDCl_3$, 300.0 MHz).

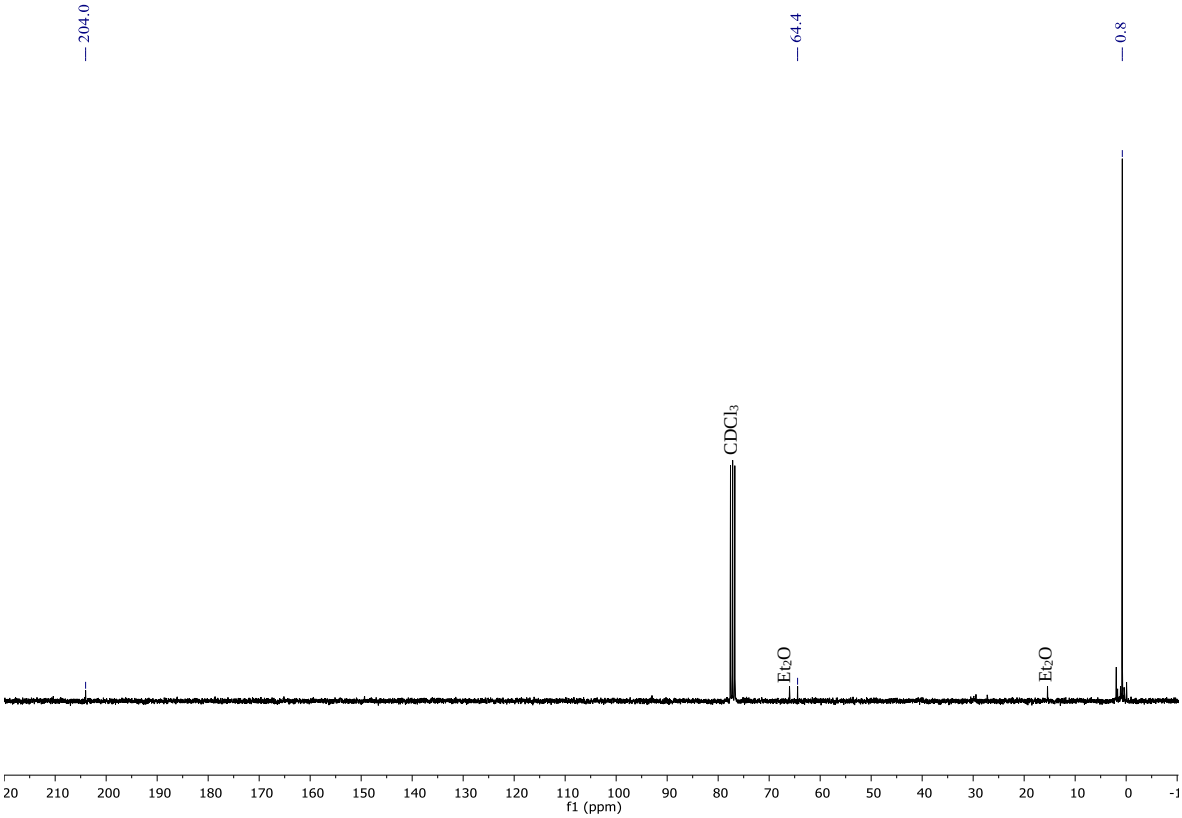

Figure S38: $^{13}C\{^{1}H\}$ NMR spectrum of the product from the reaction of *in situ* generated Li[**4**] with Me_3SiCl, which could be identified as **I** ($CDCl_3$, 75.5 MHz).

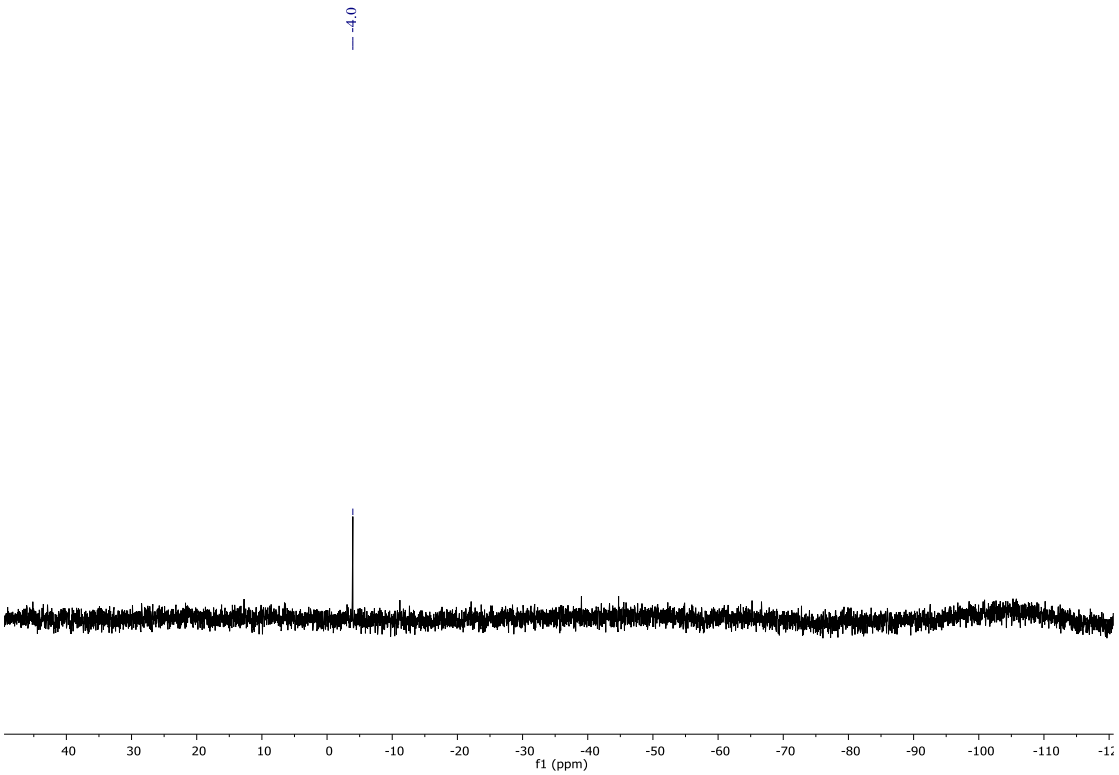

Figure S39: $^{29}Si\{^{1}H\}$ NMR spectrum of the product from the reaction of *in situ* generated Li[**4**] with Me_3SiCl, which could be identified as **I** ($CDCl_3$, 59.6 MHz).

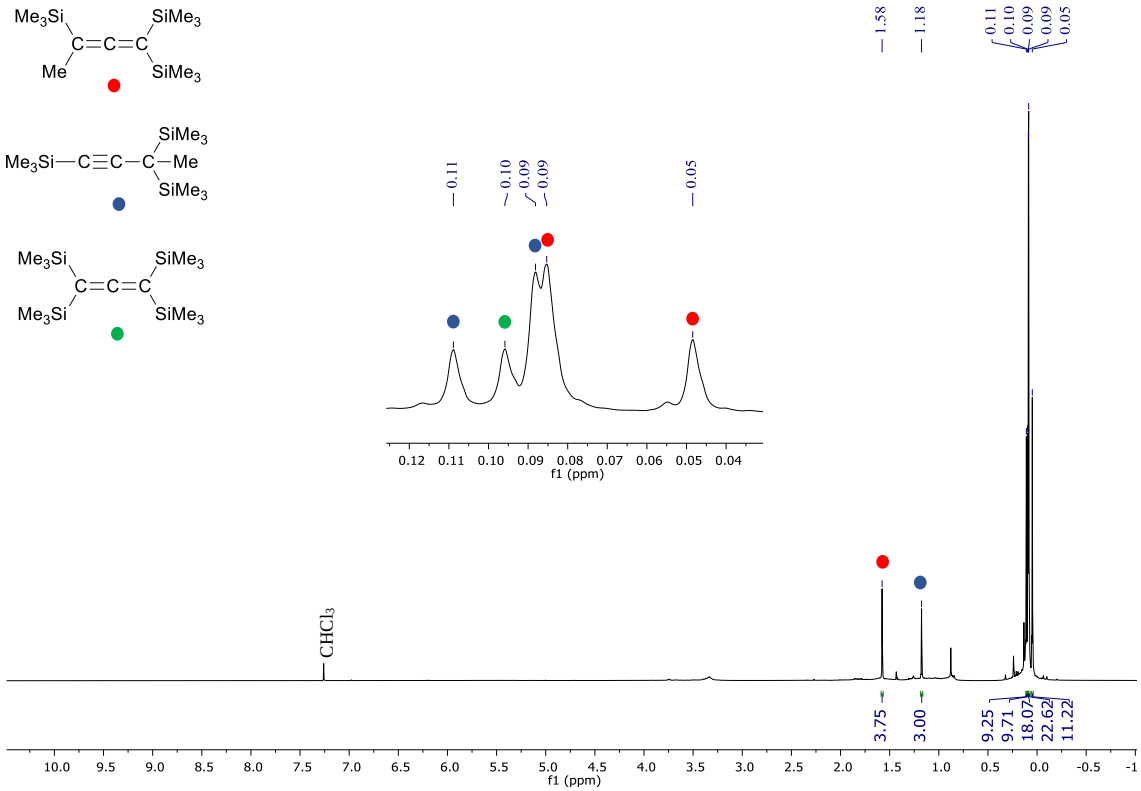

Figure S40: ^{1}H NMR spectrum of the product from the reaction of *in situ* generated Li[**4**] with MeI, identified as **J** and **K** and containing small amounts of **I** ($CDCl_3$, 300.0 MHz).

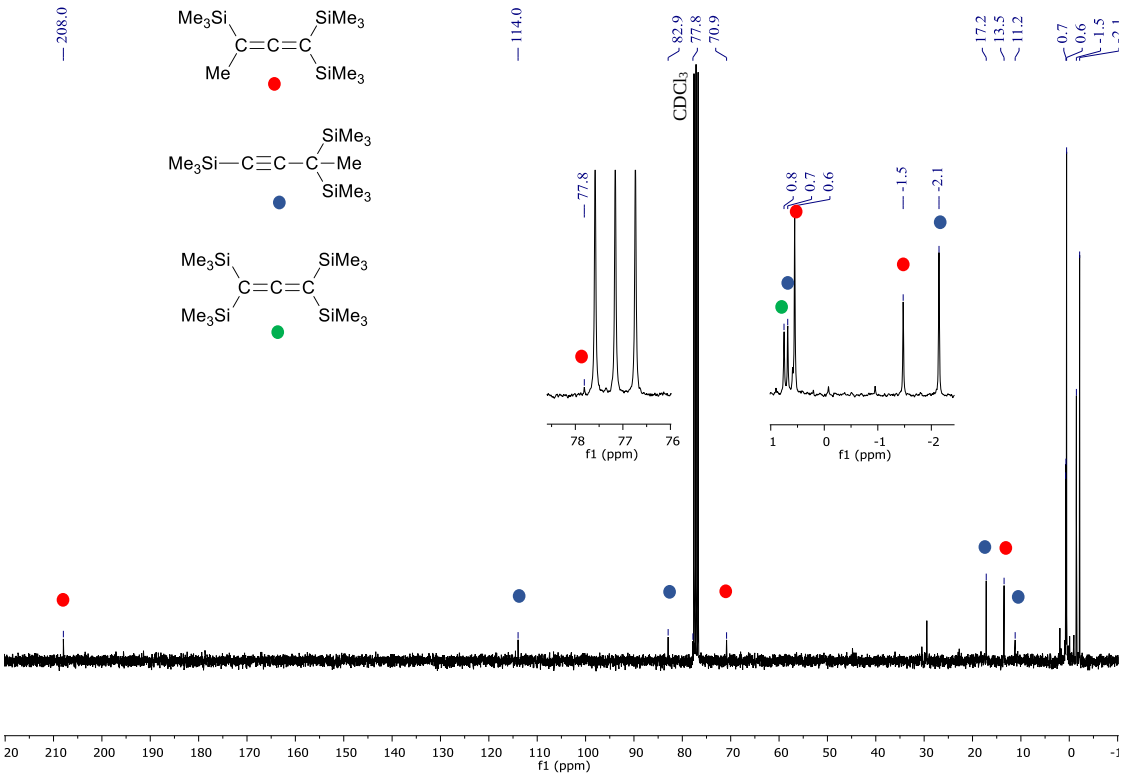

Figure S41: $^{13}C\{^{1}H\}$ NMR spectrum of the product from the reaction of *in situ* generated Li[**4**] with MeI, identified as **J** and **K** and containing small amounts of **I** ($CDCl_3$, 75.5 MHz).

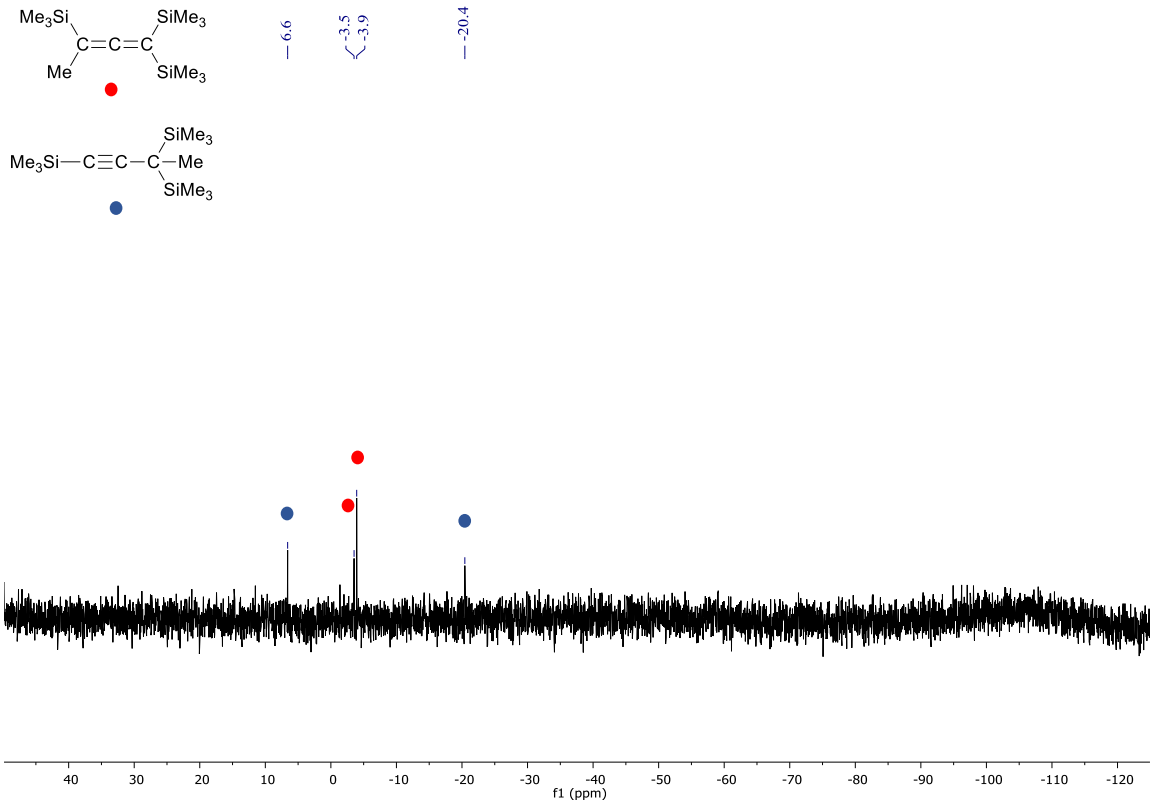

Figure S42: $^{29}Si\{^{1}H\}$ NMR spectrum of the product from the reaction of *in situ* generated Li[**4**] with MeI, identified as **J** and **K** ($CDCl_3$, 59.6 MHz).

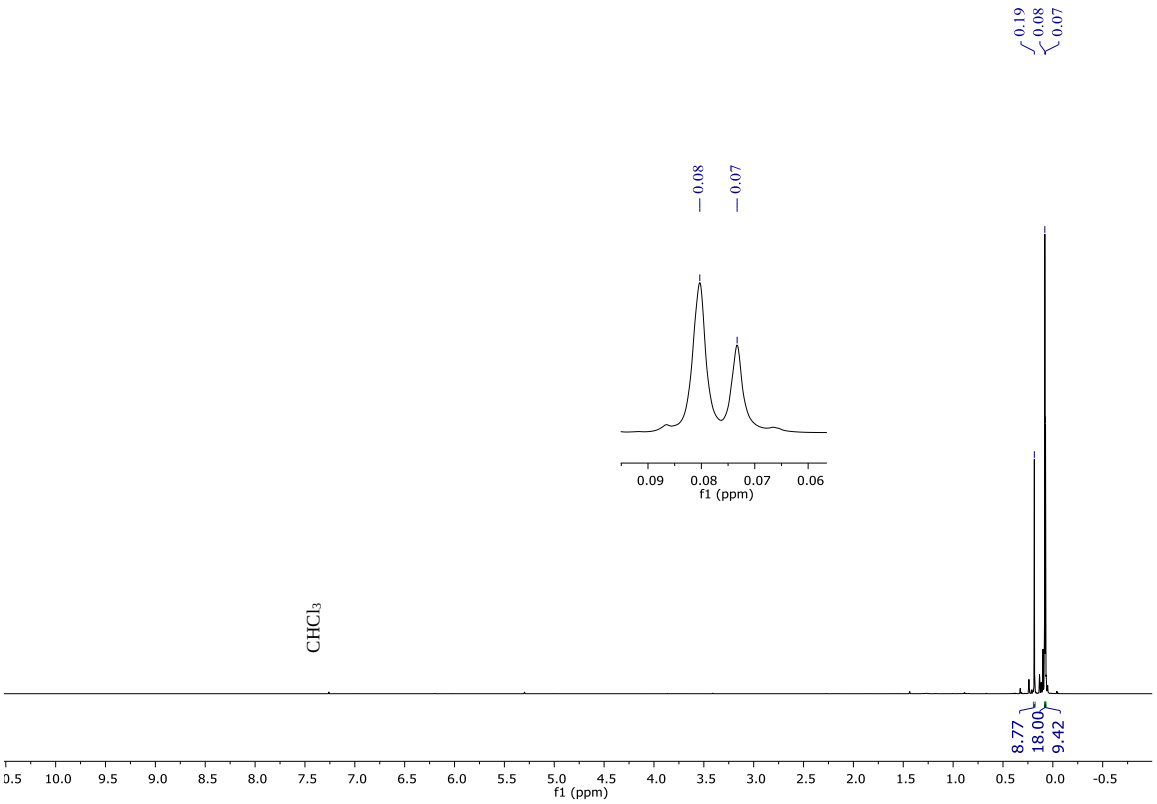

Figure S43: ^{1}H NMR spectrum of the product from the reaction of *in situ* generated Li[**4**] with Me_3SnCl, which was identified as **5** ($CDCl_3$, 500.2 MHz).

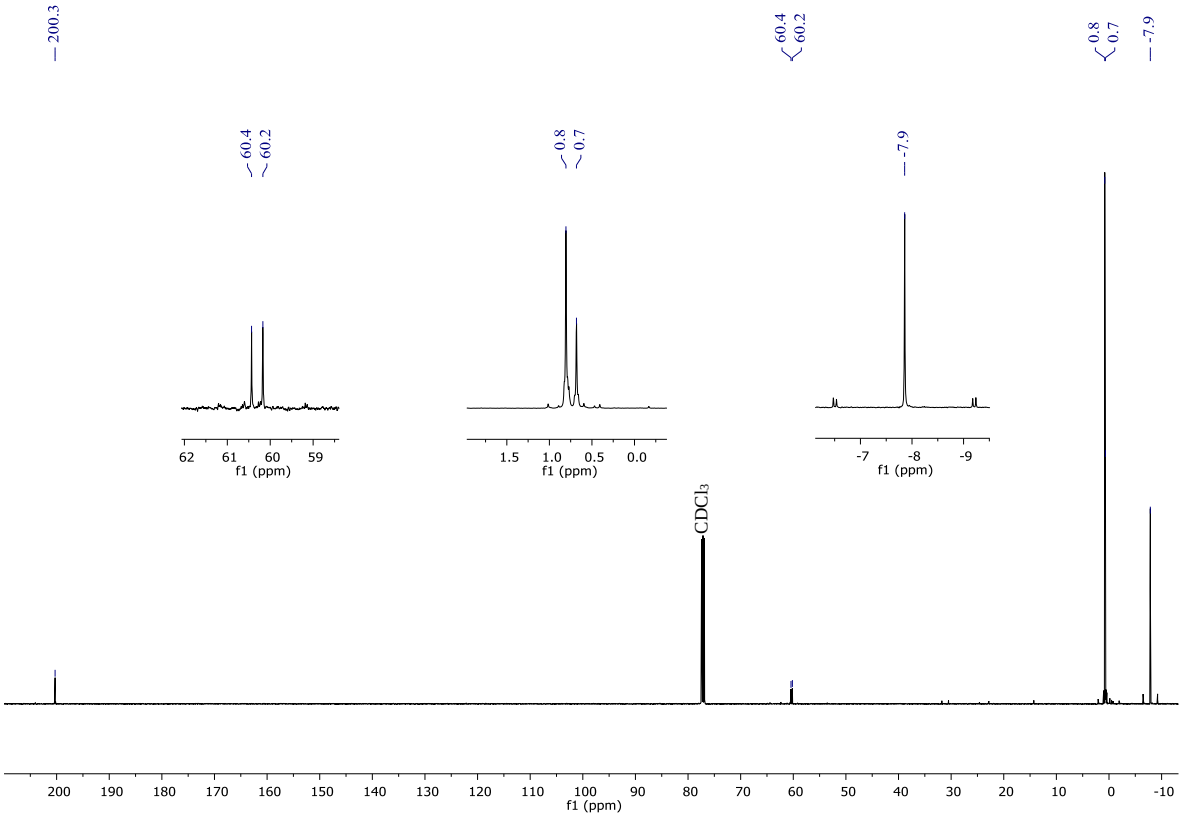

Figure S44: $^{13}C\{^{1}H\}$ NMR spectrum of the product from the reaction of *in situ* generated Li[**4**] with Me_3SnCl, which was identified as **5** ($CDCl_3$, 125.8 MHz).

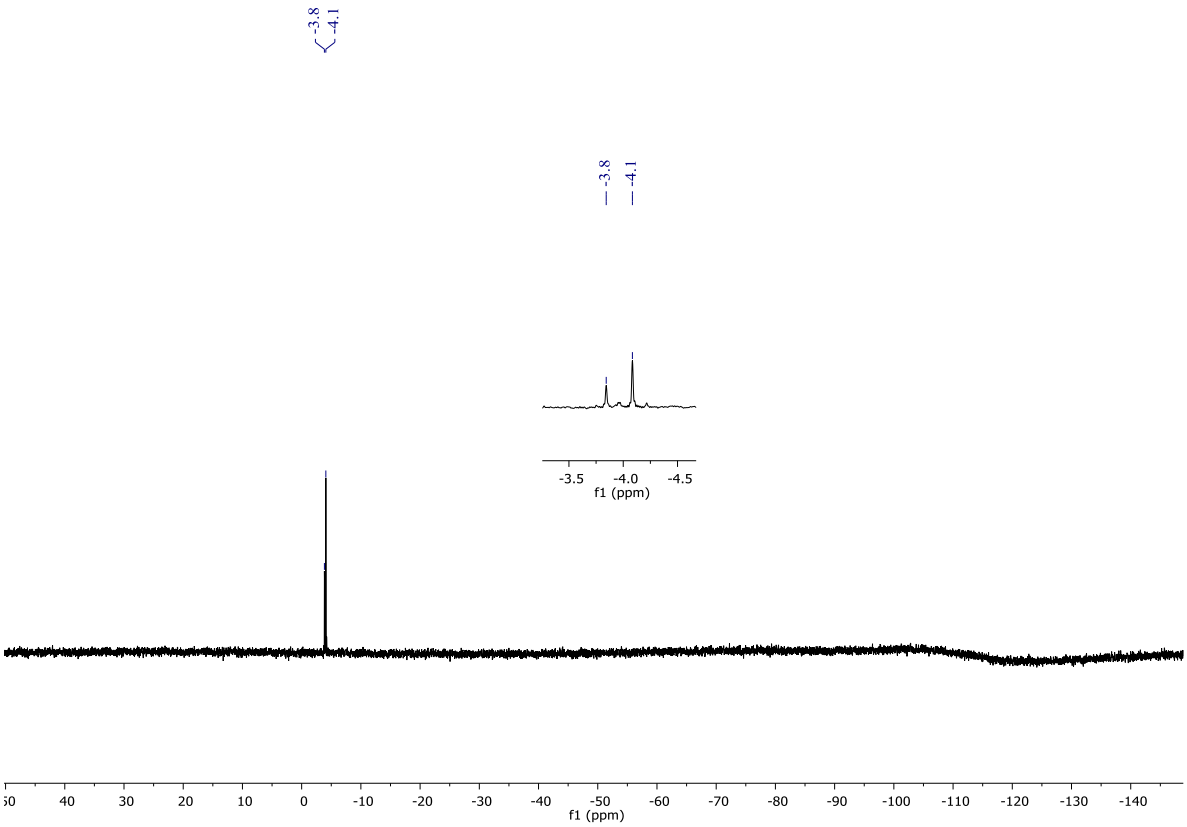

Figure S45: $^{29}Si\{^{1}H\}$ NMR spectrum of the product from the reaction of *in situ* generated Li[**4**] with Me_3SnCl, which was identified as **5** ($CDCl_3$, 99.4 MHz).

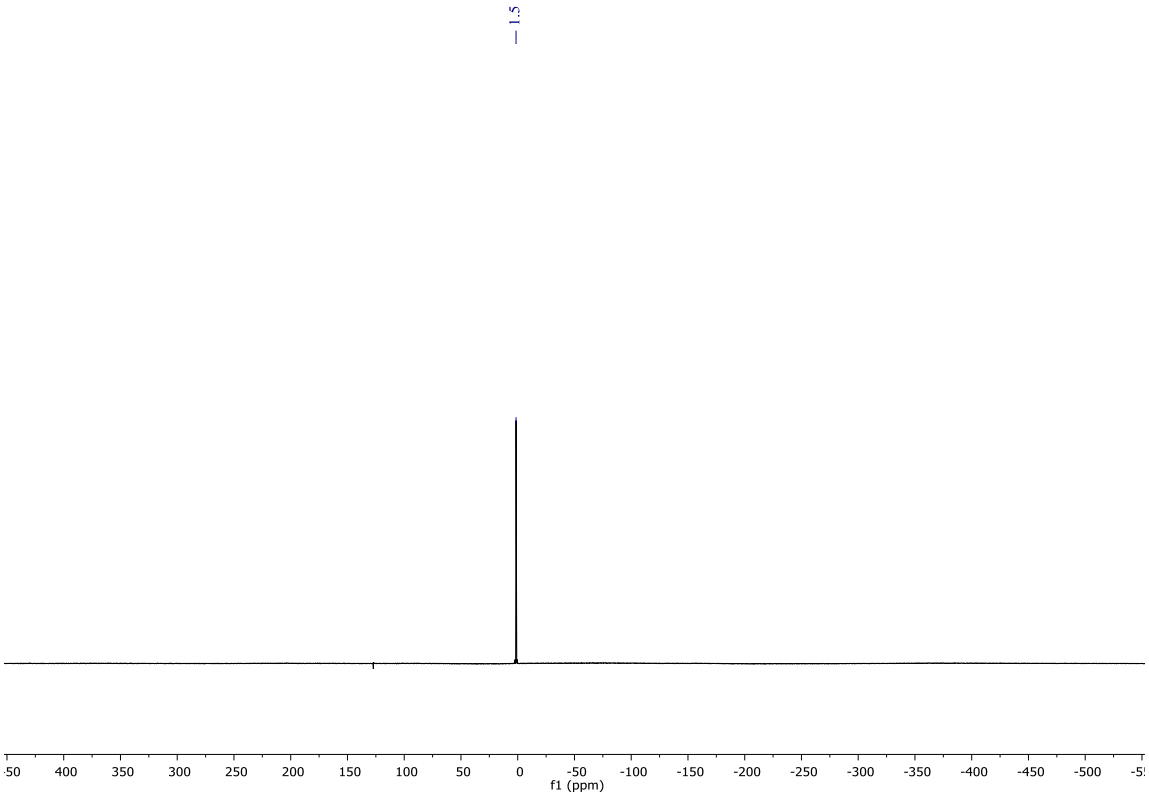

Figure S46: $^{119}Sn\{^{1}H\}$ NMR spectrum of the product from the reaction of *in situ* generated Li[**4**] with Me_3SnCl, which was identified as **5** ($CDCl_3$, 186.5 MHz).

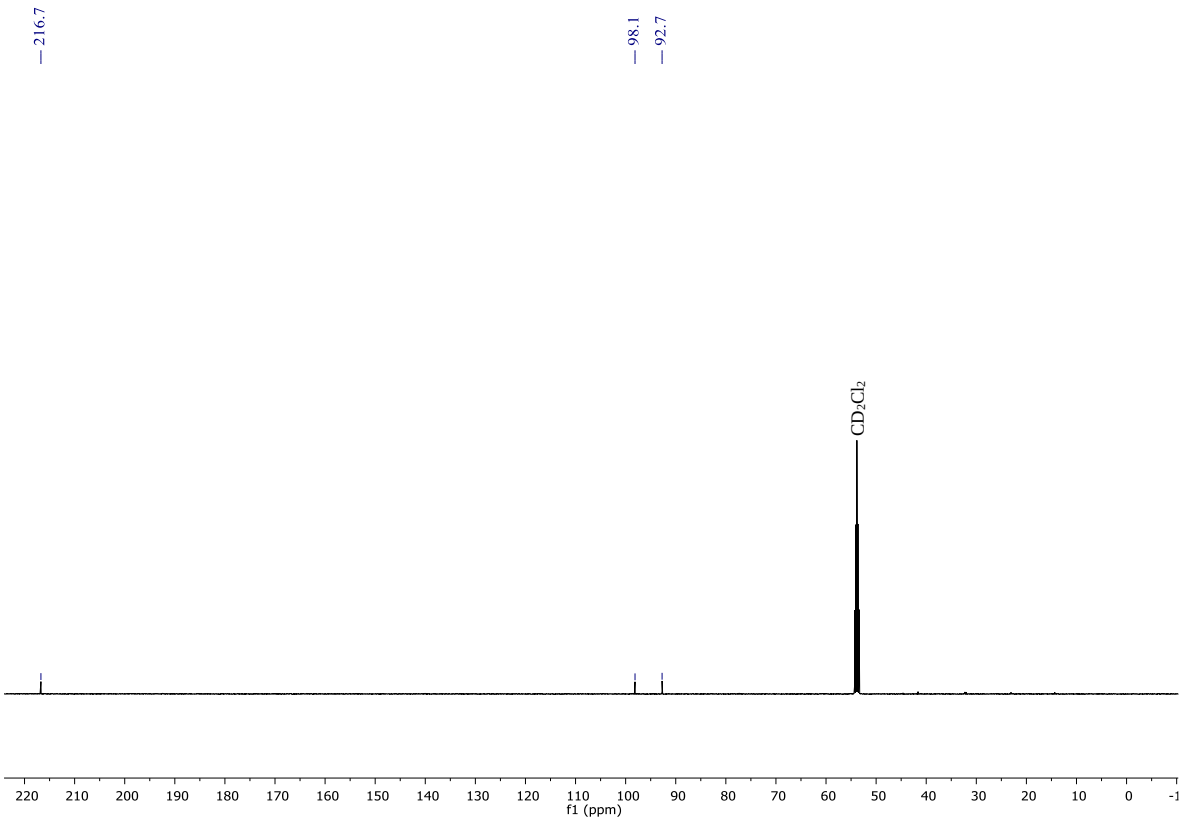

Figure S47: $^{13}C\{^{1}H\}$ NMR spectrum of **6** (CD_2Cl_2, 125.8 MHz).

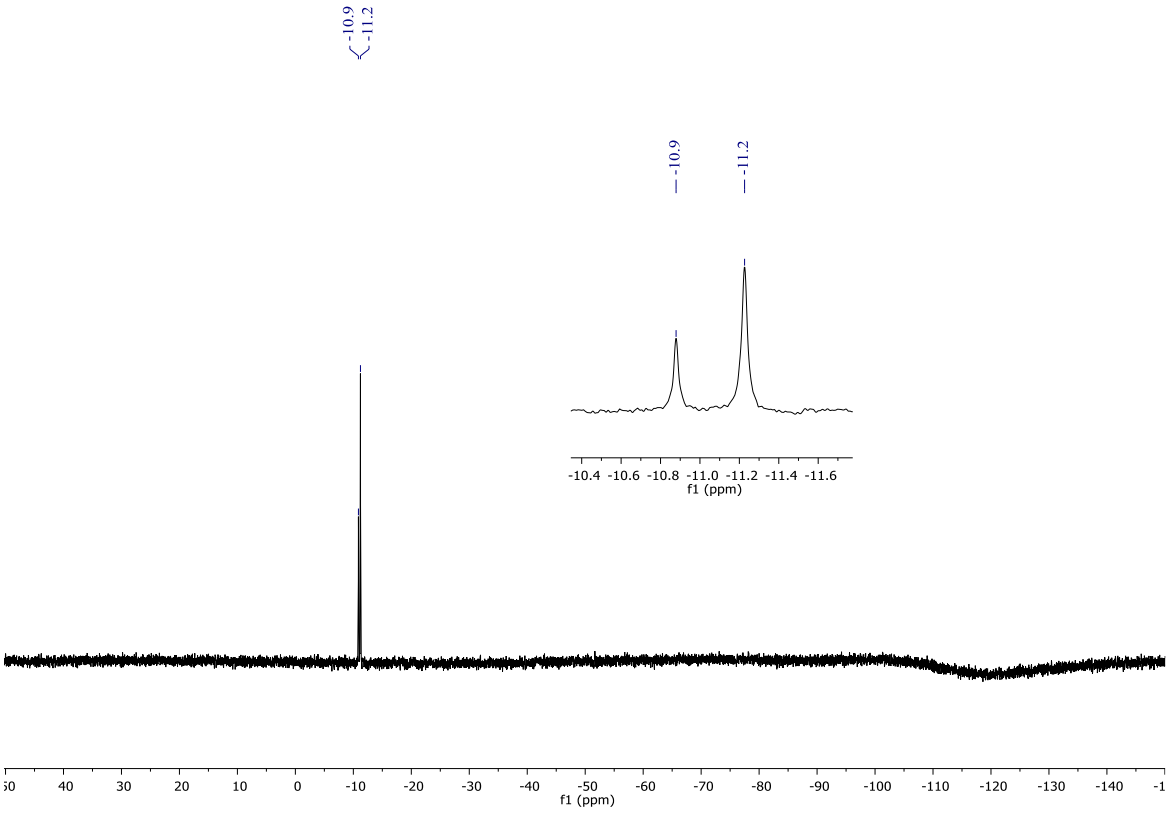

Figure S48: $^{29}Si\{^{1}H\}$ NMR spectrum of **6** (CD_2Cl_2, 99.4 MHz).

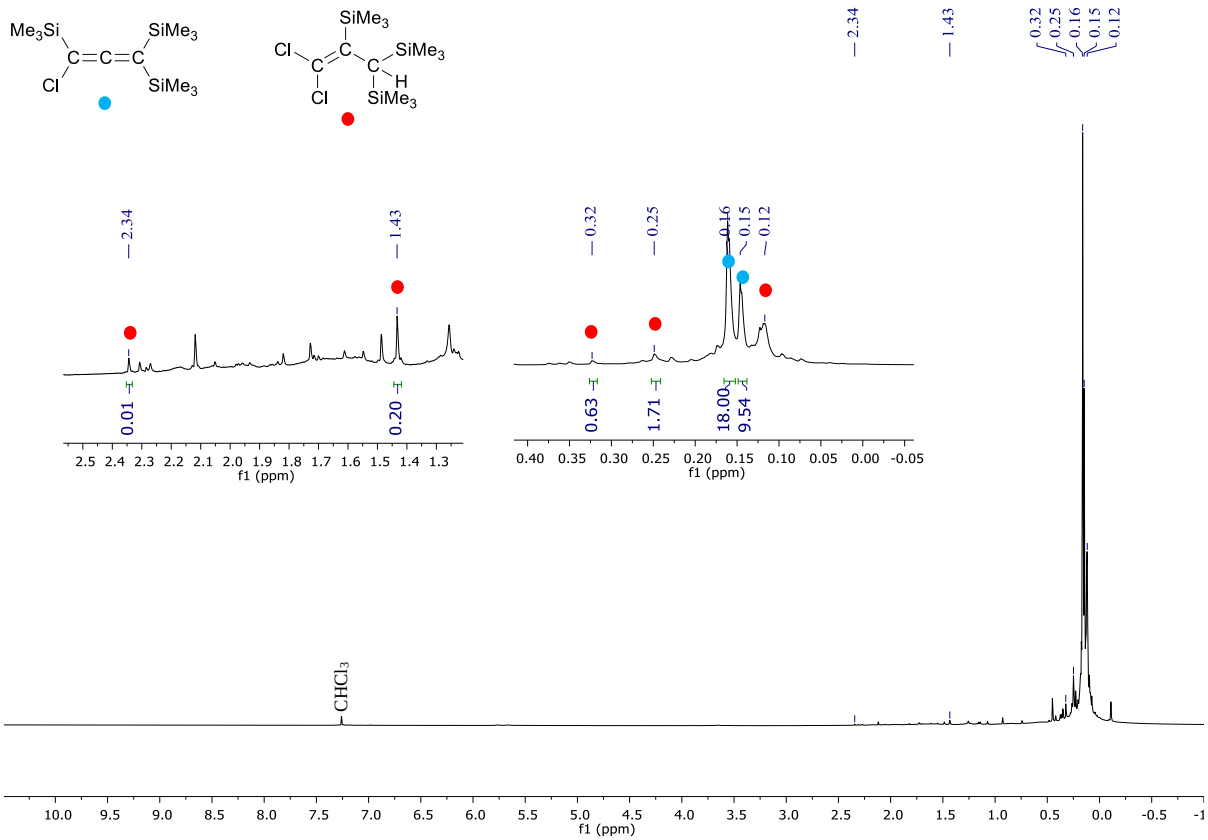

Figure S49: ^{1}H NMR spectrum of the product mixture consisting of **6**^{Me} and **2**^{Me} which results from the reaction of **6** and **2** with MeMgBr ($CDCl_3$, 500.2 MHz).

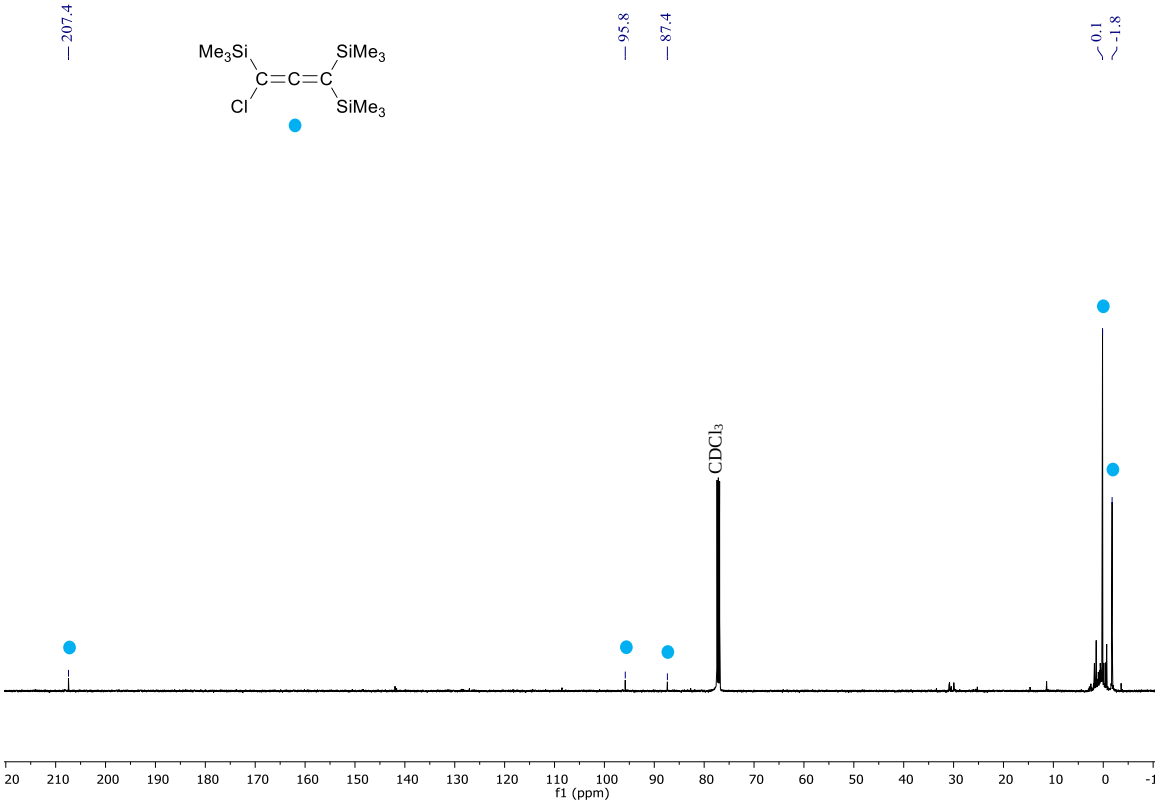

Figure S50: $^{13}C\{^{1}H\}$ NMR spectrum of the product mixture consisting of **6**^{Me} and **2**^{Me} which results from the reaction of **6** and **2** with MeMgBr ($CDCl_3$, 125.8 MHz). Due to the small amount of **2**^{Me}, the signals are only detectable in ^{1}H NMR spectrum.

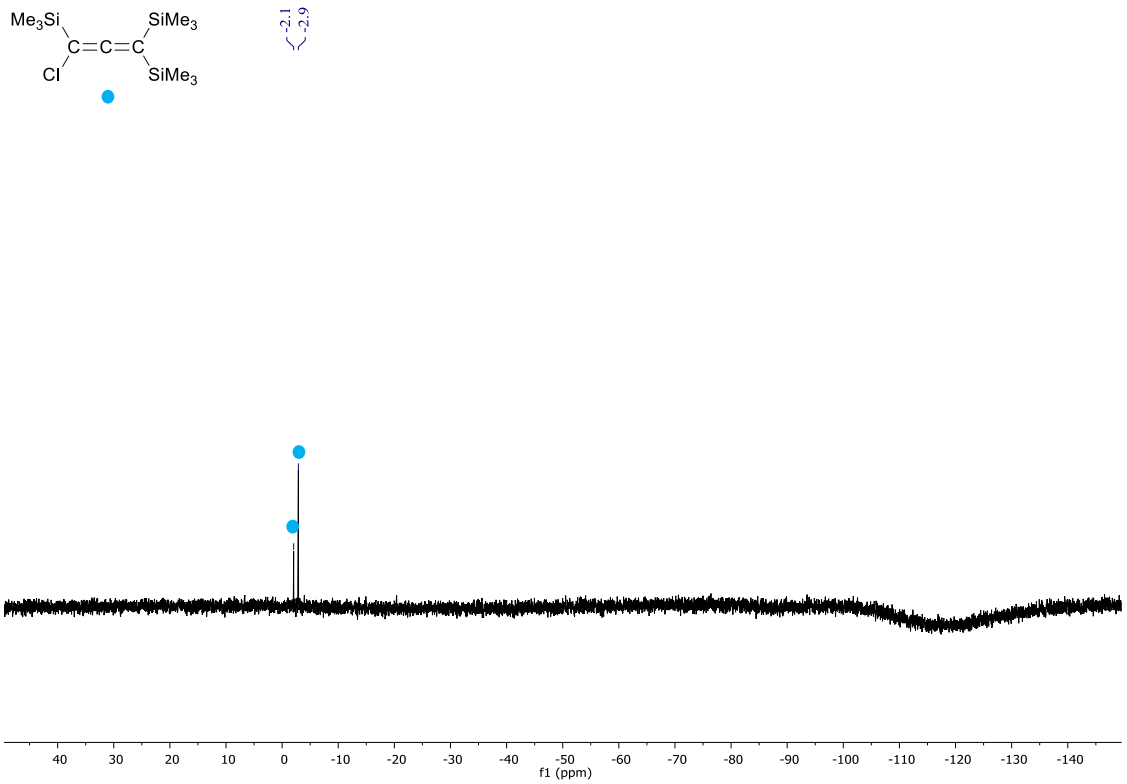

Figure S51: $^{29}Si\{^{1}H\}$ NMR spectrum of the product mixture consisting of **6**^{Me} and **2**^{Me} which results from the reaction of **6** and **2** with MeMgBr ($CDCl_3$, 99.4 MHz). Due to the small amount of **2**^{Me}, the signals are only detectable in ^{1}H NMR spectrum.

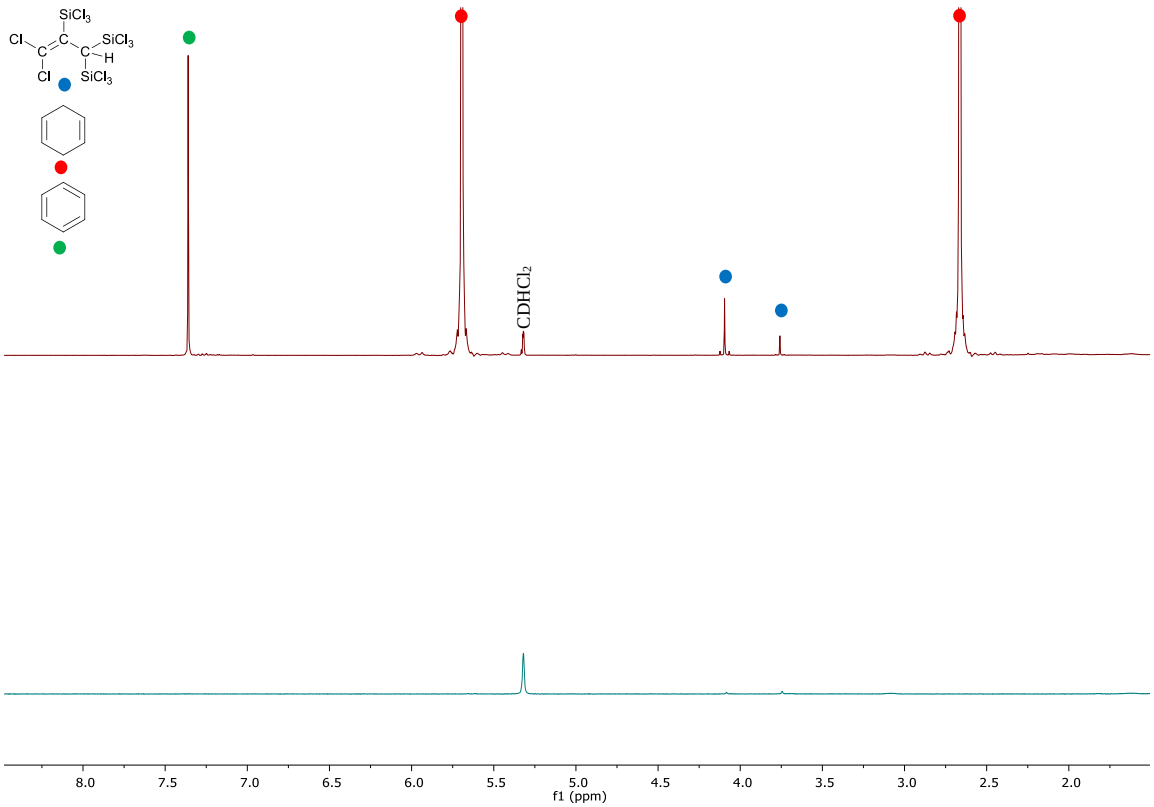

Figure S52: ^{1}H NMR spectra of **1**$^{\bullet}$ (blue, bottom) and 6 h after the addition of 1,4-cyclohexadiene (red, top) which furnishes **2** and benzene (CD_2Cl_2, 300.0 MHz).

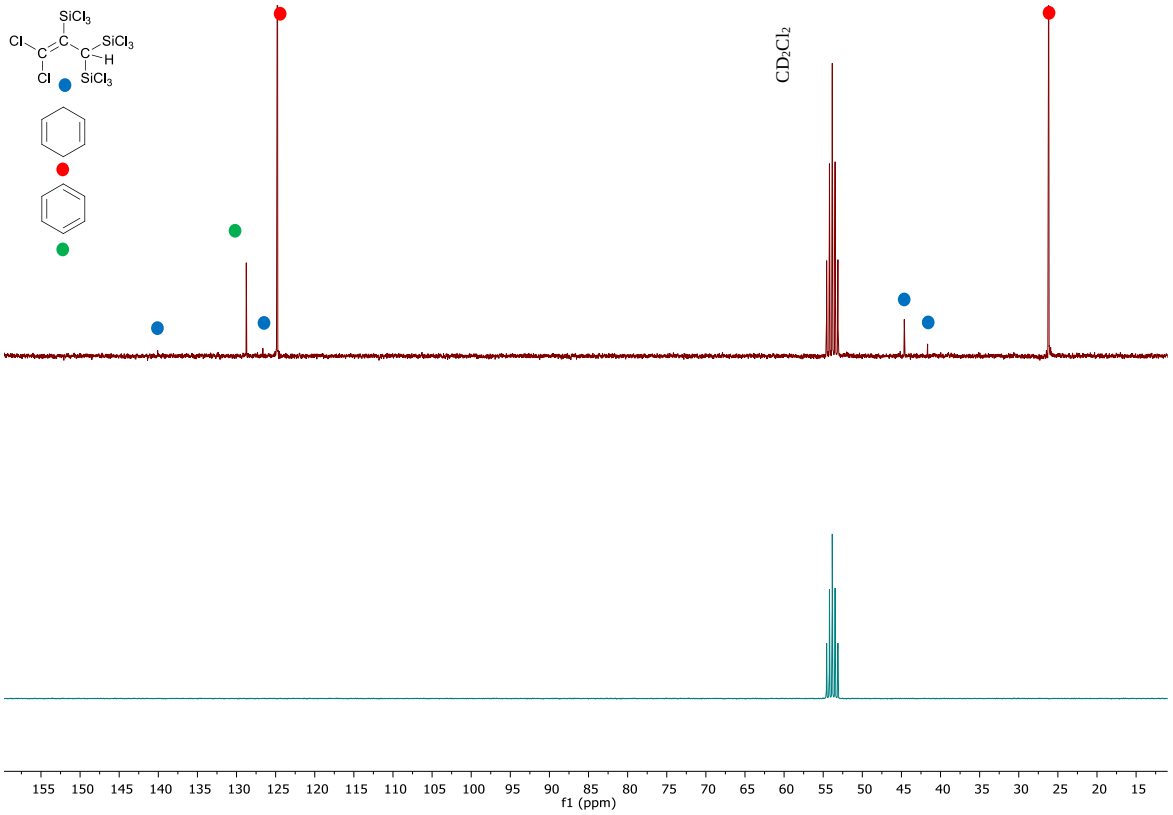

Figure S53: $^{13}C\{^{1}H\}$ NMR spectra of **1˙** (blue, bottom) and 6 h after the addition of 1,4-cyclohexadiene (red, top) which furnishes **2** and benzene (CD_2Cl_2, 75.5 MHz).

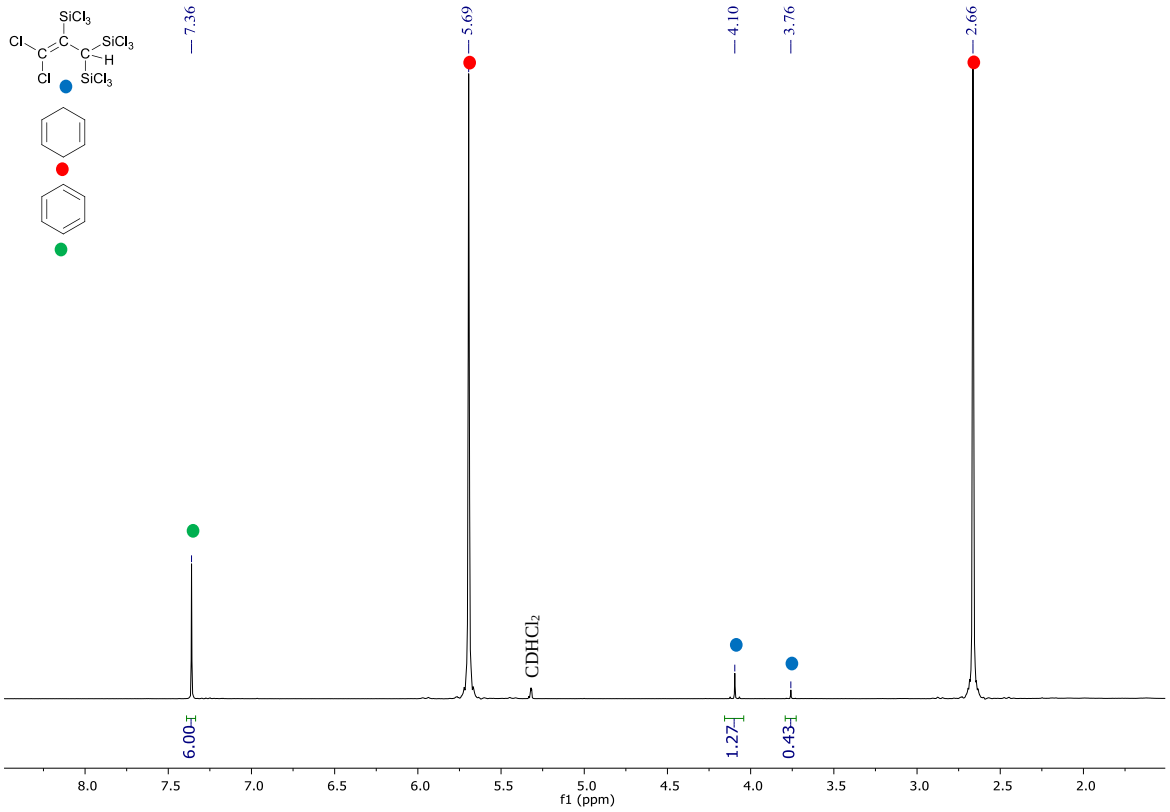

Figure S54: ^{1}H NMR spectrum of the reaction mixture of **1˙** and 1,4-cyclohexadiene which furnishes **2** and benzene (CD_2Cl_2, 300.0 MHz).

3. Low-temperature NMR-spectroscopic monitoring of the formation of [*n*Bu$_4$N][1]

Neat Si_2Cl_6 (0.108 g, 0.402 mmol) was added dropwise via syringe at –198 °C to an NMR tube charged with a solution of [*n*Bu$_4$N]Cl (0.028 g, 0.101 mmol) and C_3Cl_6 (0.026 g, 0.105 mmol) in CD_2Cl_2 (0.5 mL). The tube was flame-sealed under vacuum and held at –198 °C until it was placed in the pre-cooled NMR spectrometer (–32 °C). Inside the spectrometer, the sample was warmed to –32 °C and $^{13}C\{^1H\}$ NMR spectra were recorded directly one after the other at intervals of about 30 min. All in all, the sample was held at –32 °C for 140 min, then stepwise warmed to –17 °C, –7 °C, 5 °C, and 15 °C and held for about 30 min at each of these temperatures. After storing the sample for 1 d at room temperature, the final $^{13}C\{^1H\}$ NMR spectrum was recorded (Figure S56).

Note: The purchased C_3Cl_6 batch was contaminated. The impurity has no effect on the reaction but gives rise to a signal at 50.3 ppm in the $^{13}C\{^1H\}$ NMR spectrum (Figure S55). For all other reactions described herein C_3Cl_6 was purified by flash chromatography prior to use.

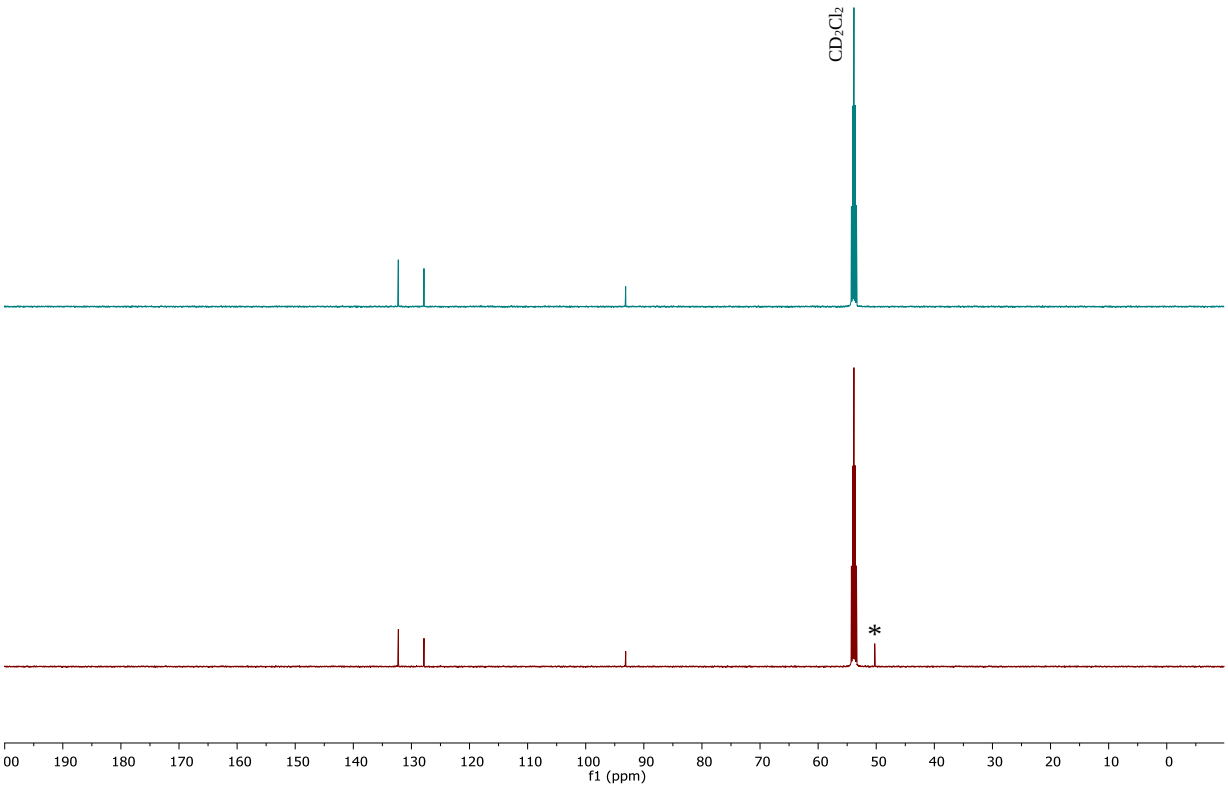

Figure S55: $^{13}C\{^1H\}$ NMR spectra of C_3Cl_6 as received (red, bottom) and after purification by flash chromatography (top, blue; CD_2Cl_2, 125.8 MHz). The signal marked with * belongs to the above-mentioned impurity

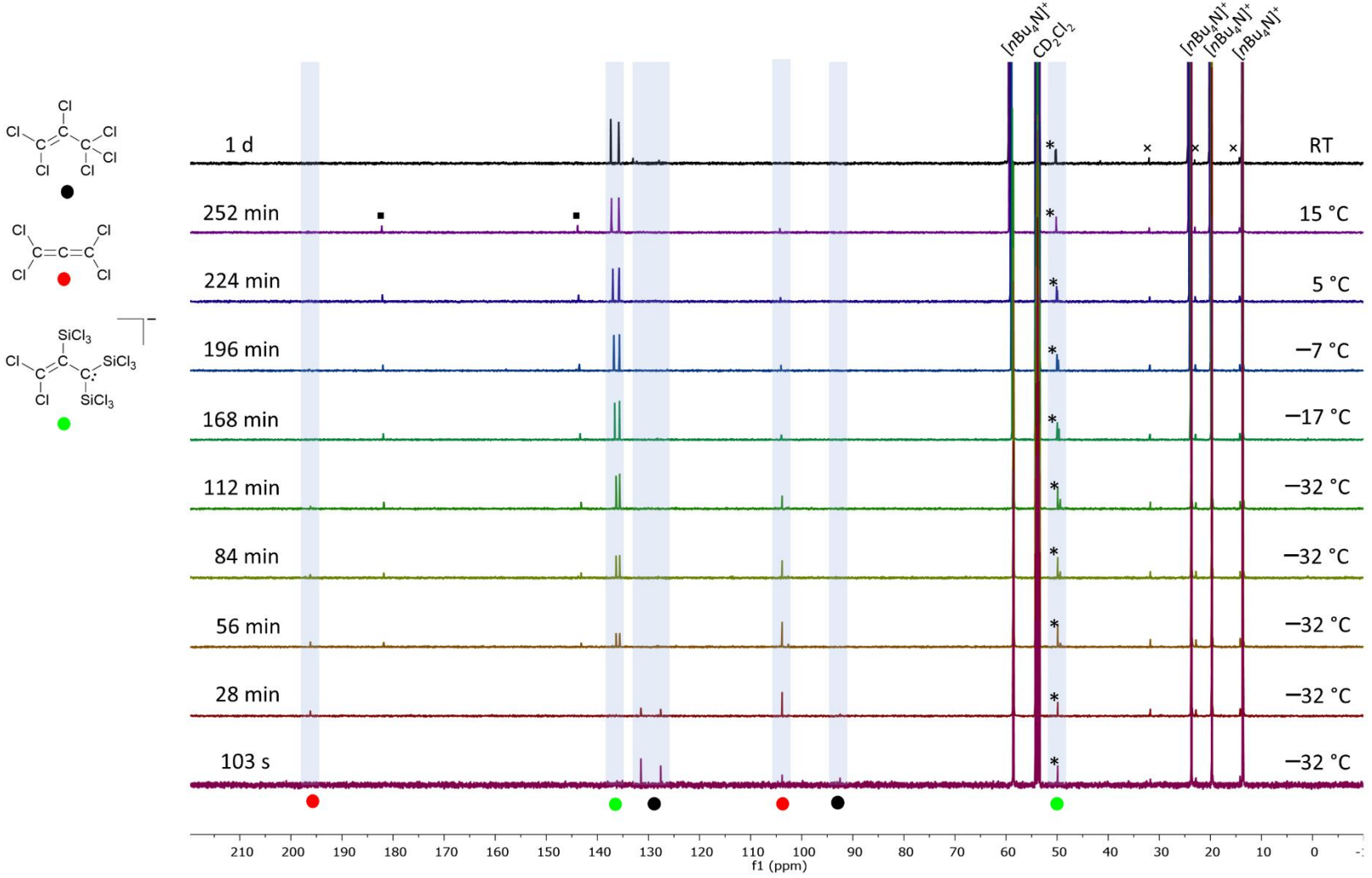

Figure S56: $^{13}C\{^{1}H\}$ NMR spectra recorded at the reaction mixture of C_3Cl_6 and Si_2Cl_6/Cl^- starting at –32 °C and stepwise warmed to room temperature (1:4:1; CD_2Cl_2, 125.8 MHz). The signal marked with * belong to the above-mentioned impurity from the purchased C_3Cl_6 batch. The signals marked with ▪ may be assigned to an unknown intermediate and signals marked with × belong to *n*-hexane.

4. X-ray crystal structure analysis of [Ph_4P][1]

Data were collected on a STOE IPDS II two-circle diffractometer with a Genix Microfocus tube with mirror optics using MoK_α radiation (λ = 0.71073 Å). The data were scaled using the frame-scaling procedure in the *X-AREA* program system.[S21] The structure was solved by direct methods using the program *SHELXS* and refined against F^2 with full-matrix least-squares techniques using the program *SHELXL*.[S22]

CCDC file CCDC 2078581 contain the supplementary crystallographic data for the structure [Ph_4P][**1**] and can be obtained free of charge from The Cambridge Crystallographic Data Centre via www.ccdc.cam.ac.uk/data_request/cif.

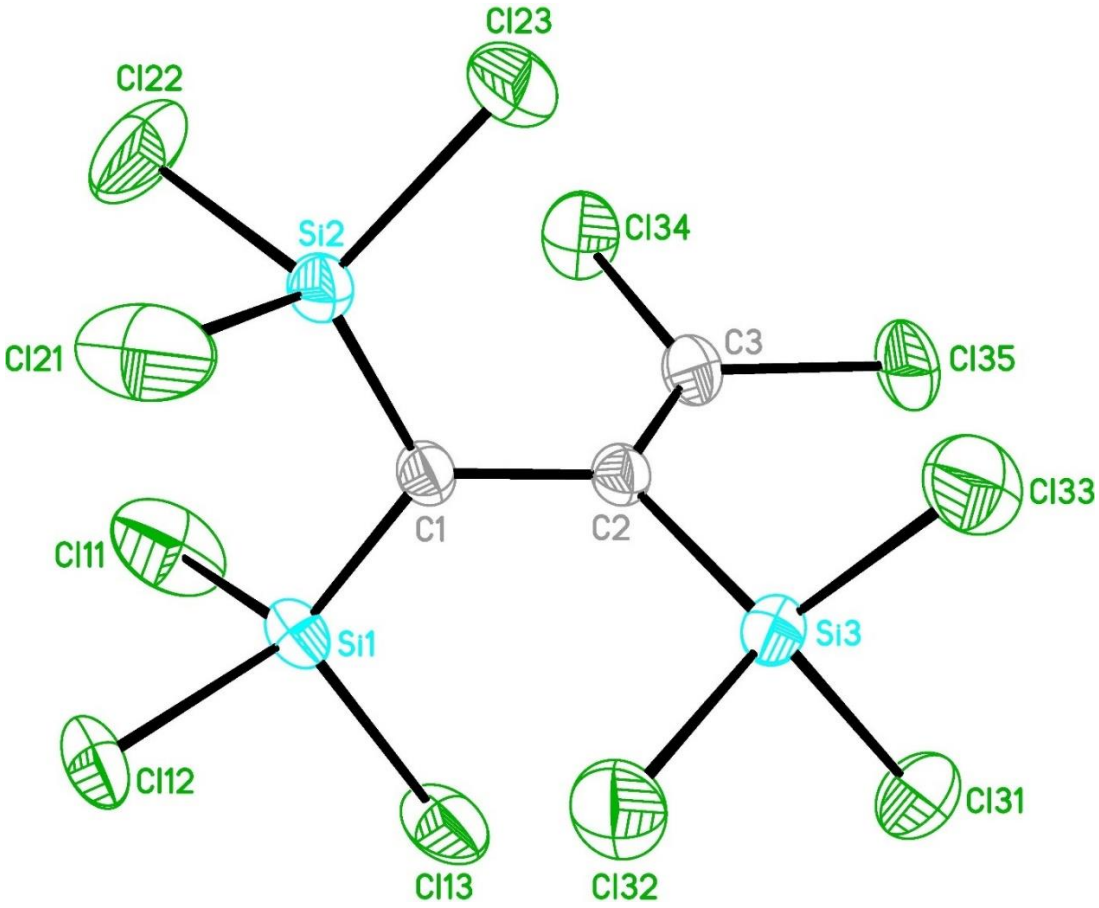

Figure S57: Molecular structure of [Ph_4P][**1**] in the solid state. Displacement ellipsoids are shown at the 50% probability level. The $[Ph_4P]^+$ cation is omitted for clarity. Selected bond lengths [Å], bond angles [°], torsion angles [°], and dihedral angle [°]: C(1)–C(2) = 1.484(3), C(2)–C(3) = 1.338(4), C(1)–Si(1) = 1.760(2), C(1)–Si(2) = 1.762(3), C(2)–Si(3) = 1.859(3), C(3)–Cl(34) = 1.724(3), C(3)–Cl(35) = 1.735(3); C(1)–C(2)–C(3) = 123.1(2), C(1)–C(2)–Si(3) = 117.8(2), C(2)–C(1)–Si(1) = 119.0(2), C(2)–C(1)–Si(2) = 120.3(2), C(3)–C(2)–Si(3) = 118.9(2), C(2)–C(3)–Cl(34) = 123.9(2), C(2)–C(3)–Cl(35) = 123.4(2), Si(1)–C(1)–Si(2) = 120.4(1), Cl(34)–C(3)–Cl(35) = 112.7(2); Si(1)–C(1)–C(2)–C(3) = 100.8(3), Si(2)–C(1)–C(2)–C(3) = –72.8(3), Si(1)–C(1)–C(2)–Si(3) = –83.9(2), Si(2)–C(1)–C(2)–Si(3) = 102.6(2); Si(1)C(1)Si(2)//Si(3)C(2)C(3) = 78.3(1).

Table S2. Crystal data and structure refinement for $[Ph_4P][\mathbf{1}]$.

Identification code	wa3034	
Empirical formula	$C_{27}\ H_{20}\ Cl_{11}\ P\ Si_3$	
Formula weight	849.62	
Temperature	173(2) K	
Wavelength	0.71073 Å	
Crystal system	Monoclinic	
Space group	$P\ 2_1/n$	
Unit cell dimensions	a = 13.4583(5) Å	α = 90°.
	b = 18.6349(7) Å	β = 95.151(3)°.
	c = 14.6168(5) Å	γ = 90°.
Volume	3651.0(2) Å^3	
Z	4	
Density (calculated)	1.546 Mg/m^3	
Absorption coefficient	0.999 mm^{-1}	
F(000)	1704	
Crystal size	0.350 x 0.240 x 0.180 mm^3	
Theta range for data collection	3.039 to 25.830°	
Index ranges	–16<=h<=16, –22<=k<=22, –17<=l<=17	
Reflections collected	31190	
Independent reflections	6838 [R(int) = 0.0349]	
Completeness to theta = 25.000°	99.8 %	
Absorption correction	Semi-empirical from equivalents	
Max. and min. transmission	1.000 and 0.316	
Refinement method	Full-matrix least-squares on F^2	
Data / restraints / parameters	6838 / 0 / 379	
Goodness-of-fit on F^2	1.032	
Final R indices [I>2sigma(I)]	R_1 = 0.0382, wR_2 = 0.0940	
R indices (all data)	R_1 = 0.0512, wR_2 = 0.1019	
Largest diff. peak and hole	0.532 and –0.519 e Å^{-3}	

5. Plots of the LDI-MS(–) of [*n*Bu$_4$N][1]

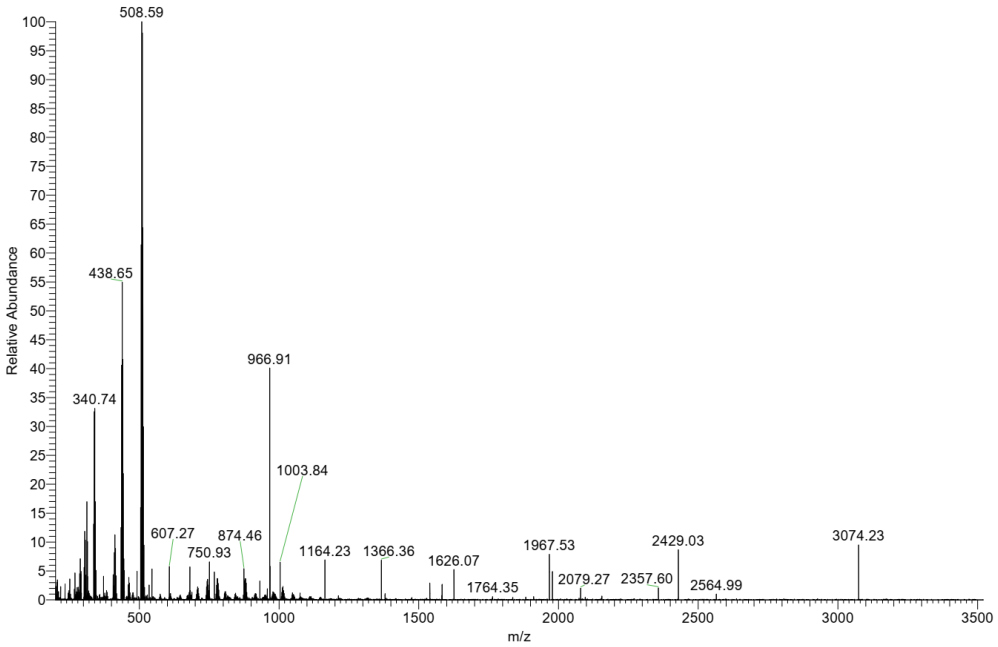

Figure S58: LDI(–) mass spectrum of [*n*Bu$_4$N][**1**]; *m*/*z* = 508.59 is the molecular-ion peak of [**1**]$^-$.

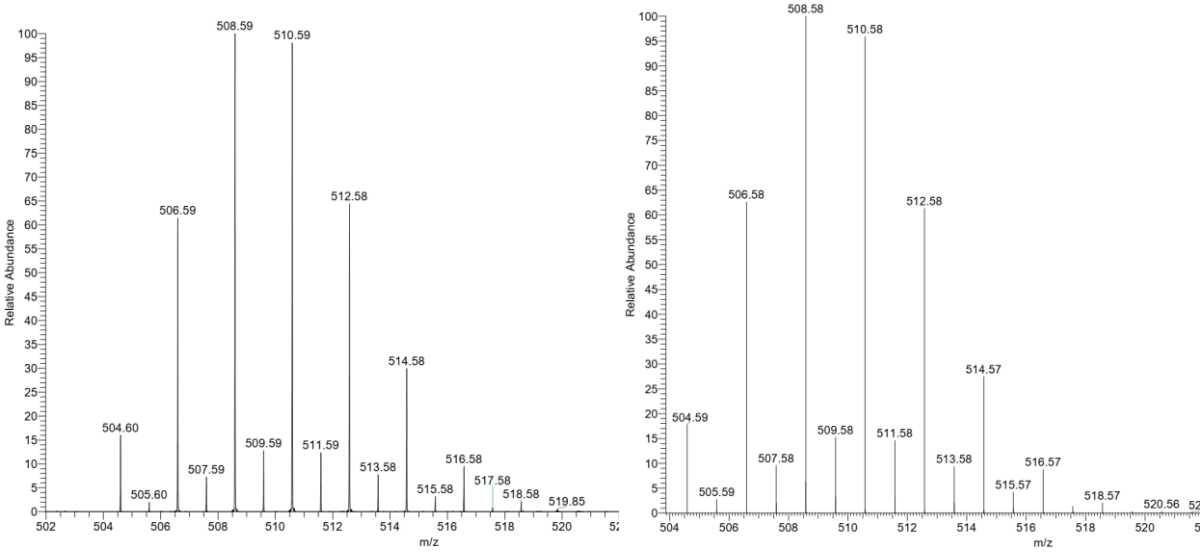

Figure S59: Isotopic pattern of the molecular-ion peak of [**1**]$^-$ (left: experimental signal pattern from LDI(–) mass spectrum; right: simulated signal pattern).

6. Plots of the IR spectra of I, 5, and 6

The highlighted bands originate from the characteristic antisymmetrical C=C=C stretching vibrations, which are specific for the allene bond system.[S23]

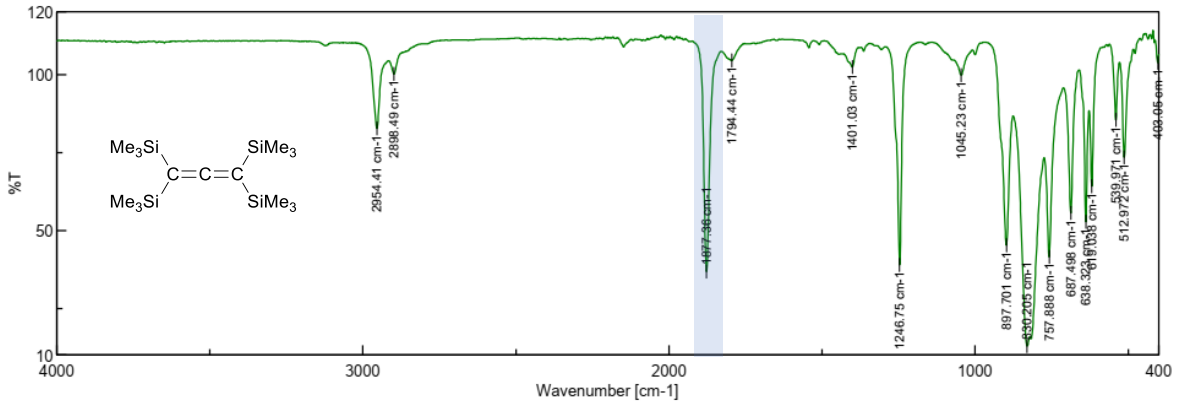

Figure S60: IR spectrum (ATR) of **I**.

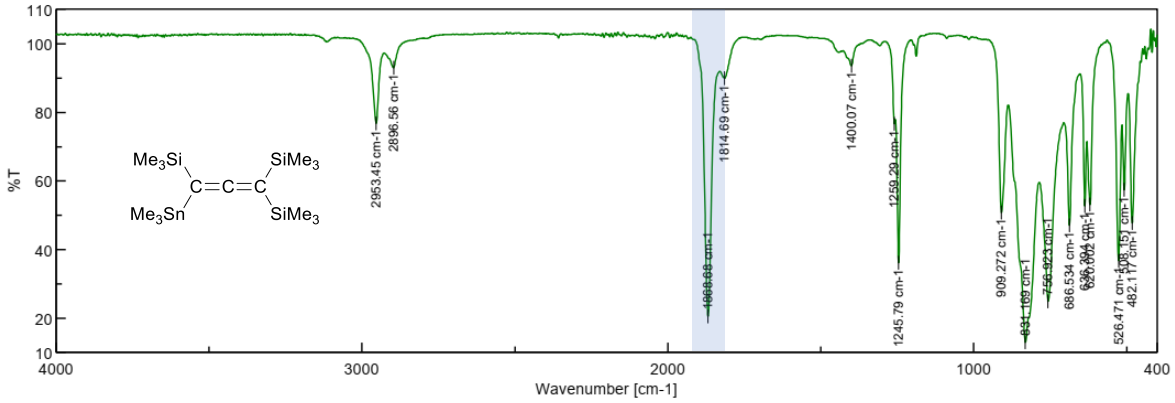

Figure S61: IR spectrum (ATR) of **5**.

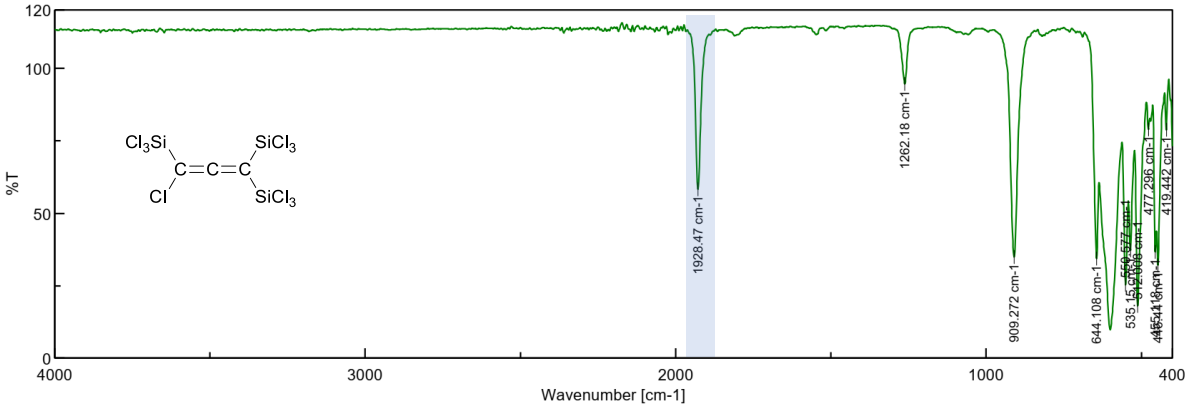

Figure S62: IR spectrum (ATR) of **6**.

7. EPR spectrum of 1$^{\bullet}$

In the glove box, a small volume (0.05 mL) of **1**$^{\bullet}$ in CH_2Cl_2 (c = 0.48 mM) was transferred via syringe into a 3 mm EPR quartz tube (inner diameter: 2 mm). The tube was covered with a plastic cap. The CW EPR spectrum was recorded at room temperature on an EMXnano (*Bruker*) tabletop EPR spectrometer using its Xenon controlling/recording software. Parameters of the shown EPR spectrum: microwave frequency = 9.64 GHz; power = 1 mW; field modulation = 1 G; recording time = 80 sec. The EPR spectrum was simulated and finally fitted using the garlic (isotropic and fast motion) and esfit function (least-squares fitting) of the program easyspin.[S24]

8. UV/vis absorption spectrum of 1• and monitoring of its decomposition in air

UV/vis absorption spectra were measured on a solution of **1•** in CH_2Cl_2 (c = 150 µM). The sample was prepared inside the glove box, transferred to the cuvette, and the cuvette was closed. After the first UV/vis measurement (see Figure S63 black curve "inert sample", ε = 11023 $M^{-1} \cdot cm^{-1}$), the cuvette was opened under ambient atmosphere for ~5 s and was closed again. A second spectrum was measured (see violet curve "opened"). Measurements were repeated every 30 min for a total of 4 h. A final spectrum was recorded after 14 h, during which time the color had completely disappeared (Figure S63). After each measurement, a photo of the cuvette was taken (Figure S65).

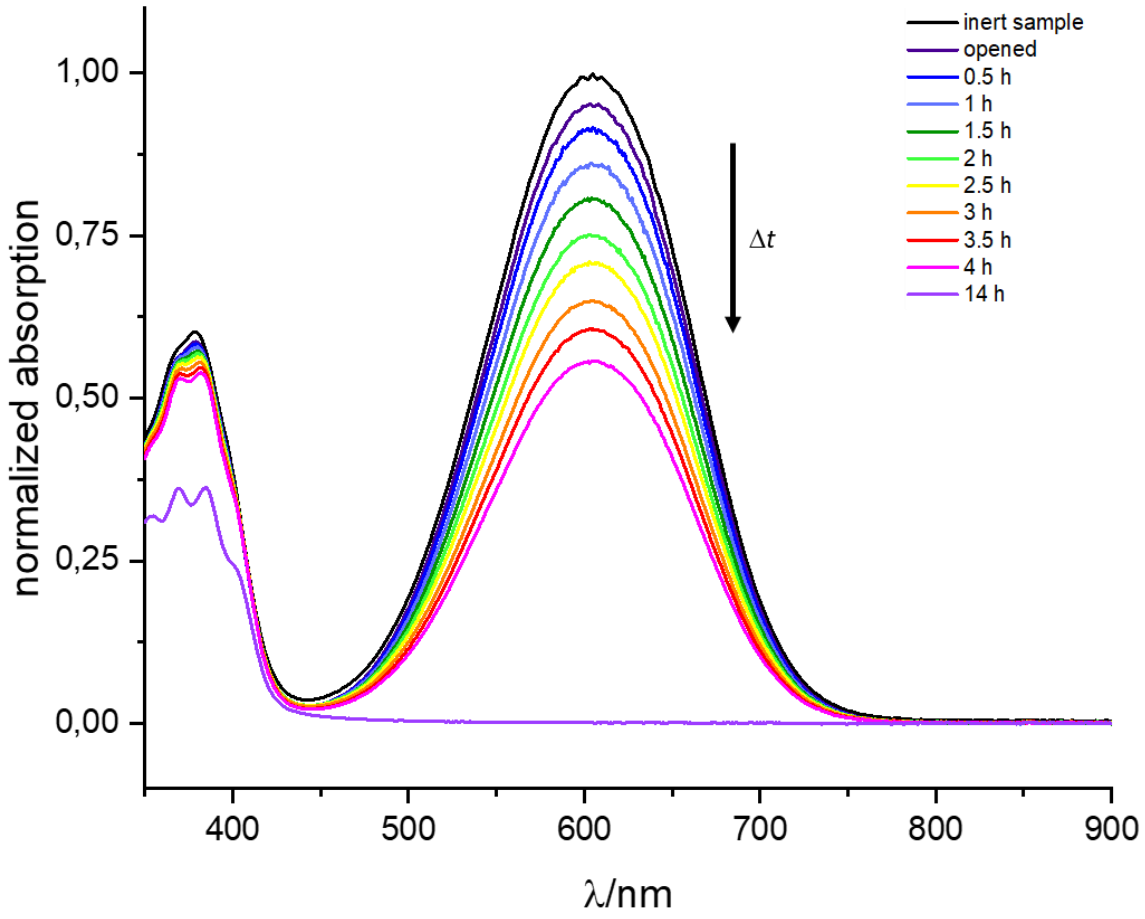

Figure S63: UV/vis absorption spectra of **1•** in CH_2Cl_2, recorded under inert conditions (black curve) and after the cuvette was opened to the ambient atmosphere (c = 150 µM, λ_{max} = 605 nm).

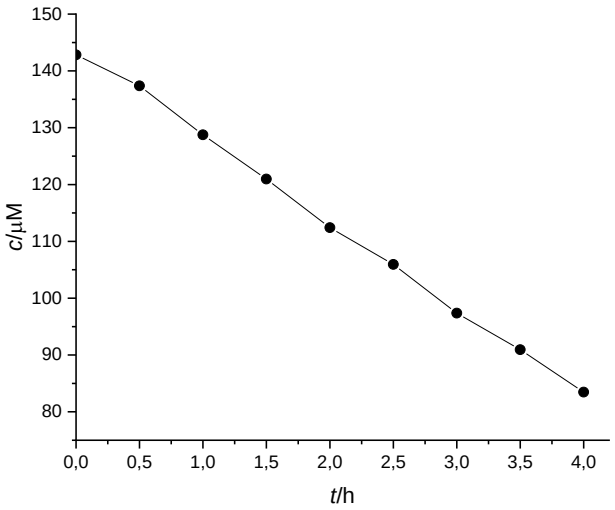

Figure S64: Linear decrease of the concentration of **1**$^{\bullet}$ in CH_2Cl_2 over time after the cuvette was opened to the ambient atmosphere (t = 0 h).

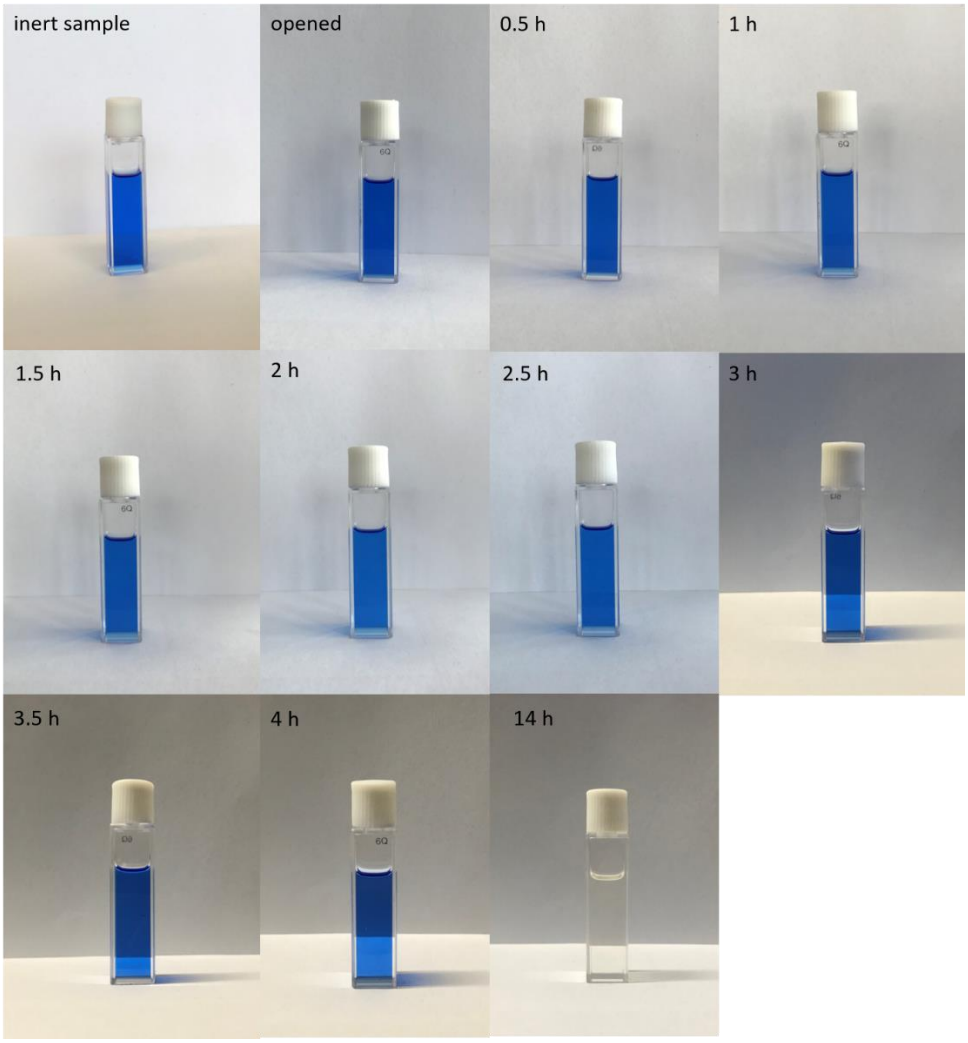

Figure S65: Cuvette charged with **1**$^{\bullet}$ in CH_2Cl_2 under inert conditions, after the cuvette was opened to ambient atmosphere, and after 0.5 – 14 h standing at room temperature.

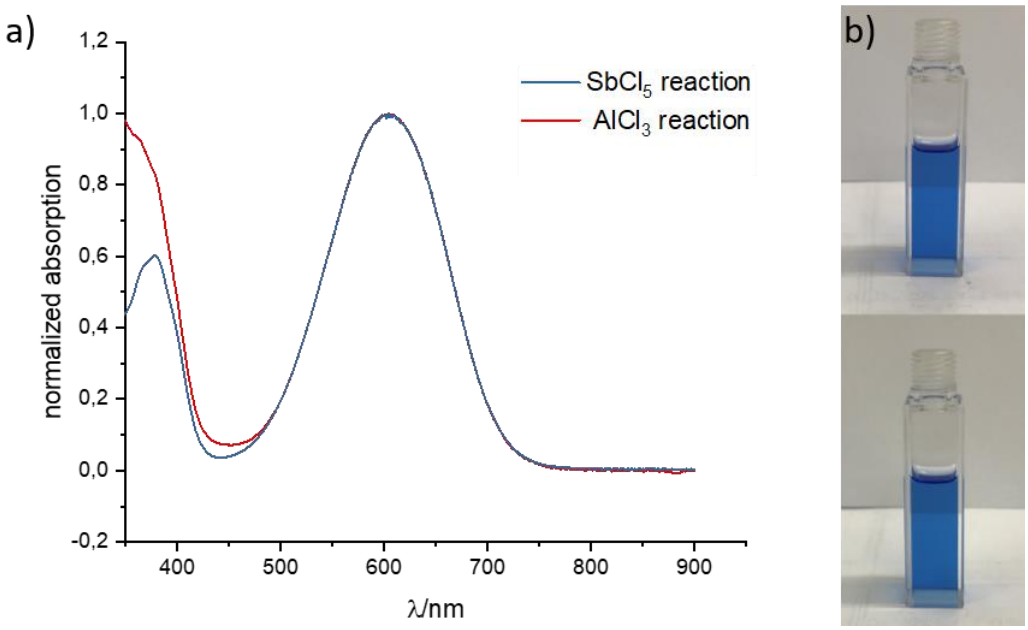

Figure S66: a) UV/vis absorption spectra of **1**$^{\bullet}$ in CH_2Cl_2. The radical was generated from the reaction of [*n*Bu_4N][**1**] with $SbCl_5$ (blue; *c* = 150 µM, λ_{max} = 605 nm) or $AlCl_3$ (red; mixture with colorless **6**, λ_{max} = 604 nm); b) **1**$^{\bullet}$ in CH_2Cl_2 immediately after exposure to ambient atmosphere (top) and after exposure to ambient atmosphere for 15 min (bottom). The still persistent blue color indicates a surprisingly low sensitivity of the radical toward air and moisture.

9. Cyclic voltammogram of [*n*Bu$_4$N][1]

The cyclic voltammogram of [*n*Bu$_4$N][**1**] in CH_2Cl_2 shows one (quasi)reversible redox process at a half-wave potential of $E_{1/2}$ = 0.06 V.

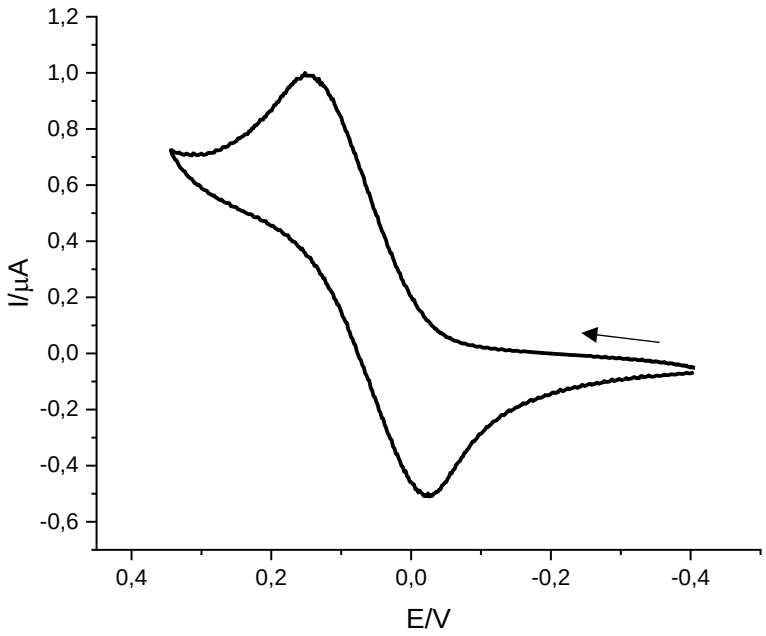

Figure S67: Cyclic voltammogram of [*n*Bu$_4$N][**1**] in CH_2Cl_2 at room temperature; vs. FcH/FcH+, supporting electrolyte: [*n*Bu$_4$N][B(C_6F_5)$_4$] (0.05 M), scan rate: 200 mVs^{-1}.

10. Computational details

General remarks, geometry optimizations and single point energies

Structures, orbitals and densities were visualized with UCSF Chimera[S25] 1.10.2. Quantum-mechanical calculations were performed with the ORCA 4.2.1[S26,S27] and xtb 6.5[S28,S29] program packages. Geometries were pre-optimized with the GFN2-xTB[S30] extended tight binding method applying the generalized born solvation with solvent accessible surface (GBSA)[S31] model for CH_2Cl_2. Final geometries were optimized applying the London dispersion-corrected ωB97X-D3BJ[S32–S34] range-separated hybrid density functional in conjunction with the minimally augmented ma-def2-TZVP[S35] basis set including diffuse basis functions to improve the description of anionic systems and the CPCM[S36] implicit continuum solvation model for CH_2Cl_2 as implemented in ORCA. For geometry optimizations, the *GRID4* option was employed and default convergence criteria for energies and gradients were applied as implemented in ORCA. Minimum structures were verified as minima on the potential energy surface by the absence of imaginary frequencies ($i\omega > 35$ cm^{-1}) in the harmonic vibrational frequency calculation. Imaginary frequencies below this threshold were inverted and included in the thermostatistical correction except for very flat transition states. All calculations were accelerated by applying the resolution-of-identity (RI) approximation for Coulomb integrals[S37] with matching default auxiliary basis sets.[S38] Transition state search was performed with the molecular growing string method (GSM) by Zimmermann and co-workers in conjunction with GFN2-xTB(GBSA).[S39–41]

Ro-vibrational corrections to obtain free energies were obtained from a modified rigid rotor harmonic oscillator statistical treatment[S42] (T = 25.0 °C, 1 atm pressure) based on harmonic frequencies calculated at the geometry optimization level. To avoid errors in the harmonic approximation, frequencies with wave numbers below 100 cm^{-1} were treated partially as rigid rotors.[S42]

Gas phase single point energies were calculated at the ωB97X-D3BJ/ma-def2-QZVPP[S43] level applying the *GRID7* option.

Solvation corrections and Gibbs free energies

Solvation effects were further considered by the COSMO-RS[S44,S45] model, used as implemented in COSMOtherm (Version C3.0, release 16.01)[S46] with the 2016 fine parameterization for CH_2Cl_2 (parameter file: BP_TZVPD_FINE_C30_1601.ctd; default G_{solv} option). Calculated solvation corrections were further corrected for the volume work of 1 bar to 1 M ideal gas.

Final Gibbs free energies were obtained by summing the gas phase single point energy E, the dispersion correction $E_{Disp.}$, the ro-vibrational correction G_{RRHO} and the solvation correction $\delta G_{solv., corr.}$ (Eq. S1).

$$G_{tot.} = E + E_{Disp.,} + G_{RRHO} + \delta G_{solv., corr.} \quad \text{(Equation S1)}$$

UV/vis and EPR spectra calculations

UV/vis spectra were calculated applying the Tamm-Dancoff approximation (TDA)[S47] to time-dependent density functional theory (TDA-DFT) at the ωB97X-D3BJ/ma-def2-TZVP(CPCM) level. The range-separation parameter μ was optimally tuned[S48] with μ = 0.158 being finally used for the calculation. The calculation was accelerated by applying RIJCOSX with the *GRID6*, *GRIDX6* option and *TightSCF* convergence criteria as implemented in ORCA.

EPR parameter were calculated at the ωB97X-D3BJ/ma-def2-TZVP(CPCM) level applying the *GRID6* option and the GIAO[S49] approach.

Tabulated energy contributions

Table S3. Tabulated contributions to G_{tot}.

#	imag. freq.	E(ωB97X-D3BJ/ma-def2-QZVPP) / a.u.	E(ωB97X-D3BJ/ma-def2-QZVPP) / kcal·mol^{-1}	G_{RRHO} (25 °C) / kcal·mol^{-1}	$\delta G_{solv., corr.}$ (25 °C) / kcal·mol^{-1}	G_{tot} / kcal·mol^{-1}
[**1**]$^-$	0	-6046.20	-3794046.11	-8.19	-39.91	-3794094.21
[**1'**]$^-$	0	-6046.21	-3794053.67	-9.12	-39.79	-3794102.58
[**1''**]$^-$	0	-6046.17	-3794031.09	-9.75	-39.61	-3794080.45
[**1'''**]$^-$	0	-6046.208	-3794052.65	-8.860	-39.716	-3794101.23
F	0	-1955.256458	-1226941.95	-7.62	-3.52	-1226953.09
G	0	-3910.601888	-2453939.73	1.88	-8.67	-2453946.52
$SiCl_3^-$	0	-1670.445693	-1048220.50	-16.35	-45.24	-1048282.09
$SiCl_4$	0	-2130.684651	-1337024.81	-14.43	-2.33	-1337041.56
C_3Cl_6	-10	-2875.752522	-1804561.95	-6.95	-5.62	-1804574.52
Cl^-	0	-460.301300	-288843.43	-9.43	-67.21	-288920.07
Si_2Cl_6	-9	-3340.810952	-2096390.52	-16.54	-4.03	-2096411.10
INT1	0	-3625.752390	-2275193.98	-9.97	-43.19	-2275247.14
INT2	0	-5756.478067	-3612244.53	-8.09	-44.06	-3612296.67
INT3	0	-5296.124717	-3323368.44	-7.87	-8.89	-3323385.20
INT4	0	-4835.974400	-3034619.75	-9.71	-40.46	-3034669.92
INT5	0	-6506.313178	-4082773.16	-7.46	-10.23	-4082790.85
TS1	-132	-3625.708494	-2275166.43	-11.41	-41.49	-2275219.33
TS3	-113	-5756.455013	-3612230.06	-8.37	-55.05	-3612293.48
TS2	-11	-5756.447464	-3612225.32	-10.64	-42.26	-3612278.22
TS4	-324	-6966.579748	-4371594.80	-10.34	-41.53	-4371646.66
TS5	-131	-6966.639757	-4371632.45	-8.37	-54.34	-4371695.16
TS6	-303	-8176.776045	-5131004.44	-9.20	-41.76	-5131055.40
TS7	-270	-3910.486057	-2453867.05	-1.23	-7.68	-2453875.95
2A	0	-6046.720026	-3794374.10	-1.26	-9.47	-3794384.83
2B	0	-6046.720037	-3794374.11	-0.57	-9.46	-3794384.14
2^{Me}A	0	-2263.862048	-1420594.88	197.12	-7.25	-1420405.01
2^{Me}B	0	-2263.858403	-1420592.60	198.91	-7.20	-1420400.89
TS8	-39	-6046.149079	-3794015.83	-7.75	-40.51	-3794064.09
TS9	-36	-6046.667863	-3794341.37	0.35	-10.33	-3794351.35
TS10	-72	-2263.815138	-1420565.45	202.22	-7.78	-1420371.00
$[C_3(SiCl_3)_5]^-$	0	-8466.568244	-5312851.79	-8.02	-40.42	-5312900.23

11. References

S1 I. Georg, J. Teichmann, M. Bursch, J. Tillmann, B. Endeward, M. Bolte, H.-W. Lerner, S. Grimme and M. Wagner, *J. Am. Chem. Soc.*, 2018, **140**, 9696–9708.

S2 G. R. Fulmer, A. J. M. Miller, N. H. Sherden, H. E. Gottlieb, A. Nudelman, B. M. Stoltz, J. E. Bercaw and K. I. Goldberg, *Organometallics*, 2010, **29**, 2176–2179.

S3 J. Tillmann, L. Meyer, J. I. Schweizer, M. Bolte, H.-W. Lerner, M. Wagner and M. C. Holthausen, *Chem. Eur. J.*, 2014, **20**, 9234–9239.

S4 W. E. Billups and R. E. Bachman, *Tetrahedron Lett.*, 1992, **33**, 1825–1826.

S5 C. Korhummel and M. Hanack, *Chem. Ber.*, 1989, **122**, 2187–2192.

S6 H. Hopf, R. Stamm and P. G. Jones, *Chem. Ber.*, 1991, **124**, 1291–1294.

S7 Y. Y. Rusakov, L. B. Krivdin, V. M. Nosova, A. V Kisin and V. G. Lakhtin, *Magn. Reson. Chem.*, 2012, **50**, 665–671.

S8 L. B. Krivdin and Y. Y. Rusakov, *eMagRes*, 2014, **3**, 87–110.

S9 G. Maier, J. Neudert, O. Wolf, D. Pappusch, A. Sekiguchi, M. Tanaka and T. Matsuo, *J. Am. Chem. Soc.*, 2002, **124**, 13819–13826.

S10 R. West and P. C. Jones, *J. Am. Chem. Soc.*, 1969, **91**, 6156–6161.

S11 M. Pitkänen, K. Laihia and K. Schulze, *Org. Magn. Reson.*, 1984, **22**, 543–546.

S12 S. W. Collins, T. D. Alger, D. M. Grant, K. F. Kuhlmann and J. C. Smith, *J. Phys. Chem.*, 1975, **79**, 2031–2037.

S13 R. B. Bates, L. M. Kroposki and D. E. Potter, *J. Org. Chem.*, 1972, **37**, 560–562.

S14 J. Clayden and S. A. Yasin, *New J. Chem.*, 2002, **26**, 191–192.

S15 F. T. Oakes, F. A. Yang and J. F. Sebastian, *J. Org. Chem.*, 1982, **47**, 3094–3097.

S16 F. Reiß, M. Reiß, A. Spannenberg, H. Jiao, W. Baumann, P. Arndt, U. Rosenthal and T. Beweries, *Chem. Eur. J.*, 2018, **24**, 5667–5674.

S17 W. Priester and R. West, *J. Am. Chem. Soc.*, 1976, **98**, 8421–8425.

S18 J. Teichmann, C. Kunkel, I. Georg, M. Moxter, T. Santowski, M. Bolte, H. W. Lerner, S. Bade and M. Wagner, *Chem. Eur. J.*, 2019, **25**, 2740–2744.

S19 L. Liu, Z. Wang, X. Fu and C.-H. Yan, *Org. Lett.*, 2012, **14**, 5692–5695.

S20 D. Gleason, W. B.; Britton, *Cryst. Struct. Commun.*, 1982, **11**, 1159–62.

S21 Stoe & Cie., *X-AREA. Diffractometer control program system*, Stoe & Cie, Darmstadt, Germany, 2002.

S22 G. M. Sheldrick, *Acta Crystallogr. A.*, 2008, **64**, 112–122.

S23 J. H. Wotiz and D. E. Mancuso, *J. Org. Chem.*, 1957, **22**, 207–211.

S24 S. Stoll and A. Schweiger, *J. Magn. Reson.*, 2006, **178**, 42–55.

S25 E. F Pettersen, T. D. Goddard, C. C. Huang, G. S. Couch, D. M. Greenblatt, E. C. Meng, T. E. Ferrin, *J. Comput. Chem.* 2004, **25** , 1605–1612.

S26 F. Neese, Software Update: The ORCA Program System, Version 4.0. *Wiley Interdiscip. Rev.*

Comput. Mol. Sci. 2018, **8**, e1327.

S27 ORCA: An Ab Initio, Density Functional and Semiempirical Program Package , V. 4.2.1; MPI Für Kohlenforschung: Mülheim a. d. Ruhr, Germany, 2019. *ORCA: An ab initio, density functional and semiempirical program package , V. 4.2.1; MPI für Kohlenforschung: Mülheim a. d. Ruhr, Germany, 2019.*

S28 *Semiempirical Extended Tight-Binding Program Package Xtb, Version 6.5, Https://Github.Com/Grimme-Lab/Xtb. Accessed: 2021-07-18.*

S29 C. Bannwarth, E. Caldeweyher, S. Ehlert, A. Hansen, P. Pracht, J. Seibert, S. Spicher, S. Grimme, Extended Tight-Binding Quantum Chemistry Methods. *Wiley Interdiscip. Rev. Comput. Mol. Sci.* Blackwell Publishing Inc. March 1, 2021, p e1493. https://doi.org/10.1002/wcms.1493.

S30 C. Bannwarth, S. Ehlert, S. Grimme, *J. Chem. Theory Comput.* 2019, **15**, 1652–1671.

S31 S. Ehlert, M. Stahn, S. Spicher, S. Grimme, *J. Chem. Theory Comput.* 2021, **17**, 4250–4261.

S32 Y.-S. Lin, G.-D. Li, S.-P. Mao, J.-D. Chai, *J. Chem. Theory Comput.* 2013, **9**, 263–272.

S33 S. Grimme, J. Antony, S. Ehrlich, H. Krieg, *J. Chem. Phys.* 2010, **132**, 154104.

S34 S. Grimme, A. Hansen, J. G. Brandenburg, C. Bannwarth, *Chem. Rev.* 2016, **116**, 5105–5154.

S35 J. Zheng, X. Xu, D. G. Truhlar, Minimally Augmented Karlsruhe Basis Sets. *Theor. Chem. Acc.* 2011, **128**, 295–305.

S36 V. Barone, M. Cossi, *J. Phys. Chem. A* 1998, **102**, 1995–2001.

S37 K. Eichkorn, O. Treutler, H. Öhm, M. Häser, R. Ahlrichs, *Chem. Phys. Lett.* 1995, **240**, 283–289.

S38 F. Weigend, *Phys. Chem. Chem. Phys.* 2006, **8**, 1057–1065.

S39 S. Dohm, M. Bursch, A. Hansen, S. Grimme, *J. Chem. Theory Comput.* 2020, **16**, 2002–2012.

S40 P. M. Zimmerman, *J. Chem. Phys.* 2013, **138**, 184102.

S41 P. M. Zimmerman, *J. Chem. Theory Comput.* 2013, **9**, 3043–3050.

S42 S. Grimme, *Chem. Eur. J.* 2012, **18**, 9955–9964.

S43 D. Rappoport, F. J. Furche, *Chem. Phys.* 2010, **133**, 134105.

S44 A. J. Klamt, *Phys. Chem.* 1995, **99**, 2224–2235.

S45 F. Eckert, A. Klamt, *AIChE J.* 2002, **48**, 369–385.

S46 A. Klamt, F. Eckert, L. Pohler, *COSMOtherm 2016, COSMOlogic GmbH & Co. KG, Leverkusen, Germany*; COSMOtherm 2016, COSMOlogic GmbH & Co. KG, Leverkusen, Germany, 2016.

S47 S. Hirata, M. Head-Gordon, *Chem. Phys. Lett.* 1999, **314**, 291–299.

S48 T. Stein, L. Kronik, R. Baer, *J. Chem. Phys.* 2009, **131**, 244119.

S49 R. Ditchfield, *Mol. Phys.* 1974, **27**, 789–807.